THE UNIVERSITY OF CHICAGO

NEURAL MECHANISMS UNDERLYING VITAMIN B6 DEFICIENCY-INDUCED EPILEPSY AND ALCOHOL USE PATHOLOGY

A DISSERTATION SUBMITTED TO

THE FACULTY OF THE DIVISION OF THE BIOLOGICAL SCIENCES

AND THE PRITZKER SCHOOL OF MEDICINE

IN CANDIDACY FOR THE DEGREE OF

DOCTOR OF PHILOSOPHY

COMMITTEE ON NEUROBIOLOGY

BY

BENJAMIN L WANG

CHICAGO, ILLINOIS

AUGUST 2024

To my family and friends

Thank you

Table of Contents

Table of Figures

Table of Supplemental Materials

Abstract

As the primary inhibitory neurotransmitter in the central nervous system, γ-aminobutyric acid (GABA) plays a critical role in controlling neural activity. Dysregulation of GABA synthesis and release or disruptions in the excitation and inhibition balance of the brain have devastating pathological consequences, such as epilepsy. Epilepsy is a highly heterogeneous neurological condition which can stem from purely genetic, gene-environment interaction, or non-genetic etiologies. Since discovery of the first epilepsy-associated gene in 1995, nearly 1000 contributing loci and mutations have been found. However, how individual mutations may lead to excitation and inhibition imbalance and seizures remains poorly understood. One group of drug-resistant epilepsies occurs in human patients with mutations in the pyridox(am)ine-5'-phosphate oxidase (*PNPO*) gene. PNPO metabolizes dietary inactive forms of vitamin B6 into the active pyridoxal-5'-phosphate (PLP), which is a critical cofactor for synthesis of GABA. We generated two novel genetic knock-in mouse models containing *PNPO* point mutations identified in human epilepsy patients: D33V and R116Q. Homozygous D33V mutants require supplemental PLP feeding for survival and exhibit spontaneous seizures around P15. Meanwhile, homozygous R116Q and heterozygous D33V do not have spontaneous seizures but exhibit decreased latency to chemically-induced seizures, increased hyperactivity, and impaired spatial learning and memory. Using electroencephalography (EEG) and virally-expressed fluorescent GABA sensors, we found that heterozygous D33V mice exhibited increased theta rhythm power which could be rescued with PLP supplementation, increased ictal propagation speed across the cortex, and decreased GABA neurotransmitter release compared to wild-type controls. The data suggests that *PNPO* mutant mice recapitulate phenotypes exhibited in epilepsy patients, and that GABA

deficiency in *PNPO* mutant mice contributes to a collapse of feedforward inhibitory control and increased seizure susceptibility.

One of the largest contributors to new onset of seizures in humans is excessive alcohol use and withdrawal, and the variable behavioral and psychosocial consequences of alcohol consumption between individuals suggests a strong genetic component affecting alcohol response. In a second project, we examined the role of *PNPO* and PLP in alcohol use and behavioral response to alcohol consumption. In the central nervous system, one of the main targets of alcohol are $GABA_A$ receptors, where it acts as a positive allosteric modulator. Moreover, chronic alcohol consumption has been shown to cause deleterious effects on PLP content in humans. However, the intricate inter-relationship between alcohol use, PLP content, and GABAergic transmission has not yet been systematically explored. We previously generated and characterized knock-in fly models in which we replaced the fly *PNPO* gene with mutant human *PNPO* from epilepsy patients. Taking advantage of these fly models, we found that 1) alcohol consumption leads to PLP reduction; 2) PLP deficiency increases alcohol consumption; 3) *PNPO* mutations impair alcohol clearance; and 4) *PNPO* mutations have potentially lethal consequences which are worsened by alcohol consumption and rescued with PLP supplementation. Therefore, *PNPO* mutant flies exhibit an increase in alcohol consumption and decreased alcohol clearance, both of which lead to increased body alcohol and exacerbation of endogenous PLP deficiencies.

Chapter 1: Introduction

GABA and inhibition in the central nervous system

γ-aminobutyric acid (GABA) is the primary inhibitory neurotransmitter of the brain and plays a central role in control of neural activity, whereas glutamate is the primary excitatory neurotransmitter[1–3]. Often working in opposition to one another, changes in GABA and glutamate neurotransmission directly contribute to neural and network excitability and, in extreme cases, neuropathological states[3,4]. First discovered in 1950 by Eugene Roberts and Sam Frankel using ninhydrin-staining of primary amines on paper chromatography[5], GABA was initially theorized to mediate excitatory neural activity due to its structural similarities to excitatory amine-containing neurotransmitters acetylcholine and norepinephrine. 7 years after its discovery, GABA was revealed to instead mediate inhibitory effects on crayfish neural activity[6]. These inhibitory effects are mediated by highly selective $GABA_A$ and $GABA_B$ receptors, which differ in signaling mechanisms as well as in pharmacological, electrophysiological, and biochemical properties.

$GABA_A$ receptors are ionotropic chloride ion (Cl^-) channels, and activation by GABA-binding at physiological neuron membrane resting potentials mediates a Cl^- ion influx which in turn hyperpolarizes the cell membrane and reduces probability of action potential initiation[7,8]. Due to the ionotropic properties of direct coupling between receptor activation and ion channel opening, $GABA_A$ receptors mediate fast inhibition and are the primary molecular target for many drugs involved in control of inhibition within the brain[9]. In most cells, the reversal potential of $GABA_A$ receptors remains close to the neuronal resting membrane potential, leading to a relatively small driving force upon channel opening. Instead, a $GABA_A$ receptor Cl^- channel activation can mediate shunting inhibition, wherein inhibitory effects on the synapse are mediated by local

changes in membrane resistance rather than membrane potential change[10,11]. Opening of $GABA_A$ receptor-associated Cl^- channels will generate a 'shunt' effect on adjacent currents due to decreased membrane input resistance[12,13]. When a positive charge from an activated excitatory synapse arrives at the inhibitory synapse, Cl^- ions are attracted through the activated Cl^- channels, reducing the strength of the excitatory post-synaptic potential (EPSP) and allowing for highly localized temporal integration of inhibition with incoming excitatory synaptic input[12–14].

Slow inhibition is meanwhile mediated through G-protein coupled $GABA_B$ metabotropic receptors[9,15]. $GABA_B$ receptors associate specifically with Gi/o G-proteins to stimulate activity of G-protein coupled inwardly rectifying potassium channels (GIRKs), reducing activity of adenylyl cyclase (cAMP), and decreasing calcium ion (Ca^{2+}) conductance through regulation of voltage gated Ca^{2+} (Ca_V) channel activity[16]. The varied ability of GABA to mediate its inhibitory effects through both direct fast coupling to ionotropic $GABA_A$ receptors and slow coupling to metabotropic $GABA_B$ receptors highlights its importance and versatility in controlling neural excitability and normal brain function.

Outside of generalized inhibition via release of GABA into the synaptic cleft, interneurons have complex roles depending critically on synapse location and timing[17,18] such as generation of rhythmic activities in neural networks. One example is cortical PV-expressing interneurons synchronizing activity of pyramidal cells to generate and maintain cortical theta and gamma frequency oscillations[19,20]. The fast inhibition mediated by $GABA_A$ receptors is essential for synchronization of these fast frequencies, and similar phasic inhibition for generation of synchronous activity has been demonstrated in thalamic brain regions[21].

Both long-term and acutely disrupted GABA neurotransmission can cause a broad variety of neuropathological states and neurological diseases, including anxiety and mood disorders,

depression, schizophrenia, and epilepsy, to name a few[22,23]. Many of these diseases are associated with a disturbance in the optimal excitatory and inhibitory network balance and disruption of neurocircuit integrity[3], and control of GABAergic signaling through pharmacological agonism and antagonism have played a central role in treatment development for these neurological diseases. Currently, many medications aimed at increasing GABAergic signaling fall under one of several classes: 1) $GABA_A$ receptor positive allosteric modulators including benzodiazepines and non-benzodiazepine Z-drugs; 2) $GABA_B$ receptor positive modulators such as baclofen; and 3) drugs preventing breakdown or reuptake of GABA such as vigabatrin and tiagabine. Non-GABAergic medications prescribed for seizure treatment aim to decrease neural excitatory signaling, such as levetiracetam and valproic acid. Yet, no existing commonly prescribed medications are focused on addressing underlying deficiencies in GABA synthesis.

GABA is synthesized in the presynaptic neuron from precursor glutamate molecules and loaded into synaptic vesicles by vesicular GABA transporters (VGAT)[24]. Production of GABA neurotransmitter utilizes α-ketoglutarate taken from the citric acid (TCA) cycle and glutamate dehydrogenase to first generate L-glutamate, followed by decarboxylation and loss of a CO_2 molecule via glutamate decarboxylase (GAD) to generate GABA[25]. This synthesis pathway is unique among neurotransmitters in that GAD has two separate mammalian isoforms, GAD65 and GAD67 (named after their molecular weights 65 and 67 and transcribed by *Gad2* and *Gad1* genes, respectively), with GAD65 predominantly localized in nerve terminals whereas GAD67 is spread throughout the neuron[26,27]. Outside of localization differences, these two enzymes are also post-translationally regulated at two levels. The first level of regulation is achieved through phosphorylation-induced activation of GAD67 by protein kinase A (PKA) and phosphorylation-

induced inactivation of GAD65 by protein kinase C[28,29]. The second level of regulation is achieved through requirement of cofactor pyridoxal 5'-phosphate (PLP), the active form of vitamin B6, for GAD enzymatic activity. The active GAD holoenzyme, or GAD with a bound PLP cofactor, decarboxylates glutamate to form GABA neurotransmitter whilst also catalyzing a transanimation reaction producing an inactive GAD apoenzyme, or GAD without a bound PLP cofactor. At saturating glutamate concentrations *in-vitro*, GAD65 is roughly 15 times faster than GAD67 at converting from holoenzyme to apoenzyme form[28,29]. This striking kinetic difference contributes to nerve terminal-specific GAD65 predominantly existing in an inactive state (72% inactive), whereas GAD67 predominantly exists in an active state (92% active)[28].

Vitamin B6 metabolism and its role in GABAergic signaling

Isolated by Paul György in the early 1934 whilst investigating deficiencies leading to skin lesions in rodents[30,31], vitamin B6 is an essential water-soluble nutrient for organismal survival and is involved in many aspects of metabolism, macromolecule synthesis, and gene expression. Vitamin B6 is synthesized in plants, but animals cannot synthesize any of the forms of vitamin B6 in physiologically sufficient amounts and must rely upon dietary consumption and absorption through the small intestines and liver. Following dietary absorption, vitamin B6 is bound to albumin whilst circulating in plasma and predominantly stored in the muscles in liver. As a generally abundant nutrient present in a variety of meat and plant food sources, cases of dietary vitamin B6 deficiency are relatively rare. However, genetic and/or dietary factors causing long-term abnormal vitamin B6 bodily content have been demonstrated to cause dermatitis, confusion, paresthesia, peripheral neuropathy, and even seizures[32,33].

Comprised of 6 chemically similar compounds with a pyridine ring as their core structure, vitamin B6 includes pyridoxine (PN), pyridoxal (PL), pyridoxamine (PM), and their phosphorylated states pyridoxine 5'-phosphate (PNP), pyridoxal 5'-phosphate (PLP), and pyridoxamine 5'-phosphate (PMP)[34]. The enzyme pyridox(am)ine 5'-phosphate oxidase (PNPO) is responsible for catalyzing the conversion of inactive forms of vitamin B6 into PLP, the active form, which is a cofactor for nearly 4% of all known catalytic processes within the human body[35,36]. Among these processes, PLP is a critical cofactor for GAD in the primary synthesis pathway of GABA, and is a cofactor for AADC during one of the synthesis pathways for serotonin and dopamine[35–37]. Therefore, it is unsurprising that genetic deficiencies in PNPO enzymatic activity or long-term dietary deficiencies in vitamin B6 consumption have been reported to have severe neuropathological consequences, possibly due to altered neurotransmission and weakened inhibitory control of neural activity[32,38].

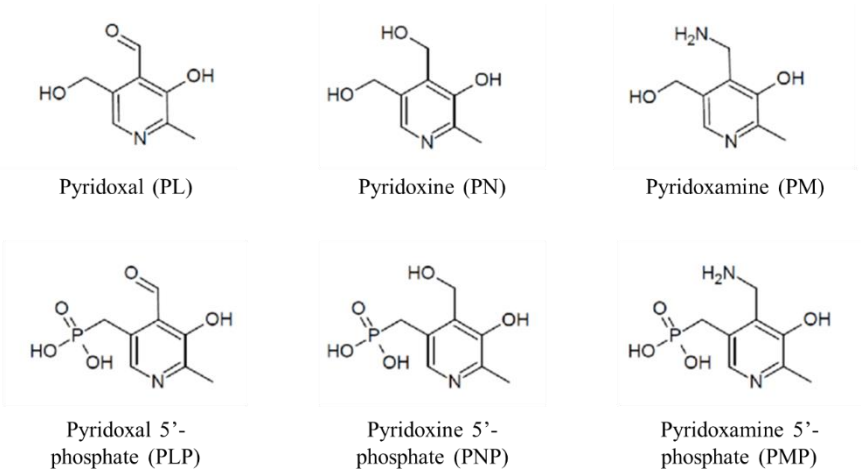

Fig 1: Chemical structures of the vitamin B6 vitamers.

In humans, 27 neuropathological mutations contributing to severe neonatal encephalopathies have been identified and published so far, of which 13 are missense mutations[32]. Interesting, the

severity of reported phenotypes varied depending on the genomic location of the mutation[39]. Additionally, *PNPO* was also identified as 1 of 16 epilepsy susceptibility genes in a recent large scale GWAS[40], suggesting that *PNPO* represents a unique case in which different variants cover a spectrum of genetic mechanisms. Severe but rare loss-of-function *PNPO* mutant variants can directly cause severe neonatal seizures and other neuropathological phenotypes, whereas less severe but more common variants likely influence seizure development through interacting with other genetic and/or environmental factors. Furthermore, in long-term alcohol users, studies have identified significantly decreased PLP in circulating plasma[41,42]. Together with the fact that metadoxine, a pyridoxine carboxylate drug, is used to treat alcohol intoxication and alcohol abuse may influence up to 25% of new onset seizures in humans[43], there are clear connections between *PNPO* deficiency and a host of neuropathological and neuropsychological disorders outside of only seizures arising from imbalance between excitation and inhibition. Despite this complex interplay between *PNPO* mutation-mediated PLP deficiency, GABAergic signaling, seizures, and alcohol-use disorder, there have been no systematic studies investigating these relationships using physiologically applicable models.

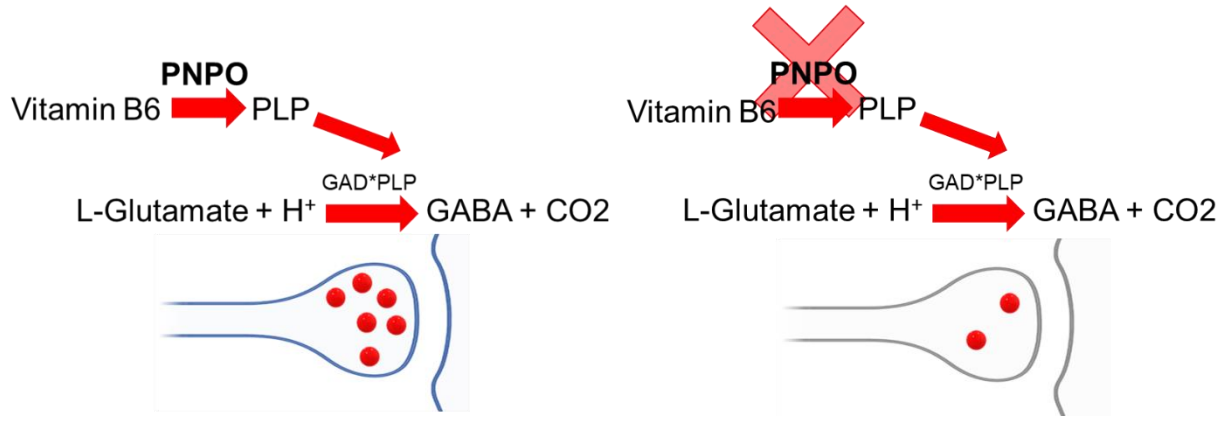

Fig 2: Schematic of how deficiency in PNPO enzymatic activity may influence GABA production via the glutamate-GAD production pathway. Red dots represent GABA neurotransmitter molecules.

Epilepsy and neural microcircuits

Epilepsy is an ancient disease with documented cases appearing in records from Mesopotamia and ancient Egypt, where individuals experiencing seizures could as likely be blessed by the gods or cursed by demons, depending on the physicians and religious leaders of the time[44]. Hippocrates dispelled some of the mysticism in the 5th century BC, when he attributed the cause of epilepsy to the brain and suggested a hereditary, rather than contagious, etiology[44]. Although Hippocrates' assertion gained traction throughout the 17th century medical community in Europe through the work of Samuel Tissot and William Cullen[45], our current understanding of the neural network mechanisms of epilepsy only evolved following discovery of electrical signaling and neuronal synapses by Santiago Ramon y Cajal and invention of the electroencephalography (EEG) in 1913[46].

Epilepsy is a highly heterogeneous neurological disorder manifesting as recurrent hypersynchronous neural discharges due to imbalances in excitatory and inhibitory signaling. The most common symptom of epilepsy are recurrent convulsive seizures, which may appear only briefly for nearly undetectable periods or appear for prolonged periods of violent convulsions. Left untreated, these seizures can result in disability or death[40,47]. As one of the most common serious neurological disorders, epilepsy is estimated to affect 1% of the population by age 20 and 3% of the population by age 75[48]. Epileptic generalized seizures generally fall into 6 main categorizations: 1) tonic-clonic seizures, involving cycles of tonic contraction of the limbs and arching of the back followed by uncontrolled clonic limb shaking; 2) tonic seizures, comprised of constant limb contractions and possible cessation of adequate breathing; 3) clonic seizures, comprised of uncontrolled limb shaking; 4) myoclonic seizures, comprised of brief

muscle spasms in one or more locations; 5) non-motor or absence seizures which can be typical (shorter, quick onset) or atypical (longer, slow onset); comprised of slight head tilt and/or repetitive eye blinking with impaired consciousness; and 6) atonic seizures, comprised of loss of muscle and/or postural control for greater than 1 second. Focal seizures, or seizures originating from a single location due to tissue injury, tumors, or GABAergic dysfunction, are a separate category to these generalized seizures[40,49]. Epilepsy etiology is highly varied, with the largest causes being structural damage and/or injury, genetic mutations, infections, metabolic disorders, and immune disorders, in no particular order[40,49]. Recently, advances in genetic sequencing technologies have allowed the identification of nearly 1000 contributing genetic loci and mutations since the discovery of the first epilepsy-associated gene in 1995[49–51]. Despite the continual expansion of etiological classifications for epilepsy, treatment options and research remain hindered by a poor understanding of the pathophysiology leading to epileptic seizures.

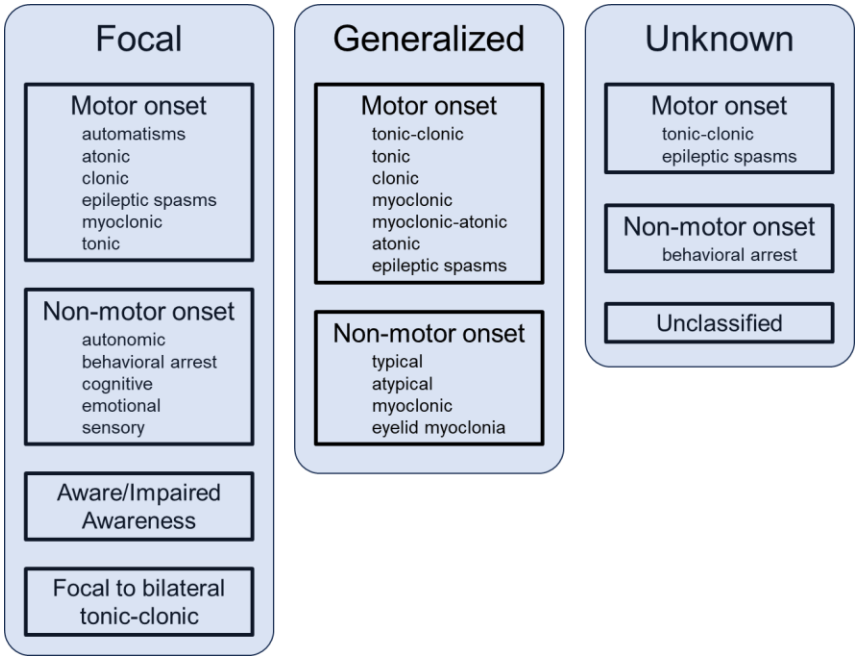

Fig 3: Classification of epileptic seizures issued by the International League Against Epilepsy (ILAE) in 2017[40].

Epilepsy arises from a disruption of the balance between GABA-mediated inhibitory signaling and primarily glutamate-mediated excitatory signaling in the brain, contributing to hypersynchronous neural discharges rapidly spreading across the cortical regions. However, how hypersynchronous activity originates and spreads to local networks or generalizes to both hemispheres is still incompletely understood. Under normal conditions, sensory stimuli from the peripheral nervous system reach the thalamus and are relayed to the sensory receptive zone in cortex layer 4[52]. There, intracortical circuits amplify and process these sensory stimuli through excitatory microcircuits from superficial to deeper cortical layers[3,53]. In order to avoid uncontrolled outward spread of excitation from hyperexcitable regions, inhibitory cortical interneurons, predominantly parvalbumin (PV)-expressing, are recruited by these excitatory sensory stimuli to provide feedforward inhibition[54–57]. This feedforward inhibition mechanism displays several levels of connective complexity to allow fine control of inhibition, such as an increase in GABAergic cortical interneuron spike generation reliability through receiving inputs from multiple thalamocortical axonal projections[57,58], and divergent inhibitory outputs from inhibitory interneurons targeting multiple downstream targets[59]. This feature is consistent with inhibitory neurons in the hippocampal CA1 region, where GABAergic basket cells inhibit only specific subsections of downstream glutamatergic neurons rather than all downstream neurons[60]. Feedforward inhibition differs from common inhibitory feedback control motifs, which operate through excitatory neurons providing drive to local inhibitory neurons which then directly form synapses back to the original excitatory population[61]. The intricacy of these inhibitory systems highlight the importance of adequate inhibition for regular brain function[54,57] and information processing by division and subtraction of input[62,63].

Feedforward inhibition is intrinsically dependent upon function of GABAergic neurons and several mechanisms leading to its failure during epilepsy have been proposed, including the exhaustion of GABA neurotransmitter[64] and depolarization block preventing interneuron firing[65,66]. Pharmacological block of inhibitory synaptic inputs promotes epileptic activity[1,65] and current AEDs commonly target $GABA_A$ receptors to allosterically upregulate inhibitory signaling[2]. Furthermore, when GABAergic inhibitory signaling fails and disrupts the balance between excitatory and inhibitory processes, cortical pyramidal neurons are recruited in glutamatergic epileptiform activity[66]. Repeated pharmacological induction of epileptiform spiking in a mouse slice preparation also weakens local feedforward inhibition, leading to increased ictal activity propagation[67]. Epileptiform activity can manifest in the form of interictal epileptiform discharges (IEDs), high-amplitude discharges of neuronal activity interspersed between seizures[68,69], ictal discharges, spikes of neuronal activity during seizures, and postictal discharges, spikes of activity following seizures.

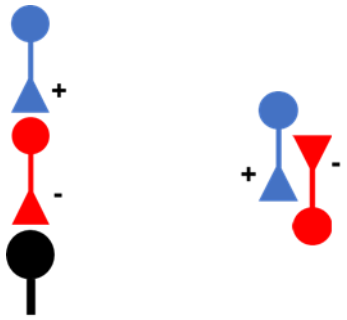

Fig 4: Schematic comparison between feedforward inhibition (left) and feedback inhibition (right). Blue color represents cortical glutamatergic excitatory neurons, red color represents cortical GABAergic inhibitory interneurons, and black represents downstream glutamatergic neurons.

Current treatment options for epilepsy are predominantly palliative rather than curative, with the primary objective of suppressing seizure severity and/or occurrence through pharmacological manipulation of the central nervous system. To complicate matters, despite the explosion of FDA-approved anti-epilepsy drugs (AEDs) and advancing genetic sequencing technologies since the mid-20th century, one third of patients remain resistant/refractory to current pharmacological treatments or develop resistance over time[70–72]. Surgical resection of seizure foci in patients with focal refractory epilepsies are evaluated on an individual basis and usually result in complete cessation of seizures[73] but may not be viable for patients with focal seizures in critical brain regions for survival or when socioeconomic conditions do not allow for surgical follow up and post-operative care. Additionally, surgical resection is not a viable option in patients with generalized epileptic seizures since there is no single seizure foci to target. Recently, clinical outcomes have shown a long-term ketogenic diet may reduce seizure severity and occurrence in children with refractory epilepsy[74,75]. The mechanisms surrounding this treatment remain poorly understood, although possible availability of alternative neuronal energy source and influence on reduction of inflammation and reactive oxygen species (ROS) have all been proposed[76].

As there are many difficulties associated with direct manipulation of neural networks and surgical resections in human epilepsy patients for purposes of research, animal models have been developed to replicate features observed in bedside patients. The use of animal models to investigate epilepsy and test potential therapeutic strategies began in the early 20th century, when an electroshock seizure model in cats was used to discover the antiseizure properties of phenytoin[77]. The electroshock seizure model was later developed into a therapy and modified for mice and rats[78]. Simultaneously, a pentylenetetrazole (PTZ) chemoconvulsant seizure model was also developed for mice[79] and used to demonstrate the efficacy of trimethadione in blocking

absence seizures, as well as to show that phenytoin was ineffective at blocking PTZ-induced absence seizures[79]. This began the use induced seizures in animal models for research and epilepsy therapy development.

Currently, animal epilepsy models can be roughly divided into acute and chronic seizure models. Acute animal models consist of triggering seizures in healthy animal subjects, whether through administration of electroshock or chemoconvulsant stimulation including flurothyl, pentylenetetrazole, kainic acid, or pilocarpine[71,72,80–82]. Although these models cannot replicate the epileptogenic process of seizure development that occurs in patients (neonate or adult) that develop epilepsy, they still offer temporal control for induction of seizures and are useful for investigating mechanisms involving generation and progression of seizure activity[72,81]. Meanwhile, chronic seizure models aim to completely replicate epileptogenesis and may involve genetic manipulations mimicking mutations observed in human epilepsy patients[71,72,83]. These models oftentimes reproduce structural and functional changes found in human patients, and usually present with spontaneous seizure development[84–86]. Commonly used chronic seizure models include the *Scn1a* mutant model of Dravet syndrome[84,87], the *Gabrg2* mutant model of generalized absence epilepsy[88], or the genetic absence epilepsy rat from Strasbourg (GAERS) model[89]. Most animal studies utilize rodent models, due to rapid and relatively inexpensive breeding, the rich variety of genetic tools available for genetic manipulations, *in-vivo* and *ex-vivo* neural recording techniques, and close behavioral and physiological relevance to human subjects compared to invertebrate models[72,83,86].

Although chronic seizure models offer a more faithful reproduction of seizure phenotypes found in human patients compared to acute seizure models, current genetic animal models of epilepsy carry either severe, extremely rare, monogenic epilepsy mutations[84,87,90], or common, extremely

mild, polygenic epilepsy mutations that require chemoconvulsive induction or kindling to produce seizures[72,82]. Clearly, development of new animal models remains crucial for more accurate modeling of epilepsy patients that do not fall on either ends of the spectrum of phenotypic severity.

Alcohol use and GABAergic signaling

Alcohol is a leading contributor to disease and preventable deaths in the United States, with one in four adults aged 26 and older engaging in binge drinking each month (5 or more drinks for men or 4 or more drinks for women on one occasion)[91]. Alcohol use disorder (AUD) comprises of an impaired ability to stop or control alcohol use despite adverse health, social, and/or occupational consequences, and about one in three adults will meet the criteria defining AUD[92]. In the United States, it is estimated that excessive alcohol intake is the fifth leading risk factor for death and disability[93] and the cost of excessive alcohol use is estimated to cost the American healthcare system more than $28 billion each year. Outside of cognitive behavioral therapy (CBT), pharmacological treatment of AUD is hindered by an incomplete understanding of the neurobiology underlying addictive behaviors and the heterogeneity of patient symptoms[94,95]. Furthermore, longitudinal studies have revealed individuals from disadvantaged socioeconomic backgrounds bear a disproportionately large burden of consequences related to excessive consumption of alcohol[96], indicating a need for additional cost-effective, tailored AUD treatment strategies.

Acute alcohol consumption in humans increases GABAergic inhibitory signaling through allosteric upregulation of $GABA_A$ receptor activity[97,98] and decreases glutamatergic excitatory signaling[99,100], leading to tipping of the brain excitation/inhibition (E/I) balance toward inhibition. However, under chronic alcohol consumption conditions, the brain compensates through

increased excitatory glutamatergic signaling[101] which may lead to hyperexcitability and resultant anxiety and seizures upon cessation of alcohol consumption. This is supported by the prevalence of epilepsy and new-onset seizures being greater than 3-4 times that of the general human population in individuals with chronic alcohol abuse[102–104]. Several other factors have been proposed that may contribute to this severe prevalence, such as cerebral atrophy reported in 74% of long-term heavy alcohol users[105], the prevalence of cerebrovascular infarctions, lesions, and head traumas in individuals with alcohol dependence[105,106], and acute and chronic alcohol exposure contributing to opposing epigenetic effects on gene regulation and expression[107]. Regardless, the clear pathologic effects of chronic alcohol use on inhibitory signaling and resultant seizure susceptibility among individuals with AUD necessitates further research into the relationship between alcohol intake and GABAergic neurotransmission.

The prevailing model for development of addictive behaviors suggests addiction stems not from homeostatic adaptations but through allostatic maladaptations to maintain a new stability outside of the normal homeostatic range[101,108]. Addictive behaviors are believed to bring about tonic brain-body adaptations to new drug reward set points, including changes in hormones and neurotransmitters[109], leading to chronic stress to maintain allostatic load of adapting the body to the new set point. As the increased chronic stress leads to prolonged allostatic maladaptations beyond normal homeostatic conditions, breakdown and illness can occur[101,109]. Neurotransmitters and signaling molecules related to reward, such as dopamine, may have limited ability to maintain such allostatic maladaptations, further exacerbating the breakdown of prolonged allostatic stability[101,108]. Although biologically poorly understood, genetic contributions toward alcohol use disorder vulnerability have long been hypothesized based on twin studies with adoption[110–112].

Current treatments for AUD rely predominantly on cognitive behavioral therapy, with 3 FDA-approved (dilsulfiram, acamprosate, and naltrexone) and several repurposed pharmacological treatments offered as alternative options[94,95]. Many of the repurposed pharmacological treatments, including baclofen, are anti-epilepsy drugs aiming to strengthen GABAergic signaling through increasing GABA neurotransmitter concentration in the synaptic cleft or positively modulating the activity of GABA receptors. Future development and research toward tailored AUD treatment strategies require an improved understanding of contributors toward alcohol addictive behavior development.

Summary

In this thesis, we generated novel genetic models of *PNPO* deficiency to investigate behavioral and molecular phenotypes and GABAergic signaling alterations underlying seizures in *M. musculus* mouse models, and behavioral and neurobiological changes related to alcohol addictive behavior development in *D. melanogaster* fly models. Our findings indicate that *PNPO* mutant mice containing mutations identified in human epilepsy patients are a robust model for severe neonatal encephalopathies and recapitulate many behavioral and molecular phenotypes associated with human epilepsy. Additionally, *PNPO* mutant mice exhibit altered GABAergic neurotransmission and *in-vivo* recording using iEEG and fiber photometry with a fluorescent virally expressed GABA sensor suggests a progressive collapse of feedforward inhibition leads to increased seizure susceptibility and propagation. *PNPO* mutant flies exhibit significant vulnerability to falling into 2 separate vicious cycles fed by endogenous PLP deficiency, increased alcohol consumption, impaired clearance of alcohol, and increased body alcohol content. Together, these findings demonstrate the importance of *PNPO* and PLP in maintenance

of GABAergic neurotransmission, and the consequences of disruptions in inhibitory signaling in epileptic seizures and addictive behaviors.

Chapter 2: Genetic errors in vitamin B6 metabolism induces seizures and GABAergic signaling deficiency

Introduction

Epilepsy is a highly heterogeneous neurological condition estimated to be one of the most globally common severe neurological conditions[48]. Patients with epilepsy frequently present with seizures, events in which regions of the brain will transition into a pathological hypersynchronous state presumably due to disrupted balance of neuronal excitation and inhibition. Despite continual research and development of anti-epilepsy drugs (AEDs) since the mid-20th century[71,72], there is still no cure for epilepsy and existing treatments are merely palliative. Furthermore, more than a third of epilepsy patients are drug-resistant or develop drug-resistance to existing AEDs over the course of treatment[70,71]. Generation of novel mouse models for treatment research and for understanding of the mechanisms underlying seizure development are therefore critical for future epilepsy treatment.

Pyridoxine-5'-phosphate oxidase (PNPO) is a homodimer enzyme responsible for metabolism of dietary vitamin B6 into pyridoxal 5'-phosphate (PLP), a cofactor for nearly 4% of all known catalytic processes[35] and required for synthesis of neurotransmitters GABA, serotonin, and dopamine[35–37,113]. Identified in 2005 as a genetic mediator for severe refractory neonatal epilepsy, *PNPO* has 27 documented pathogenic mutations contributing to epileptic seizures of varying severity depending on residual enzymatic activity[32,38], of which 12 are missense mutations[32,39]. Interestingly, *PNPO* has also been identified as 1 of 16 most high-risk epilepsy susceptibility genes in a large scale GWAS[49], suggesting this gene represents a unique case in which different variants cover a spectrum of genetic mechanisms. Severe but rare loss-of-function *PNPO* mutant variants can directly cause early onset severe seizures, while less severe but more common

variants are unlikely to cause epileptic seizures on their own but can influence seizure development when combined with other genetic and/or environment factors[32,38]. *PNPO* represents an excellent genetic target for understanding genetic, neuronal, and network mechanisms of not just epileptogenesis, but also GABAergic signaling and the effect of environmental long-term vitamin B6 dietary deficit on neuronal function.

We previously generated genetic fruit fly models containing knocked in human *PNPO* mutant variants selected across a spectrum of partial enzymatic loss-of-function[114,115]. These fly models recapitulate many of the symptoms found in human epilepsy patients, and their seizure characteristics suggest GABA neurotransmitter deficiency[115]. We've now generated knock-in mouse models carrying the severe D33V and mild R116Q *PNPO* point mutations found in human epilepsy patients. These genetic mouse models allow leveraging of the rich genetic and imaging tools available in mouse models to investigate epileptiform activity and GABA neurotransmitter release *in-vivo* without local drug injections or reduced slice preparations.

We characterized these *PNPO* mutant mice using a battery of *in-vivo* neuronal recording strategies and behavioral assays to confirm applicability to human genetic epilepsy patients and to evaluate them as potential platforms for future epilepsy drug development studies. We also used *in-vivo* recording and molecular strategies to investigate effects of *PNPO* deficiency on GABAergic signaling and feedforward inhibition. *PNPO* mutant mice homozygous for the severe D33V mutation (D33V/D33V) displayed severe seizures and death from P15. *PNPO* mutant mice heterozygous for the D33V mutation (D33V/+) and homozygous for the mild R116Q mutation (R116Q/R116Q) exhibited mutation severity-dependent seizure susceptibility, hyperactivity, and spatial learning and memory phenotypes, which were accompanied with loss of endogenous PNPO protein expression and altered glutamate decarboxylase (*GAD*) mRNA

expression specifically in R116Q/R116Q. D33V/+ exhibited dramatically increased power in EEG theta frequencies and increased speed of ictal propagation during seizures compared to controls, both of which could be rescued along with the seizure phenotype through dietary administration of PLP. *In-vivo* GABA release measured using the virally expressed fluorescent sensor iGABASnFR revealed reduced D33V/+ maximal GABA neurotransmitter release compared to controls following administration of a selective GABA reuptake inhibitor, and a severe progressive weakening of GABAergic signaling preceding seizures. These results were coupled with decreased mIPSP frequency in CA1 pyramidal neurons of D33V/+, suggesting a decrease in presynaptic GABA release in mutant mice. Our data characterizes epilepsy and seizure phenotypes in a new genetic model of *PNPO* deficiency and illustrates how collapse of feedforward inhibitory restraint during seizures is influenced by failure of GABA release.

Methods

Animals: All experiments used male and female C57Bl/6 mice. Similarly to human PNPO, the mouse PNPO gene has 7 exons with 89% homology. Amino acid D33 and R116 are conserved in both species, allowing direct introduction of point mutations found in human epilepsy patients into the mouse genome. Mice carrying the R116Q and D33V PNPO mutations were generated using single-guide RNA (sgRNA) and donor DNA sequences created using PNPO sequences flanking the D33V (NM_018129.4(PNPO):c.98A>T (p.Asp33Val); 17:47941773) and R116Q (NM_018129.4(PNPO):c.347G>A (p.Arg116Gln) mutation sites and an online tool available at Integrated DNA Technologies, Inc. (IDT). The sgRNAs, donor ssDNAs, and Cas9 ribonucleoprotein were purchased from IDT and microinjected into C57Bl/6 zygotes by the University of Chicago Transgenic Mouse Facility. PCR of genomic DNA isolated from tail biopsies followed by DNA sequencing through the University of Chicago DNA Sequencing

Facility allowed screening for positive founders, which were further backcrossed over 5 generations to C57Bl/6 mice. Afterward, heterozygote D33V/+ and R116Q/+ breeding cages were set up to obtain homozygote, heterozygote, and wild type littermates for experiments. For PCR genotyping, DNA was isolated from mouse tail biopsies at P12. Breeding cages were fed 150mg/kg/day pyridoxal 5'-phosphate (PLP, #82870, SigmaAldrich, MO) mixed in water, based on clinical human PLP treatment doses[116,117]. All studies were approved by the University of Chicago Institutional Animal Care and Use Committee (IACUC) in accordance with the National Institutes of Health Guide for the Care and Use of Laboratory Animals.

Induced seizure paradigm: Flurothyl seizure induction was conducted as previously described[80,118]. Briefly, mice were placed inside a clear plexiglass chamber and 10% flurothyl (#287571 SigmaAldrich, MO) in EtOH was infused via syringe pump at a flow rate of 6mL/h. The seizure latency was measured as the time from when flurothyl infusion began to loss of postural control. Mice were continually observed until onset of seizure and loss of postural control, before flurothyl flow was shut off and mice were returned to the home cage for recovery. Latency to seizure onset and Racine scale for seizure severity quantification were recorded for each individual mouse[119] by an experimenter blinded to mouse genotype. Mice were monitored every 8h for 24h following seizure induction for adequate recovery of locomotion, grooming, and feeding behaviors, and mice were given no more than one flurothyl-induced seizure every 48h, with a maximum of two seizures per mouse. Pentylenetetrazole (PTZ) was also used to induce seizures in mutant mice and controls[7,119]. All mice were continually observed for 10min in a clear plexiglass chamber before 50mg/kg PTZ (P6500 SigmaAldrich, MO) was injected intraperitoneally. Mice were returned to the clear plexiglass chamber and observed for 30min, the latency to seizure onset and Racine scale for seizure severity[119] were recorded, and then the

mice were returned to recover in their home cage. Similarly to the flurothyl seizure induction method, mice were monitored every 8h for 24h following seizure induction for adequate recovery, and mice were given no more than one PTZ-induced seizure every 48h, with a maximum of two seizures per mouse. Paired t-tests were performed to assess statistical significance between each heterozygote and homozygote mutant mouse cohort with the corresponding controls.

Rodent locomotor activity: Mice were placed inside a clear plexiglass 40cm x 40cm x 37cm chamber and allowed to freely move continuously for 2h. Light was adjusted to 16 lux as measured 1cm above chamber floor, and each chamber was surrounded by black drop cloth curtains to obscure views beyond the chamber. Mice were acclimated to the open field chamber for 60min 1 day prior to the experiment. Movement speed (cm/s) and distance travelled (cm) were recorded in 1min bins using infra-red sensors along the floor of the arena and analyzed using Activity Monitor (Med Associates, VT, USA). Movement distribution analysis was calculated by binning total distance traveled in 5min bins using Matlab. Paired t-tests were performed to assess statistical significance of total distance travelled between each heterozygote and homozygote mutant mouse cohort with the corresponding controls.

Morris water maze: Experiments were conducted as previously described[120]. Briefly, a circular 100cm diameter white, acrylic tank (Med Associates, VT, USA) was filled with room temperature water to 15cm below the lip of the tank. White, non-toxic paint (Reeves and Poole Group, Canada) was added to the water and a circular 8cm diameter platform was submerged underneath the water surface in one quadrant. Around the tank were arranged black drop cloth curtains in various patterns to provide distinct spatial cues to the north, east, south, and west cardinal directions. Mice were placed onto the platform for 10s to learn the location of the

platform on the first day, and then were trained to find the platform for 5 days, with 4 trials per day. Mice were placed into a randomized different quadrant for each trial, and a trial was terminated at 1min if the mouse did not locate the platform. The platform was removed on the probe day and mice were allowed to freely swim. Mouse swim velocity, swim trajectory, latency to the submerged platform, and time spent in each quadrant during probe days was tracked using a live camera and EthoVision software (Noldus, Netherlands). Following the probe day, the platform was relocated to the opposite quadrant, and mice were given 5 more training days followed by a probe day as completed before. In between trials, mice were placed in their home cages under a heat lamp set to 35^{o}C, and the body weight of each mouse was taken each day before trials began. Mice with body weight changes of more than 20% from prior to the assay at any point during the training or probe trials were excluded from the study. Paired t-tests were performed to assess statistical significance of time spent in correct probe quadrants between each heterozygote and homozygote mutant mouse cohort with the corresponding controls.

Western blot: Mice previously used for open field locomotor or Morris water maze assays were anesthetized using isoflurane before brains were isolated and flash frozen in liquid nitrogen. 30g cortex tissue was homogenized in pre-chilled Tris buffer with 2% SDS using a Kontes Microtube Pellet Pestle (DWK Life Sciences #749540-0000) and a Fisherbrand Model 50 Sonic Dismembrator (FB50110, FisherScientific, MA). Protein concentration was measured using the Pierce BCA protein assay kit (#23225 ThermoFisher, MA) and absorbance was read at 562nm for 500ms using a VICTOR Nivo multimode spectrophotometer (PerkinElmer). Protein concentration was calculated from absorbance using a BSA protein standard curve. 30µg protein was run at 200V for 30min after mixing 1:1 with sample buffer containing Laemmli buffer solution (S3401 SigmaAldrich, MO) and β-mercaptoethanol (M6250 SigmaAldrich, MO).

Protein was transferred to a PVDF membrane (#1620177 BioRad, CA) and stained with 1:1500 primary polyclonal rabbit anti-PNPO (NBP1-87302 Novus, MO) and 1:1000 polyclonal mouse anti-tubulin (Sigma). Membrane was incubated with 1:5000 secondary antibodies antiMs-HRP and antiRb-HRP (Sigma) and then visualized using the ChemiDoc Imaging System (BioRad, CA). Densitometric analysis was performed through ImageJ, and paired t-tests were performed to assess statistical significance between each heterozygote and homozygote mutant mouse cohort with the corresponding controls.

Immunohistochemistry: Mice previously used for open field locomotor or Morris water maze assays were anesthetized using isoflurane before perfusion with ice-cold formalin. Brains were isolated and frozen in OCT compound (#4585 FisherScientific, MA) before 20µm coronal sections were taken from Bregma -1.07 to -2.69. Slices were blocked with 1% NGS (#50197Z, Thermofisher, MA) and incubated with 1:300 primary polyclonal rabbit anti-PNPO (NBP1-87302 Novus, MO) overnight and 1:500 secondary Ms anti-Rb antibody (Sigma). Slices were visualized under a Nikon Eclipse Ti (Nikon, Japan) and analyzed with ImageJ.

Reverse transcription polymerase chain reaction (RT-PCR): RNA was isolated from cortical tissue following homogenization using Trizol reagent (#15596026 ThermoFisher, MA) and a Kontes Microtube Pellet Pestle (DWK Life Sciences #749540-0000) and aspiration of supernatant before resuspension in RNAse-free water. cDNA was prepared using 2µg RNA with a High Capacity cDNA Reverse Transcription Kit (#4368813 AppliedBiosystems, MA) with primers for PNPO (F: 5’-AGGCTAGACACACAGGCTGA-3’; R: 5’-CGGGAATGGAAGTAGTTCTCGGC-3’, results were validated with F: 5’-CCGAATCAGTTAGTGGCTGG-3’; R: 5’-GACAAGGTTGCCTCGGGAGG-3’), GAD65 (F: 5’-TCAACTAAGTCCCACCCTAAG-3’; R: 5’-CCCTGTAGAGTCAATACCTGC-3’), and

GAD67 (F: 5’-CTCAGGCTGTATGTCAGATGTTC-3’; R: 5’-AAGCGAGTCACAGAGATTGGTC-3’). qPCR was performed using EvaGreen Supermix (#1864034 BioRad, CA) loaded in triplicate into a 96 well plate and expression was quantified using a CFX Opus 96 Real-Time PCR System (BioRad, CA). The mRNA abundance was calculated with the comparative threshold (CT) method using the formula “2−ΔΔCT” where ΔΔCT is the difference between the threshold cycle of the given target cDNA expressed in PNPO mutant mouse and control tissue, normalized to the control tissue expression. The CT value was taken as a fractional cycle number at which the emitted fluorescence of the sample passes a fixed threshold above the baseline. Values were compared with the internal standard 18S gene. Purity and specificity of all products were confirmed by omitting the template and performing a standard melting curve analysis.

Electroencephalography: Continuous intracranial electroencephalography with simultaneous video recordings were obtained for 14 days using wireless Epoch 2-channel sensors with total gain 2000x, hardware bandwidth 0.1-100Hz, and +/- 1mV input range (EPTX-10212 Biopac, CA). All surgeries were conducted under aseptic conditions, and surgical tools were sterilized using a glass bead sterilizer (FST sterilization tool 18000-45). Mice were anesthetized with isoflurane (2% induction, 1.5% maintenance) and body temperature was maintained at 37^{o}C using a heating pad (Harvard Apparatus) after placement into stereotaxic surgery device. An ophthalmic gel was applied to mouse eyes, and buprenorphine (Hospira, 0.05mg/kg) and bupivacaine (Hospira, 1mg/kg) were applied subcutaneously to the site of incision. 5min afterward, an incision was made to expose the skull, and a Foredom micromotor drill was used with a drill bit (Kyocera 105-0210L310) to create bilateral openings in the skull for EEG sensor lead emplacement. The coordinates for these openings in mm relative to Bregma were AP: -1.31;

ML: -2.5 and AP: -1.31; ML: 2.5. The Epoch wireless sensor electrodes were trimmed to 5mm length and lowered into the skull openings using a modified cannula holder stereotaxic attachment (Kopf Instruments) at coordinates in mm relative to Bregma: AP: -1.31; ML: -2.5; DV: -1.25 and AP: -1.31; ML: 2.5; DV: -1.25 for bilateral recordings; AP: 1.93; ML: -2.0; DV: -1.25 for position 2 in the motor M1 region; AP: -3.51; ML: -3.0; DV: -1.25 for position 3 in the occipital V1 region. The coordinates were scaled based on the length variation between Bregma and Lambda locations on each individual mouse skull divided by 4.21 (standard distance according to Paxino's and Franklin's Mouse Brain Atlas). Dental cement (Lang Dental) was applied surrounding the EEG probe to secure it in place and form a headcap. Following surgery, mice were given 0.5mL sterile saline via intraperitoneal injection and 5mg/kg Meloxicam (71125-38-7 Sigma, CA) subcutaneously and allowed to recover in the home cage on a heat pad at 32^{o}C for 48h.

Cortical LFP electrical signals were received by an Epoch Receiver and MP160 Data Acquisition System (Biopac, CA) for signal amplification and processing. AcqKnowledge 5 software was used to record digitized signal from the MP160 processor, and the signal was sampled at 2000Hz with a low pass Blackman filter. Continual video recordings were taken using either a linked GoPro Hero8 or a Logitech C922 webcam time-locked to the beginning of signal recording. Baseline cortical LFPs were obtained following recovery from surgery for days 1-3, followed by flurothyl seizure induction once per day on days 4-7. 150mg/kg PLP was administered via drinking water during days 8-14, and flurothyl seizure induction occurred once per day on days 11-14. Seizure induction was immediately halted following loss of postural control and jumping. Signal analysis was performed in Matlab. 50 randomly selected 10s epochs without overlap from the baseline activity of each mouse were used to generate power spectral density (PSD) plots by

taking the discrete Fourier transformation (DFT) of a signal using fast Fourier transformations (FFT) with a high pass filter of 1Hz and low pass filter of 150Hz, and then each genotype was averaged.

Briefly, the FFT (Equation 1) decomposed the digitized EEG raw signal time series into a power by frequency spectral plot, with power referring to the square of the raw signal magnitude. The raw signal magnitude refers to the integral average of the amplitude of the EEG signal. A Hamming window was used for each individual epoch to reduce spectral leakage.

$$X_f = \sum_{n=0}^{N-1} E_n * e^{-i2\pi kn/N}$$

Equation 1, where E_n is the EEG signal at sample n, X_f is the DFT, N is the number of samples, n is the current sample, and k is the current frequency, ranging from 0 to N-1.

The PSD is computed by dividing the discrete-time signal into successive blocks and averaging the mean squared amplitude of the DFT of these blocks (Equation 2).

$$\hat{P}_x(\omega_k) = \frac{1}{B}\sum_{b=0}^{B-1} |DFT_k(x_b)|^2$$

Equation 2, where $x_b(n) = x(n+bN)$, with n = 0, 1, 2, 3…, N-1, is the b^{th} signal block and B is the number of blocks.

Area under curve of each power spectra was calculated using the integral under segmented regions correlating to the delta (1-4Hz), theta (4-7Hz), alpha (8-12Hz), beta (12-30Hz), and gamma (30-150Hz) EEG bands. This pipeline was repeated for randomly selected epochs during daytime (07:00 – 19:00) and nighttime (19:00 – 07:00) to rule out circadian rhythm-driven changes, and video recordings were consulted to visually determine whether mice were asleep or

awake during chosen epochs. All analysis was performed using epochs from awake animals during daytime. While fast Fourier transformations and quantification of area under curve on power spectra were all performed using raw data, plotted data traces were downsampled by factor of 2 for improved visualization.

Fiber photometry: Surgeries to create openings in the skull using a Foredom micromotor drill and drill bit (Kyocera 105-0210L310) were conducted as previously described in electroencephalography methods. A stereotaxic surgery device (Kopf Instruments) was used to position viral injection syringes and fiberoptic cannulas. A Hamilton syringe (1700 series, 33G) was controlled using a syringe pump (World Precision Instrument, UMP3T) to inject 300nL virus at a rate of 150nL/min. After injection, the injection needle was kept in place for 8min to allow viral diffusion. Injection coordinates in mm relative to Bregma were AP: -2.15; ML: 2.2; DV: -1.7. Fiber optic cannulas (MFC 400/430-0.48 5mm MF1.25 FL, Doric) were implanted using a cannula holder stereotaxic attachment (Kopf Instruments). Cannulas were lowered into the brain at a rate of 300μm/min at coordinates relative to Bregma: AP: -2.15; ML: 2.2; DV: -1.7. Dental cement (Lang Dental) was used to secure the cannulas in place to the skull via a headcap and mice were observed for 30min following surgery to ensure sufficient dental cement rigidity.

AAV1-hSynapsin-iGABASnFR (#112159 Addgene, MA) was injected at titer 7*1012vg/mL unilaterally 21-25 days prior to recording. A TDT-Doric system was used for fiber photometry recording with the RZ5P amplifier and processor (TDT, FL) to drive and demodulate signals. We simultaneously delivered 405nm and 465nm light and monitored 525nm light using a 5-port fluorescent minicube (FMC5 Doric, Canada) and Model 2151 photodetector (Newport, CA). 465nm excitation light was calcium-dependent and isosbestic control 405nm excitation light was calcium-independent. The signal was sampled at 1017.3Hz. Animal headcaps were affixed to an

optic cord (0.48NA, 400µm diameter Doric, Canada) and Synapse software (TDT, FL) was used to record signal from the RZ5P processor. Data was analyzed using Matlab. The first 5s of recording was disregarded due to possible opto-electric artifacts that may affect the fitting parameters in the subsequent step. A smoothed 405nm signal was fitted to the 465nm signal using linear regression to obtain fitting coefficients during a 10s baseline prior to seizure induction. Using the coefficients, we calculated the fitted 405nm and 465nm signals. The fitted calcium-independent 405nm isosbestic signal was subtracted from the fitted 465nm signal to reduce movement artifacts and then divided by the 405nm signal to obtain ΔF/F ((F465-F405)/F405). A mean ΔF/F was calculated by averaging the ΔF/F across 10min baseline of all mice after filtering out high amplitude events (>2x absolute deviation from mean of individual mice).

For experiments involving tiagabine pharmacological blockade of GABA reuptake protein GAT1, mice were acclimated for 30min to the clear plexiglass recording chamber before 21mg/kg tiagabine hydrochloride mixed in DMSO (#5.06236 SigmaAldrich, MO) was injected intraperitoneally following 10min baseline fiber photometry recording. Mice were initially monitored continuously for 4h following injection to assay maximal 465nm light, and then 1h for experiments after observing maximal 465nm light declined following first hour of recording. Tiagabine hydrochloride dose response was also assayed using 42mg/kg intraperitoneal injection. For experiments involving seizure induction, mice were acclimated for 30min to the clear plexiglass recording chamber before flurothyl infusion as previously described in the seizure induction methods. Mice were continually video-monitored to record seizure progression, and fiber photometry recordings were time-locked with the video to 10min prior to flurothyl infusion.

Ex-vivo slice electrophysiology: Mice previously used for behavioral experiments not involving any seizure induction protocols were anesthetized with isoflurane and decapitated. The brains were extracted and sliced on ice-cold NMDG slicing solution (93mM NMDG, 2.5mM KCl, 1.2mM NaH2PO4, 30mM NaHCO3, 25mM Glucose, 20mM HEPES, 5mM Na-ascorbate, 2mM Thiourea, 3mM Na-pyruvate, 12mM N-acetyl cysteine, 10mM MgSO4&7H2O, and 0.5mM CaCl2). pH was adjusted to 7.3-7.4 with 12N HCl and osmolarity was confirmed to be ~310mOsm, otherwise solution was discarded and remade. During dissection, NMDG slicing solution was continuously bubbled with carbogen (95% O2 and 5% CO2). 250µm coronal midbrain sections containing the hippocampus and thalamus were sliced using a vibratome (VT100S Leica, Germany) in NMDG slicing solution with continual bubbled carbogen. Slices were transferred to carbogen-bubbled NMDG solution at 32^{o}C for 15min, then transferred to a HEPES-containing aCSF solution continuously bubbled with 95% O2 and 5% CO2 (92mM NaCl, 2.5mM KCl, 1.2mM NaH2PO4, 30mM NaHCO3, 25mM Glucose, 20mM HEPES, 5mM Na-ascorbate, 2mM Thiourea, 3mM Na-pyruvate, 2mM MgSO4&7H2O, and 2mM CaCl2) adjusted to 7.3-7.4pH with 10N NaOH and osmolarity 305-315mOsm. Slices were incubated in HEPES-containing aCSF solution for 1h before starting experiments. 2-3 slices were used from each animal for experiments.

For recordings, slices were transferred to an upright microscope (Axioskop Zeiss, Germany) and neurons were visualized under infrared illumination or a lamp (XCite, Excelitas) with a 40x water-immersion objective and video microscopy. Hippocampal pyramidal neurons were located using the distinct triangular cell morphology. aCSF was used for external solution and contained 125mM NaCl, 2.5mM KCl, 1mM MgCl2*6H2O, 2.5mM CaCl2*2H2O, 20mM Glucose, 1mM NaH2PO4, and 25mM NaHCO3. pH was adjusted to 7.3 by bubbling with CO2/O2, and

osmolarity was measured to be 305mOsm. This recording aCSF was superfused at ~2mL/min. Potassium gluconate (154mM K-Gluconate, 1mM KCl, 1mM EGTA, 10mM HEPES, 10mM Glucose, 5mM Na-ATP, 0.1mM Na-GTP) was chosen for the internal recording solution due to its ability to visualize action potentials. Internal solution was adjusted to pH 7.4 with KOH and 320mOsm. Experiments were performed at room temperature (24^{o}C). Signals were amplified with a Multiclamp 700A/Axopatch 200B amplifier, digitized with Digidata 1440A, and controlled with pCLAMP9 software (Molecular Devices). Data was sampled at 10kHz and low pass filtered at 1kHz. Borosilicate patch pipettes were created on a Flaming/Brown micropipette puller (model P-97, Sutter Instrument, Novato CA) and confirmed to have 3-6MΩ tip resistance. Miniature IPSPs were recorded following patching with bath infusion of AMPA/NMDA antagonist cocktail containing 50µM D-AP5 (#0106 Tocris,), 10µM CNQX (#0190 Tocris), and 1µM TTX (#1078 Tocris). $GABA_A$ receptor antagonist 100µM picrotoxin was later bath applied to confirm GABAergic currents. All data analysis was performed in Matlab. Spontaneous synaptic events were detected in Matlab using the findpeaks function with prominence >3 median absolute deviation from baseline noise, <0.75ms rise time, and >3 RMS noise picocoulomb charge transfer calculated using area under the curve. Frequency and amplitude of events were also provided by the findpeaks function. Function-identified events were verified visually by the experimenter.

Data visualization: All figures were prepared using GraphPad Prism 8, following analysis with Matlab and built-in GraphPad Prism 8 statistical software. When possible, results were cross-verified using manual calculations. Custom Matlab scripts for data analysis and plotting are uploaded to a publicly available cloud folder on the University of Chicago Box website.

Results

PNPO mutant mice were generated using CRISPR/Cas9 and exhibit severe spontaneous seizures which can be rescued with dietary supplementation

The *M. musculus PNPO* gene shares 89% sequence homology with the human *PNPO* gene, allowing for directed knock-in of point mutations from human patients into the mouse gene rather than knocking in the mutant gene as used in *D. melanogaster* models of *PNPO* deficiency[114,115]. Using homology-directed repair (HDR) CRISPR/Cas9 and guide RNA targeting the human *PNPO* sequence, we knocked in the D33V (56% loss-of-function) and R116Q (16% loss-of-function) point mutations into C57Bl/6 mice. Generating mutants with a range of *PNPO* enzymatic loss-of-function allowed for investigations into how D33V and R116Q may differentially affect epilepsy and seizure development, and also for comparison of physiological consequences due to severe vs mild *PNPO* loss-of-function. Genomic DNA sequencing of all *PNPO* exons from cortical tissue and comparison to the native *M. musculus PNPO* sequence on the NIH GenBank database confirmed successful CRISPR/Cas9 insertion and lack of off-target mutations.

Mice heterozygous for the severe D33V point mutation (D33V/+) were crossed and produced litters with lopsided Mendelian ratios, suggesting homozygotes carrying the D33V point mutation (D33V/D33V) were embryonically lethal. Upon supplementation of drinking water with 150mg/kg PLP based on clinical human PLP treatments[32,38], D33V/D33V pups were born with correct Mendelian ratios (1 wild type: 2 D33V/+: 1 D33V/D33V). However, these homozygote pups developed increasingly frequent severe spontaneous seizures and did not survive after P18. A battery of pharmacological and nutrient treatments was tested to reduce convulsions in early neonatal mice and rescue the seizure phenotype. Anti-epilepsy drugs

gabapentin, benzodiazepine, and levetiracetam were individually supplemented in diet or injected intraperitoneally but did not reduce seizure severity sufficiently to markedly improve survival. D-glucose injected subcutaneously and intraperitoneally improved survival but no pups survived after P18. Surprisingly, a modified rodent milk diet supplemented with dissolved 50mg/kg PLP was successful in improving survival, resulting in 80% surviving pups by weaning age. Although PLP and pyridoxine treatments have been successfully used to treat refractory PNPO-deficiency epilepsies in human neonates[116,117,121], the frequency of seizures and mortality rate observed in D33V/D33V pups are more severe than those observed in human patients.

Mice heterozygous for the mild R116Q point mutation (R116Q/+) were crossed and produced litters with correct Mendelian ratios. R116Q homozygote and heterozygote mice (R116Q/R116Q and R116Q/+, respectively) did not exhibit visible spontaneous seizures and were otherwise phenotypically normal. R116Q mutant mice did not develop spontaneous neonatal seizures, and treatment with modified rodent milk diet supplemented with 50mg/kg PLP did not visibly affect survival or development.

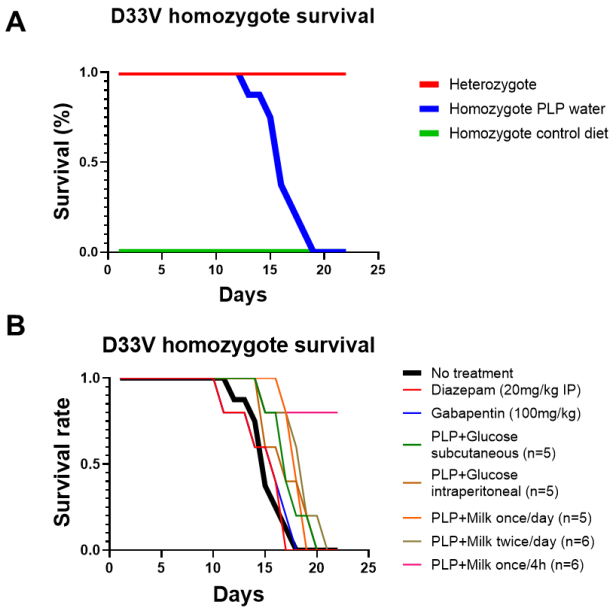

Fig 5: Survival curves of D33V homozygote mice
a) D33V homozygote pup survival rate under normal rodent diet fed to parents. Heterozygotes are denoted by red, homozygotes are denoted by green, and homozygote pups with parents fed 150mg/mL PLP-supplemented water are denoted by blue.
b) D33V homozygote pup survival rate following birth to parents fed 150mg/kg PLP-supplemented water. A battery of treatments were given to assay survival. From top to bottom: 20mg/kg IP diazepam, 100mg/kg IP gabapentin, 50mg/kg PLP+50mg/kg glucose SC, 50mg/kg PLP+50mg/kg glucose IP, 50mg/kg PLP+rodent milk once/24h, 50mg/kg PLP+rodent milk once/12h, 50mg/kg PLP+rodent milk once/4h

Pharmacologically induced seizures in PNPO mutant mice reveals increased seizure susceptibility

Since we observed severe spontaneous seizures in D33V/D33V mice, it was necessary to examine whether the mutant mice without spontaneous seizures (D33V/+, R116Q/+, and R116Q/R116Q) had altered seizure susceptibility compared to wild-type controls. To examine this, we measured the latency to seizures and loss of postural control in mutant mice and controls following administration of $GABA_A$ receptor antagonists: 2mL/min flurothyl[80] and 50mg/kg pentylenetetrazole (PTZ)[7,119]. Shortened latency to convulsions and loss of postural control compared to wild-type animals would indicate a higher susceptibility to seizure development. Utilization of flurothyl vapor to induce seizures allows for 1) avoidance of intraperitoneal injection to reduce stressors and movement artifacts during *in-vivo* recording; 2) rapid elimination of flurothyl from the body through the lungs, removing confounds for residual chemoconvulsant presence in the mice; and 3) high temporal control of seizure onset and cessation of seizures with exposure to room air[80,118]. Acute, severe seizures can also be induced through intraperitoneal injection of PTZ at a high dose[81]. Rapid recovery and sensitivity to anti-epilepsy drugs[71,81] make the PTZ-induced seizure induction method ideal for investigating the efficacy of current anti-epilepsy drugs in our *PNPO* mutant mice.

Upon exposure to flurothyl, D33V/+ mice exhibited 33.4% decreased generalized seizure threshold (GST) compared to wild type controls, suggesting increased susceptibility to seizures. Meanwhile, R116Q/+ and R116Q/R116Q mice also exhibited 20.4% and 48.2% decreased GST compared to wild type controls, respectively. Together, these results indicate that D33V/+, R116Q/+, and R116Q/R116Q mutant mice all have increased susceptibility to generalized seizures, even though they do not exhibit spontaneous seizures.

These results were also consistent in the PTZ-induced seizure model, where D33V/+ mice exhibited 28.8% decreased GST compared to wild type controls, while R116Q/+ and R116Q/R116Q mice exhibited 9.9% and 23.4% decreased GST compared to wild type controls, respectively. Together, these data suggest that both the D33V and R116Q point mutations in mice significantly decrease latency to seizure induction upon $GABA_A$ receptor blocker chemoconvulsive flurothyl inhalant or PTZ injection administration. The increased propensity for seizure activity in these mice compared to wild type make them a promising model for investigating molecular and genetic mechanisms underlying epilepsy in human patients.

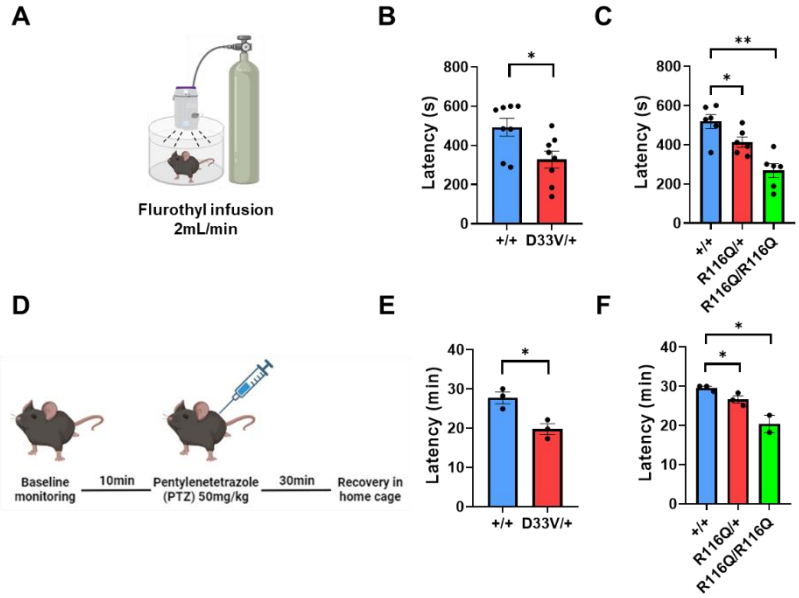

Fig 6: Seizure induction with chemoconvulsants flurothyl and pentylenetetrazole reveals reduced seizure thresholds in *PNPO* mutant mice
a) Schematic of flurothyl infusion chamber, 2mL/min flurothyl was infused into the chamber using oxygen tank.
b) Latency to seizure and loss of postural control following flurothyl infusion in wild type (blue) and D33V/+ (red) mice. Error bars correspond to standard error of the mean (SEM). *p = .0206. s = seconds.
c) Latency to seizure and loss of postural control following flurothyl infusion in wild type (blue), R116Q/+ (red), and R116Q/R116Q (green) mice. Error bars correspond to standard error of the mean (SEM). *p = .0374. **p < .001. s = seconds.
d) Schematic of pentylenetetrazole (PTZ) 50mg/kg IP injection.
e) Latency to seizure and loss of postural control following PTZ inejction in wild type (blue) and D33V/+ (red) mice. Error bars correspond to standard error of the mean (SEM). *p = .0027. s = seconds.
f) Latency to seizure and loss of postural control following PTZ injection in wild type (blue), R116Q/+ (red), and R116Q/R116Q (green) mice. Error bars correspond to standard error of the mean (SEM). *p < .05. s = seconds.

PNPO mutant mice exhibit hyperactivity

Due to the lack of visible spontaneous seizures in mice carrying the mild R116Q mutation and in order to confirm that our mice recapitulated hyperactive behavioral symptoms present in human epilepsy patients, we investigated D33V and R116Q mutant mice locomotor activity using the open field assay. Freely moving mice were continuously tracked for 2h using infrared sensors along the bottom of an arena. Total distance traveled, average travel velocity, and frequency of movement were measured to assess mouse activity. D33V/+ mice exhibited markedly increased activity over 2h compared to wild-type controls due to increased average travel velocity and frequency of movement, suggesting a strong locomotive hyperactivity phenotype. In comparison, R116Q/+ and R116Q/R116Q mice did not exhibit significantly increased total movement, average velocity, or frequency of movement compared to controls.

Surprisingly, a heterozygote carrier of the more severe loss-of-function D33V point mutation displayed heightened hyperactivity compared to wild type controls, whereas the mild loss-of-function R116Q mutation did not result in increased locomotor activity compared to controls. Together, these data suggest mice carrying the *PNPO* D33V point mutation exhibit heightened baseline locomotor activity compared to controls, mirroring that of human epilepsy patients.

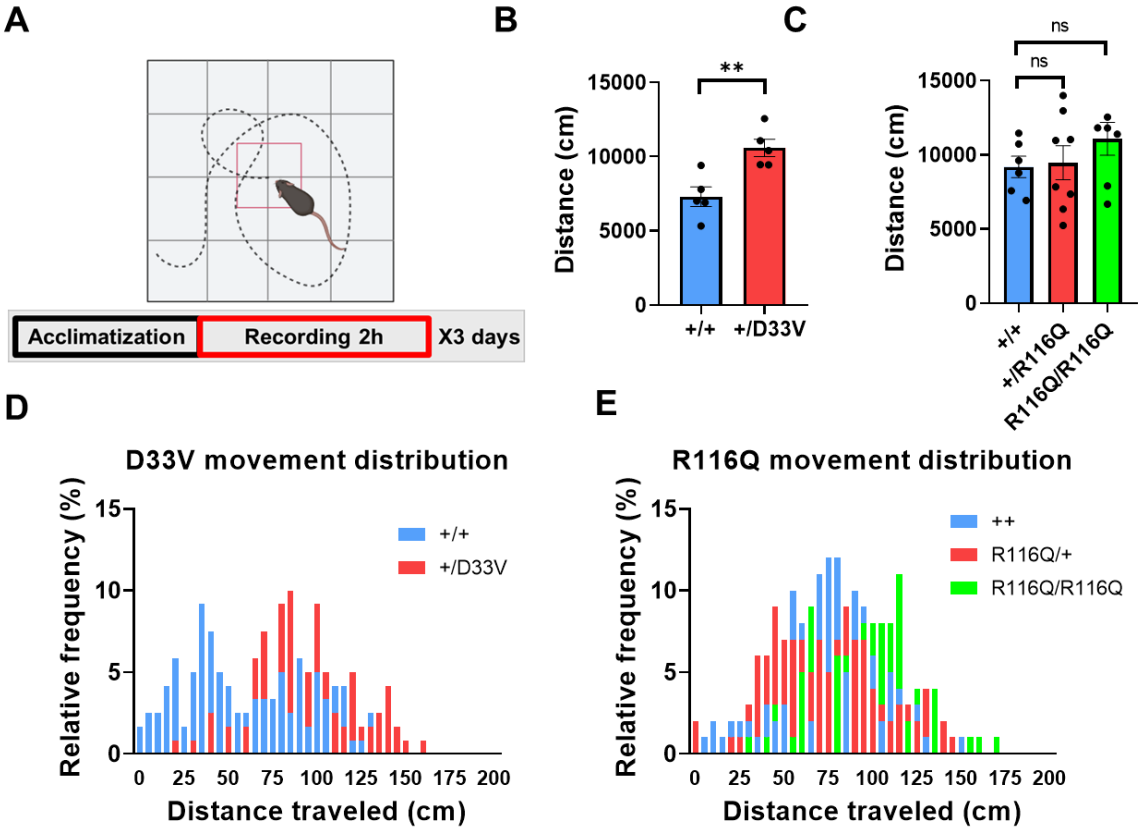

Fig 7: Open field locomotor assay reveals hyperactive phenotypes in *PNPO* mutant mice
a) Schematic of open field locomotor assay experimental paradigm. Dotted line represents mouse path, and solid lines represent infrared sensor beams across the bottom of the open field. Infrared sensor beams are not drawn to scale.
b) Total distance travelled during 2h open field locomotor assay by wild type (blue) and D33V/+ (red) mice. Error bars correspond to standard error of the mean (SEM). **p = .0057. cm = centimeters.
c) Total distance travelled during 2h open field locomotor assay by wild type (blue), R116Q/+ (red), and R116Q/R116Q (green) mice. Error bars correspond to standard error of the mean (SEM). ns = not significant. cm = centimeters.

d) Frequency distribution of distance travelled within 5min bins during 2h open field locomotor assay by wild type (blue) and D33V/+ (red) mice. cm = centimeters.
e) Frequency distribution of distance travelled within 5min bins during 2h open field locomotor assay by wild type (blue), R116Q/+ (red), and R116Q/R116Q (green) mice. cm = centimeters.

D33V and R116Q mutant mice exhibit spatial learning and memory deficit

Due to previous reports of spatial memory and learning deficits in neonatal epilepsy patients[40,122] and high expression of *PNPO* in the hippocampal, thalamic, and cortical regions of the human brain, we used a Morris water maze assay to investigate *PNPO* mutant mice spatial learning and memory. Mice were trained over 5 days to find a submerged underwater platform in the northeast quadrant of a water-filled tub using spatial cues outside of the arena, before the platform was removed during the probe test and mice were able to freely swim. Average swim velocity and time to platform were measured on training days to assess spatial learning and memory, whereas average swim velocity and time spent in the northeast platform quadrant of the water maze were measured on the probe test to assess spatial memory recall. Afterward, the submerged underwater platform was reintroduced into the opposite southwest quadrant of the water maze, and the same training regimen and probe test were repeated to assess spatial relearning and problem solving.

D33V/+ mice exhibited significant spatial learning and memory deficits during acquisition of the first underwater platform location, as evidenced by increased latency to finding the underwater platform during training days and decreased time spent in the correct northeast quadrant during the probe trial compared to wild type controls. However, D33V/+ did not exhibit significant spatial learning and memory deficits compared to controls during the relearning task, after the underwater platform was moved to the southwest quadrant and the mice were required to relearn the new location. The wild type controls performed similarly during both learning and relearning tasks, suggesting the D33V/+ mutant mice deficit occurs specifically during the initial learning

phase and not the relearning phase. R116Q/R116Q mice, on the other hand, do not exhibit learning and memory deficits during the initial learning task compared to wild type controls. Interestingly, R116Q/R116Q mice instead display significantly impaired learning during the relearning task through increased latency to find the new location of the underwater platform and decreased time spent in the correct quadrant.

Together, these results suggest that D33V and R116Q mutant mice display spatial learning deficits compared to wild type controls. Previously, severity of hyperactivity and seizure susceptibility phenotypes could be correlated with mutation severity in the D33V and R116Q mutants. However, these unique spatial learning and memory deficits are not consistent with that trend, suggesting potential neomorphic effects of the D33V and R116Q *PNPO* mutations.

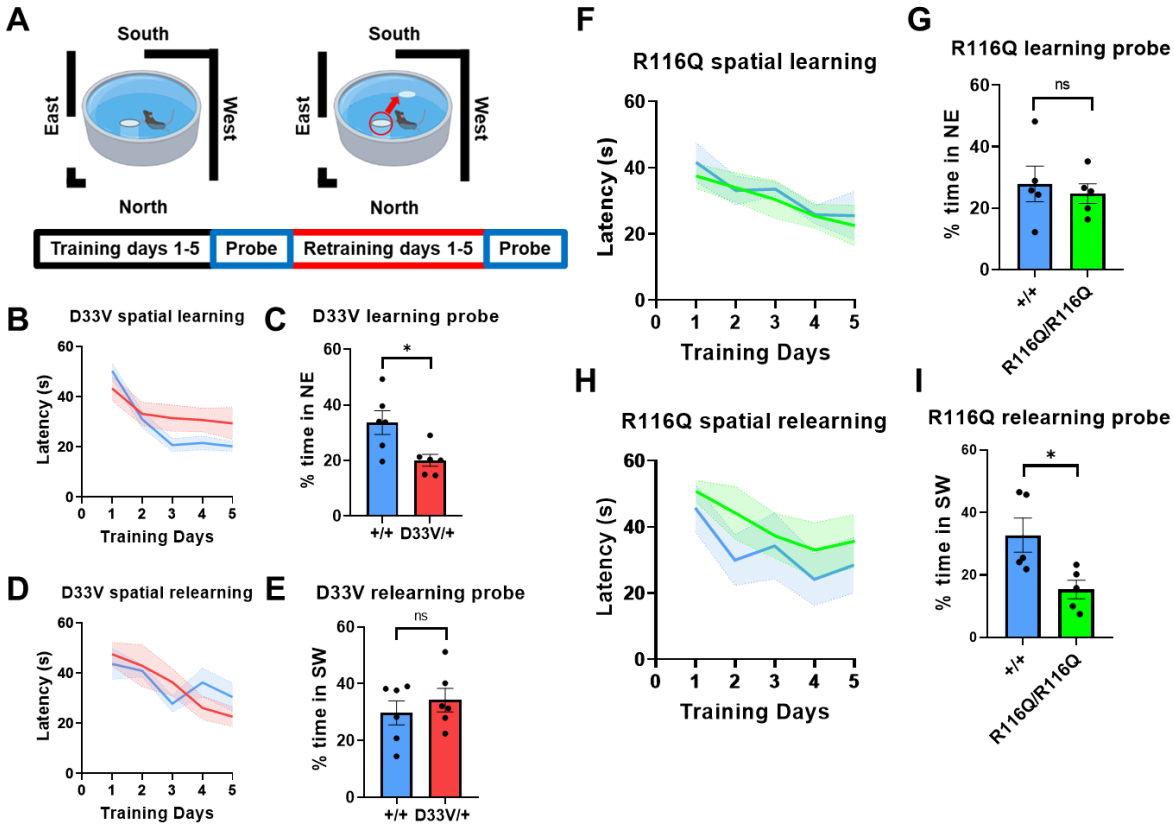

Fig 8: Morris water maze reveals *PNPO* mutant mice deficits in spatial learning and memory
a) Schematic of water maze training paradigms and probe trials. Each training day consisted of 4, 60s trials. During retraining, the underwater platform (denoted by white oval) was moved from the northeast to the southwest quadrant. Black curtains (denoted by solid black lines) provided spatial cues for underwater platform location.
b) Average latency to finding underwater platform by wild type (blue) and D33V/+ (red) mice. Standard error of the mean (SEM) is denoted in shaded regions of corresponding colors. s = seconds.
c) Average time spent in quadrant previously containing underwater platform during probe trial by wild type (blue) and D33V/+ (red) mice. Error bars correspond to standard error of the mean (SEM). *p = .0174.
d) Average latency to finding underwater platform during retraining phase by wild type (blue) and D33V/+ (red) mice. Standard error of the mean (SEM) is denoted in shaded regions of corresponding colors. s = seconds.
e) Average time spent in quadrant previously containing underwater platform following retraining phase by wild type (blue) and D33V/+ (red) mice. Error bars correspond to standard error of the mean (SEM). ns = not significant.
f) Average latency to finding underwater platform by wild type (blue) and R116Q/R116Q (green) mice. Standard error of the mean (SEM) is denoted in shaded regions of corresponding colors. s = seconds.
g) Average time spent in quadrant previously containing underwater platform during probe trial by wild type (blue) and R116Q/R116Q (green) mice. Error bars correspond to standard error of the mean (SEM). ns = not significant.
h) Average latency to finding underwater platform during retraining phase by wild type (blue) and R116Q/R116Q (green) mice. Standard error of the mean (SEM) is denoted in shaded regions of corresponding colors. s = seconds.
i) Average time spent in quadrant previously containing underwater platform following retraining phase by wild type (blue) and R116Q/R116Q (green) mice. Error bars correspond to standard error of the mean (SEM). *p = .0238.

Investigating changes in PNPO protein expression and localization in mutant mice

Our group previously generated a *Drosophila* model carrying the human *PNPO* D33V and R116Q point mutations[123] (h^{D33V} and h^{R116Q}, respectively) and found decreased protein expression in h^{D33V} mutants but altered protein localization in h^{R116Q} mutants[115]. Since these changes have not been reported in human patients but may have significant consequences on overall PNPO enzymatic activity and function, we investigated the D33V and R116Q mouse models for potential alterations in protein expression and localization. Although PNPO protein is

expressed with low region specificity in both human and mouse brains, we examined regions with relatively increased *PNPO* expression and with relation to the behavioral assays we performed. We used Western blot to quantify PNPO protein expression in the cortex, hippocampus, and thalamus in D33V/+, D33V/D33V, R116Q/+, and R116Q/R116Q mice compared to wild type littermate controls. Due to limitations on survival in D33V homozygote animals with spontaneous seizures, all tissues were collected from littermates before P30. Surprisingly, we found mutation severity- and homozygosity- dependent loss of PNPO protein expression across all brain regions examined compared to tubulin housekeeping gene. In the somatosensory cortex, quantification of PNPO expression via densitometric analysis revealed the severe loss-of-function D33V/+ and D33V/D33V mutant mice exhibited 43.8% and 96.9% decreased PNPO protein expression compared to wild type controls, respectively. Meanwhile, the mild loss-of-function R116Q/+ and R116Q/R116Q mutant mice exhibited 23.6% and 61.4% decreased PNPO expression compared to wild type controls, respectively. The baseline *PNPO* expression and genomic *PNPO* sequence between the D33V and R116Q littermate wild type mice were not significantly different, allowing for between-genotype comparisons. These protein expression-level alterations were also consistent in the hippocampus and thalamus of mutant mice.

This novel finding of the D33V and R116Q point mutations causing decreased protein expression could compound with the known PNPO mutation-mediated decreased enzymatic activity[32] to drastically decrease endogenous PLP production. The extremely low endogenous PNPO protein expression in D33V/D33V mice could provide a possible explanation for the increased seizure severity and mortality compared to human patients. These mutation- and homozygosity- dependent losses of PNPO protein expression mirrored the hyperactive and

increased seizure susceptibility phenotypes observed earlier, offering a potential mechanistic explanation for the observed behavioral alterations in mutant mice.

Following our discovery of mutation-dependent decrease in protein expression, we aimed to investigate whether the D33V and R116Q point mutations could also affect protein localization. Using immunohistochemistry, we examined PNPO protein localization in D33V and R116Q mutant mice coronal somatosensory barrel cortical, hippocampal CA1, CA2, and CA3, and medial thalamic sections compared to littermate wild type controls. D33V/+ and D33V/D33V mutant mice displayed no changes in protein localization compared to controls. Interestingly, R116Q/R116Q mutant mice displayed significantly increased PNPO protein fluorescence in non-somatic regions compared to wild type controls.

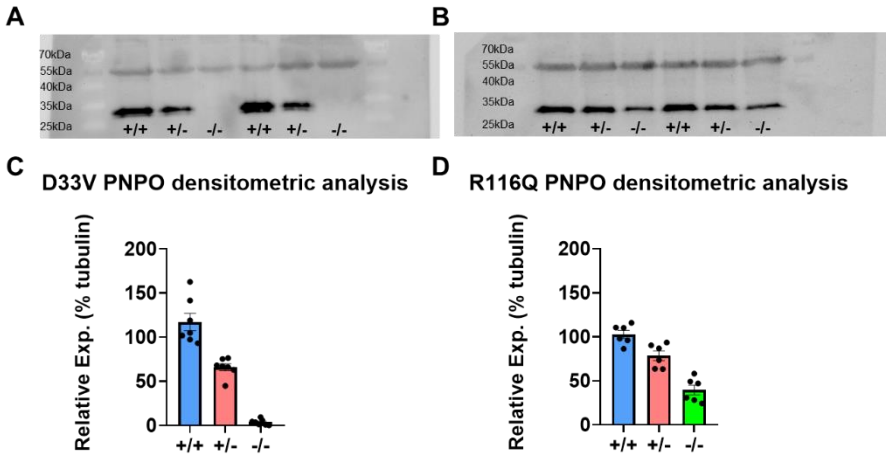

Fig 9: Western blot immunoblotting reveals decreased PNPO protein expression in *PNPO* mutant mice
a) Representative immunoblot containing wild type (+/+), D33V/+ (+/-), and D33V/D33V (-/-) homogenized cortical tissue. Tubulin molecular weight (MW) ~50kDa, PNPO MW ~30kDa.
b) Quantification of average densitometric values of PNPO expression from wild type (blue), D33V/+ (red), and D33V/D33V (green) mice. Error bars correspond to standard error of the mean (SEM).
c) Representative immunoblot containing wild type (+/+), R116Q/+ (+/-), and R116Q/R116Q (-/-) homogenized cortical tissue. Tubulin molecular weight (MW) ~50kDa, PNPO MW ~30kDa.
d) Quantification of average densitometric values of PNPO expression from wild type (blue), R116Q/+ (red), and R116Q/R116Q (green) mice. Error bars correspond to standard error of the mean (SEM).

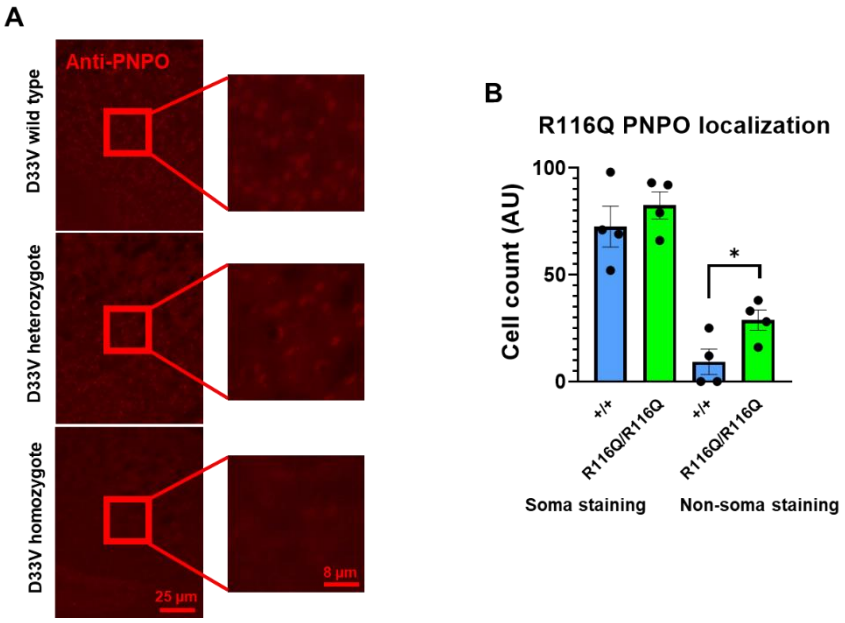

Fig 10: Immunohistochemistry reveals deceased PNPO protein expression in D33V mutant mice and altered PNPO localization in R116Q/R116Q mice
a) Representative immunostaining from somatosensory barrel cortex layer V for PNPO protein (red) from wild type (top), heterozygote (middle), and homozygote (bottom) D33V mutant mice. Red square denotes magnified panels on the right side.
b) Quantification of PNPO localization in either soma or non-somatic subcellular localized regions in wild type (blue) and R116Q/R116Q (green) mice.

Transcriptional changes suggest additional downstream consequences of PNPO mutation

To ascertain whether our finding of decreased PNPO protein expression arose from changes in mRNA transcriptional activity, we performed RT-PCR using somatosensory barrel cortex tissue from D33V and R116Q mutant mice. D33V/+ mice exhibited 44.4% decreased PNPO mRNA transcription compared to wild type littermates, almost exactly mirroring the 43.8% reduced PNPO protein expression observed in Western blots. Meanwhile, R116Q/+ and R116Q/R116Q mice exhibited very small decreases in PNPO mRNA transcription (1.5% and 5.3% respectively). These results suggest that although the decreased PNPO protein content in D33V mutant mice likely arose from deficiencies in DNA transcription as well as protein expression, the decreased

PNPO protein content in R116Q mutant mice arose predominantly from deficiencies in protein expression.

Glutamate decarboxylase GAD1 and GAD2 are two PLP-dependent enzymes important for GABA production in mice and homologous with human GAD67 and GAD65, respectively. GAD1 is constitutively active and saturated with PLP, whereas GAD2 is predominantly expressed at axon terminals and transiently binds PLP following phosphorylation[124]. To further investigate molecular adaptations resulting from decreased PNPO activity and PLP production in the brain, we examined GAD1 and GAD2 mRNA expression in D33V and R116Q mutant mice. RT-PCR quantification revealed that D33V/+ cortical tissue exhibited no changes in GAD1 and GAD2 mRNA expression, but R116Q/+ and R116Q/R116Q cortical tissue revealed decreased GAD1 and GAD2 mRNA expression. Given the mis-localization of R116Q PNPO protein toward non-somatic, axonal cellular regions and the abundance of PLP this could create in axon terminals, it could be possible that the PLP-activated GAD1 and GAD2 enzymes are downregulated through feedback inhibition mechanisms.

Historically tightly regulated enzymes, GAD1 and GAD2 expression changes were highly unexpected and further demonstrated how D33V and R116Q variant *PNPO* mutations may contribute to epilepsy and behavioral phenotypes through additional mechanisms other than decreased enzymatic activity.

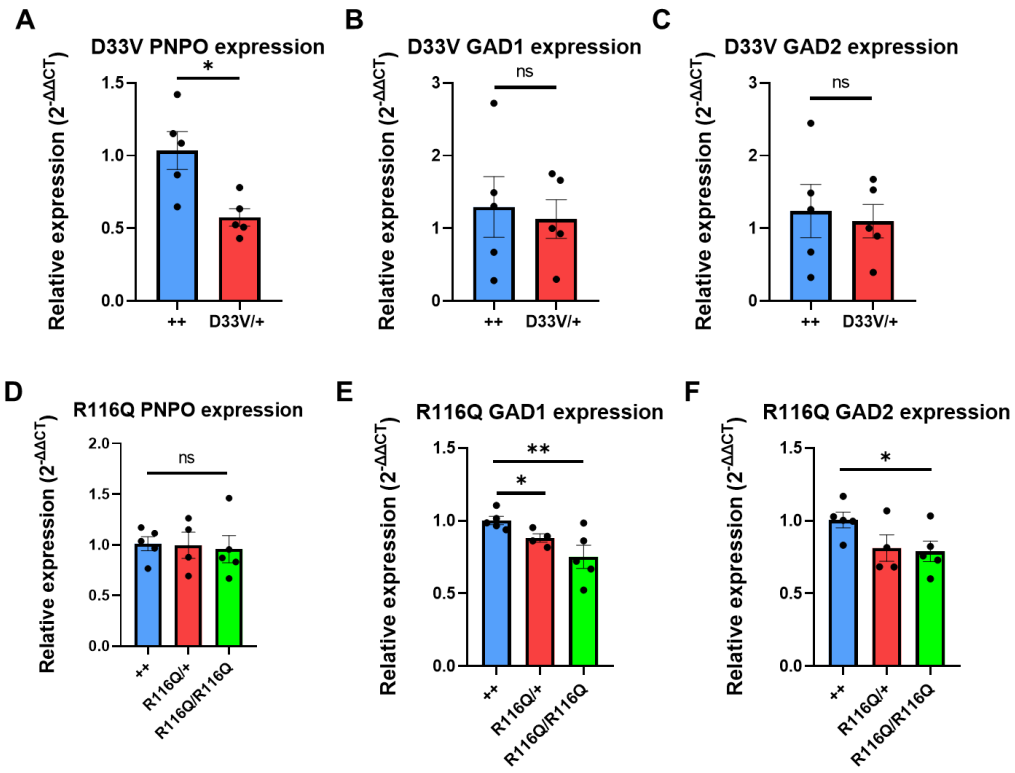

Fig 11: *PNPO* mutant mice exhibit altered *PNPO* and *GAD* transcription
a) Quantification of PNPO mRNA in cortical tissues taken from wild type (blue) and D33V/+ (red) mice. Relative expression is measured as $2^{-\Delta\Delta CT}$ normalized to internal ribosomal 18s. Error bars correspond to standard error of the mean (SEM). *p = .0129.
b) Quantification of GAD1 mRNA in cortical tissues taken from wild type (blue) and D33V/+ (red) mice. Relative expression is measured as $2^{-\Delta\Delta CT}$ normalized to internal ribosomal 18s. Error bars correspond to standard error of the mean (SEM). ns = not significant.
c) Quantification of GAD2 mRNA in cortical tissues taken from wild type (blue) and D33V/+ (red) mice. Relative expression is measured as $2^{-\Delta\Delta CT}$ normalized to internal ribosomal 18s. Error bars correspond to standard error of the mean (SEM). ns = not significant.
d) Quantification of PNPO mRNA in cortical tissues taken from wild type (blue), R116Q/+ (blue), and R116Q/R116Q (green) mice. Relative expression is measured as $2^{-\Delta\Delta CT}$ normalized to internal ribosomal 18s. Error bars correspond to standard error of the mean (SEM). ns = not significant.
e) Quantification of GAD1 mRNA in cortical tissues taken from wild type (blue), R116Q/+ (blue), and R116Q/R116Q (green) mice. Relative expression is measured as $2^{-\Delta\Delta CT}$ normalized to internal ribosomal 18s. Error bars correspond to standard error of the mean (SEM). *p = .0226. **p = .0183.
f) Quantification of GAD2 mRNA in cortical tissues taken from wild type (blue), R116Q/+ (blue), and R116Q/R116Q (green) mice. Relative expression is measured as $2^{-\Delta\Delta CT}$ normalized to internal ribosomal 18s. Error bars correspond to standard error of the mean (SEM). *p = .0406.

In-vivo electroencephalogram (EEG) recordings reveal altered baseline activity in PNPO mutant mice

The increased susceptibility to convulsions and underlying behavioral deficits despite lack of spontaneous seizures make the D33V and R116Q *PNPO* mutant mice a fascinating model to study epilepsy pathogenesis. Electroencephalogram (EEG) recordings from bilateral somatosensory barrel cortex in D33V/+ mutant mice and wild type controls allowed for quantification of baseline cortical activity during baseline and ictal activity. Simultaneous video recordings were used to visually confirm presence of seizures detected using EEG. Baseline recordings were collected from all mice on days 1-3 before flurothyl was used to induce seizures once per day on days 4-7. Seizure induction was terminated upon loss of postural control in mice and post-ictal recordings were taken for 1h following seizure cessation. Continual EEG-video monitoring was performed during both night-time and day-time hours to ascertain circadian rhythm effect on recordings. 150mg/kg PLP was supplemented in mouse drinking water during days 8-14. Baseline recordings were collected on days 8-10, and flurothyl was used to induce seizures once per day on days 11-14.

Averaged power spectral density (PSD) generated from fast Fourier transforms (FFT) comparing 50 randomly sampled D33V/+ and wild type EEG baseline traces during pre-seizure periods (days 1-4 and 8-11) reveal significant differences in baseline activity. Further analysis of individual EEG frequency bands reveals D33V/+ mutant mice display 158.85% increased theta frequency power during baseline activity compared to wild type controls. However, upon supplemented drinking water with PLP, this increased theta frequency in D33V/+ mice decreases by 44.44%. Interestingly, the theta frequency power between wild type mice and D33V/+ mutant mice on PLP water is not significantly different, suggesting that PLP supplementation to rescue

the PNPO deficiency phenotype in D33V/+ mice results in rescue of underlying neural circuitry oscillatory alterations. Recent clinical findings have suggested increased power of theta frequency in human epilepsy patients are correlated with increased susceptibility for epileptogenesis[83,125]. Therefore, we may conclude that decreased theta frequency power found in PLP supplemented D33V/+ mice may be correlated with rescue of seizure phenotype.

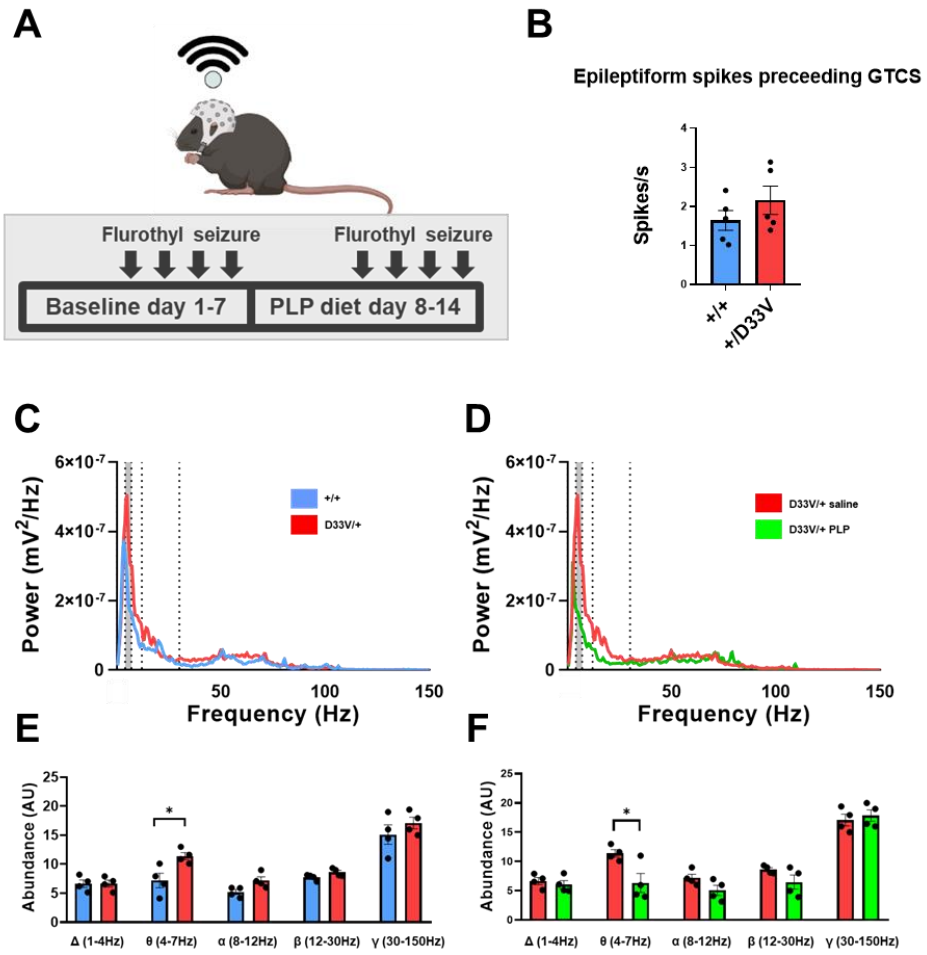

Fig 12: Electroencephalogram (EEG) recordings reveal baseline frequency abnormalities in D33V/+ mutant mice which can be rescued with dietary PLP supplementation
a) Schematic of video-iEEG recording paradigm. Baseline recordings were taken days 1-3, and flurothyl seizures were induced once a day during days 4-7. Mice were fed 150mg/kg PLP in water each day during days 8-14, and flurothyl seizures were induced once a day during days 11-14.

b) Quantification of the number of epileptiform spiking activity observed in wild type (blue) and D33V/+ (red) mice prior to complete loss of postural control and continuous convulsions as determined by simultaneous video recording. Error bars correspond to standard error of the mean (SEM).
c) Representative power spectral density plot from 50 randomly selected 10 second baseline recordings from a wild type (blue) and D33V/+ (red) mouse. Dotted lines correspond to EEG Berger bands (γ = 30-150Hz, β = 12-30Hz, α = 8-12Hz, θ = 4-7Hz, Δ = 1-4Hz), and the shaded band corresponds to θ frequencies. Hz = hertz.
d) Representative power spectral density from 50 randomly selected 10 second baseline recordings from a D33V/+ (red) and D33V/+ fed PLP-supplemented water (green) mouse. Dotted lines correspond to EEG Berger bands (γ = 30-150Hz, β = 12-30Hz, α = 8-12Hz, θ = 4-7Hz, Δ = 1-4Hz), and the shaded band corresponds to θ frequencies. Hz = hertz.
e) Quantification of area under curve of EEG Berger bands (γ = 30-150Hz, β = 12-30Hz, α = 8-12Hz, θ = 4-7Hz, Δ = 1-4Hz) from wild type (blue) and D33V/+ (red) mice. Each data point represents 50 randomly selected 10 second baseline recordings from 1 animal. Error bars correspond to standard error of the mean (SEM). *p = .0234.
e) Quantification of area under curve of EEG Berger bands (γ = 30-150Hz, β = 12-30Hz, α = 8-12Hz, θ = 4-7Hz, Δ = 1-4Hz) from D33V/+ (red) and D33V/+ fed PLP-supplemented water (green) mice. Each data point represents 50 randomly selected 10 second baseline recordings from 1 animal. Error bars correspond to standard error of the mean (SEM). *p = .0260.

Increased seizure susceptibility in PNPO mutant mice may be influenced by failure of local inhibition

We further investigated the possibility of weakened local inhibitory restraint contributing to seizure propagation using *in-vivo* video-EEG recordings from control and mutant D33V/+ mice. Implanting the EEG electrodes into ipsilateral frontal and occipital lobes to the somatosensory temporal lobe containing the recording electrode, we observed a time lag in ictal activity propagation due to the spatial distance between each region the EEG electrodes recorded from. Interestingly, the time lag of ictal propagation between somatosensory cortex to both frontal and occipital lobes in the D33V/+ mutant mice were significantly shorter compared to wild type controls, suggesting a weakening of local feedforward inhibition required to maintain control of excitatory activity. This shortened time lag was significantly rescued by PLP supplementation in drinking water, providing a potential explanation for the decreased seizure susceptibility

conferred by PLP to D33V/D33V mutant mice, and suggesting PLP supplementation strengthens feedforward inhibitory control of excitation in the cortex.

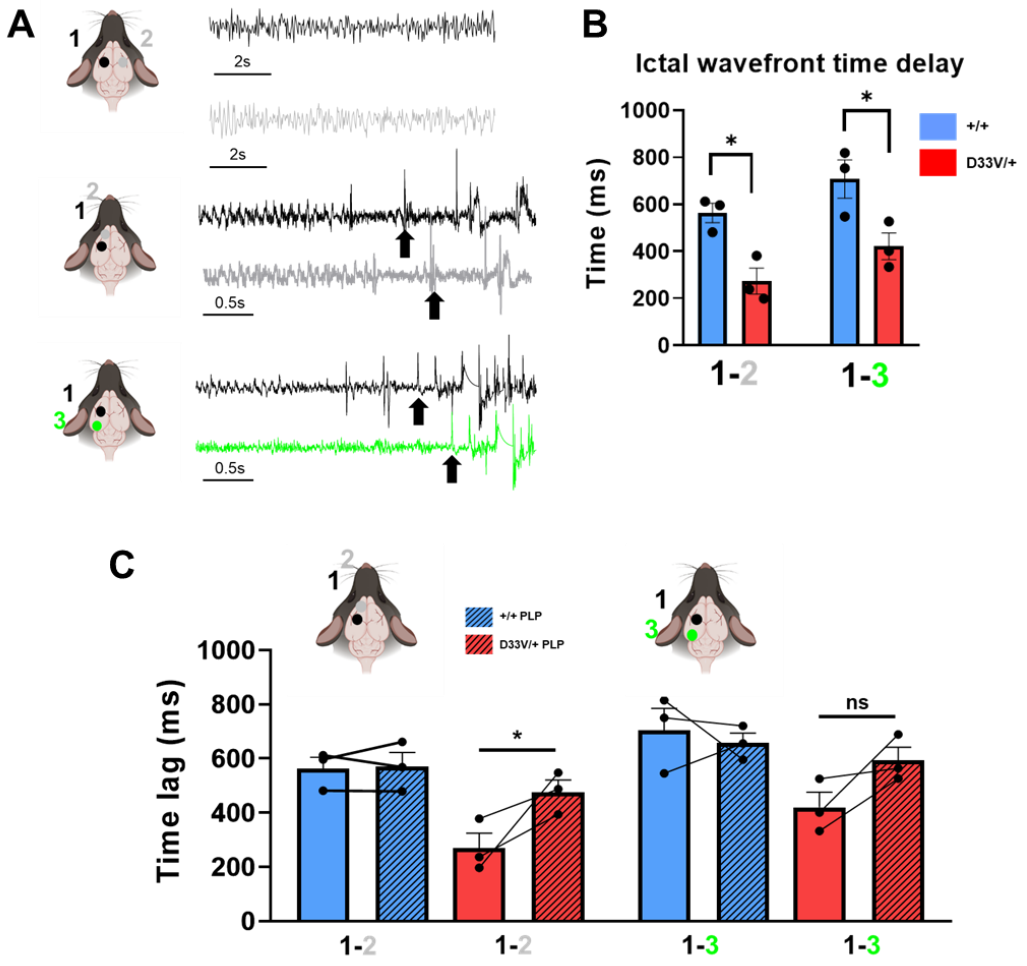

Fig 13: Increased speed of ictal propagation in D33V/+ mice suggest weakened inhibitory control which can be rescued via dietary PLP supplementation
a) Schematic with representative traces following placement of EEG intracranial electrodes at bilateral somatosensory barrel cortex (top, 1), somatosensory cortex and frontal lobe (middle, 2), and somatosensory cortex and occipital lobe locations (bottom, 3). Simultaneous recordings were taken from 1,1; 1,2; and 1,3, and the onset of ictal activity are denoted by black arrows. Severe seizures and loss of postural control are confirmed via simultaneous video capture.
b) Time delay between arrival of ictal wavefront from somatosensory cortex (position 1) to frontal lobe (position 2) are measured (left). Time delay between arrival of ictal wavefront from somatosensory cortex (position 1) to occipital lobe (position 3) are measured (right). Wild type mice are represented by the blue bars, and D33V/+ mice are represented by the red bars. Error bars correspond to standard error of the mean (SEM). *p < .05. ms = milliseconds.

c) Time delay between arrival of ictal wavefront from somatosensory cortex (position 1) to frontal lobe (position 2) before and after 150mg/kg PLP supplementation (hatched bars) are shown. Individual animals connected with lines denote time delay of propagation before and after PLP treatment. Cartoon schematics denote the location of EEG probe placement for measuring time delay between positions 1,2 and positions 1,3. Error bars correspond to standard error of the mean (SEM). *p < .05. ns = not significant.

PNPO mutant mice exhibit decreased maximal GABA release and weakened GABA fluorescent transients prior to seizures compared to controls

Although it is well-known that seizures can arise when GABA-mediated inhibition is unbalanced from glutamate-mediated excitation[3,54,67,122,126], how seizures begin and how seizures may spread remain poorly understood[3,65]. Therefore, animal models offering insight into seizure mechanisms such as PNPO-deficient mutant mice could greatly improve our understanding of ictal activity and aid in treatment development. To examine GABA neurotransmitter content preceding, during, and following ictal activity *in-vivo*, we used a virally expressed extracellular fluorescent biosensor iGABASnFR to measure GABA release in D33V/+ and controls during baseline and seizure activity. Fiber photometry recordings in the CA1 region of the hippocampus allowed for quantification of fluorescent activity following intraperitoneal injection of tiagabine, a selective inhibitor of GABA transporter (GAT-1) in the cortex and hippocampus[127]. Roughly 4000s after tiagabine administration, fluorescent signal from GABA content in the extracellular CA1 hippocampal space reached a maximum and slowly decreased back to baseline signal amplitude over several hours. The mean baseline between D33V/+ and wild type controls was not significantly different, but D33V/+ mice exhibited 42.8% decreased maximal GABA fluorescent signal compared to wild type controls after tiagabine administration. Since the maximal GABA fluorescent transients did not change in the following 2000s, it is likely that the decreased

maximal GABA fluorescence observed in D33V/+ mice was mediated by decreased GABA neurotransmitter release rather than decreased speed of release.

The mammalian cortex receives glutamatergic projections to sensory-receptive zones in Layer IV from the thalamus[52], and intracortical circuits amplifying and processing signals from superficial to deep cortical layers are mostly excitatory and recurrently connected[53]. Incoming excitatory sensory inputs also excite interneurons in Layer IV, causing feedforward inhibition[56] which normally controls the feedforward excitation recruitment of surrounding neurons[55,67]. This feedforward inhibition is also largely responsible for the 'surround inhibition[128]' originally believed to control the feedforward excitation of intracortical circuits. Similar feedforward inhibition mechanisms have been proposed in the hippocampal dentate gyrus[129], where parvalbumin-expressing interneurons target subsets of CA1 pyramidal neurons within their axonal arbor, leading to regional-specific suppression of excitatory pyramidal neuron outputs[60]. Epileptic seizures can occur when feedforward inhibition fails, although the mechanisms of failure are not yet well understood.

To examine feedforward mechanisms underlying seizure generation, we used flurothyl to induce seizures in D33V/+ mutant mice and controls while measuring GABA release in the CA1 region using iGABASnFR fluorescent transients. Interestingly, we observed a progressive decrease in interictal spike and sentinel spike frequency and amplitude directly preceding loss of postural control and onset of general tonic-clonic seizure, suggesting a progressive weakening and subsequent collapse of inhibitory restraint preceding spread of ictal activity. The progressive decrease in spike activity prior to loss of postural control was more pronounced in D33V/+ mutant mice than control mice, suggesting that D33V/+ mutants decreased GABA

neurotransmitter release could contribute to weakened inhibitory control of ictal activity upon seizure generation, ultimately leading to increased seizure susceptibility.

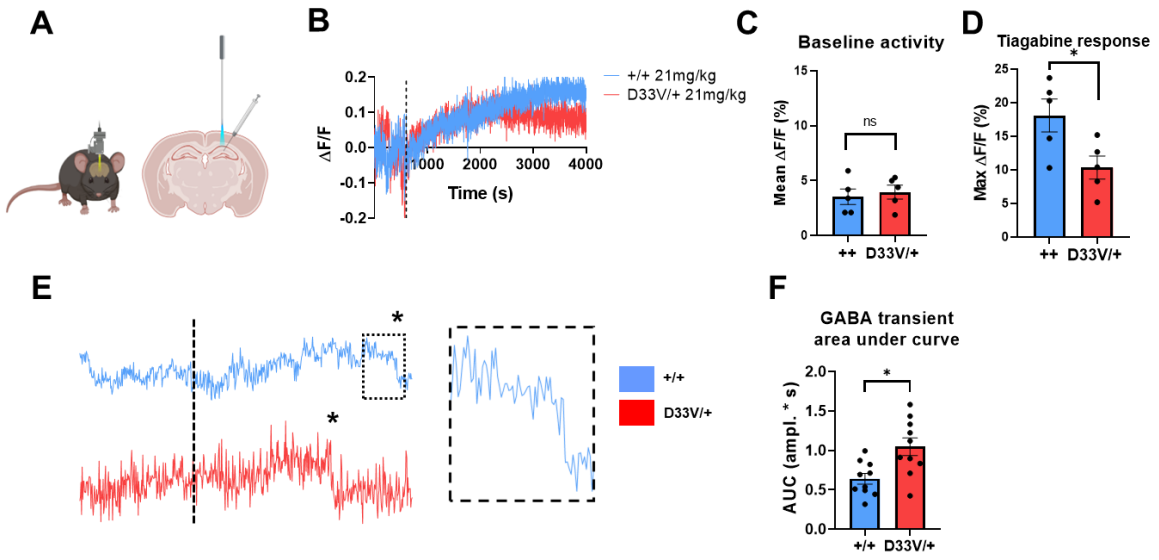

Fig 14: I*n-vivo* detection of GABA transients using a virally-expressed extracellular sensor reveals decreased maximal GABA release in *PNPO* mutant mice and progressive loss of inhibition preceding seizures

a) Schematic of injection of AAV-hSyn-iGABASnFR into CA1 region of hippocampus followed by emplacement of fiber optic to record fluorescent transients indicating GABA release.

b) Representative trace of increase in extracellular GABA following pharmacological blockade of GABA reuptake transporter (GAT1) using 21mg/kg tiagabine from a wild type (blue) and D33V/+ (red) mouse. s = seconds. F = fluorescence.

c) Quantification of mean fluorescence change over 1h baseline activity from wild type (blue) and D33V/+ (red) mice. Error bars correspond to standard error of the mean (SEM). ns = not significant. F = fluorescence.

d) Quantification of maximal fluorescence increase following 21mg/kg tiagabine injection in wild type (blue) and D33V/+ (red) mice. Error bars correspond to standard error of the mean (SEM). *p = .0324. F = fluorescence.

e) Representative traces of GABA fluorescent transients (left) following flurothyl chemoconvulsant administration (dotted line) in wild type (blue) and D33V/+ (red) mice. Star denotes start of seizure as confirmed with simultaneous video capture, and dotted square represents magnified image (right).

f) Quantification of area under curve 100 seconds prior to start of severe convulsions and loss of postural control following flurothyl seizure induction in wild type (blue) and D33V/+ (red) mice. Error bars correspond to standard error of the mean (SEM). *p = .0061. AUC = area under curve. ampl. = amplitude. s = seconds.

PNPO mutant mice exhibit decreased presynaptic GABA neurotransmitter release

To probe neuronal mechanisms underlying loss of inhibitory control, we recorded spontaneous inhibitory postsynaptic potentials (mIPSPs) in pyramidal cells following bath application of 50µM D-AP5 and 10µM CNQX. Comparison of mIPSP frequency and amplitude between D33V/+ and control slices would reveal contribution of pre- and post-synaptic changes in GABAergic neurotransmission. We observed a specific significant decrease in mIPSP frequency, but not amplitude nor signal decay time, in D33V/+ mutant mice compared to controls. These data suggest that D33V/+ mutant mice exhibit decreased presynaptic GABA release, possibly through deficits in GABA production due to endogenous decreased PNPO enzymatic activity. Consistent with our previous data, decreased presynaptic GABA release could contribute to the weakened inhibition contributing to failure of restraint and increased speed of ictal propagation in D33V/+ mutant ice.

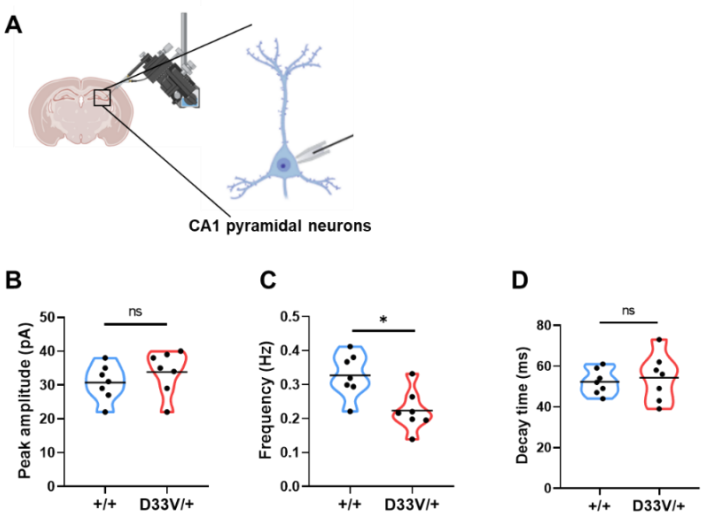

Fig 15: Weakened GABAergic signaling in *PNPO* mutant mice is due to failure of presynaptic GABA neurotransmitter release
a) Schematic of whole-cell patch clamp on pyramidal neurons in the CA1 region of a coronal slice preparation.
b) Quantification of mIPSP peak amplitudes in wild type (blue) and D33V/+ (red) mice. Each individual dot represents 1 neuron. Black lines denote group average. pA = picoamperes. ns = not significant.

c) Quantification of mIPSP frequency in wild type (blue) and D33V/+ (red) mice. Each individual dot represents 1 neuron. Black lines denote group average. Hz = Hertz. *p = .009. d) Quantification of mIPSP decay time from peak in wild type (blue) and D33V/+ (red) mice. Each individual dot represents 1 neuron. Black lines denote group average. ms = millisecond. ns = not significant.

Discussion

The present study characterizes a novel genetic mouse model for understanding epileptic seizures and GABAergic signaling in an *in-vivo* constitutive GABA-deficient neural environment. These investigations using *PNPO* mutant mice have provided interesting insights into seizure spread in a model of weakened feedforward inhibition and also offer a robust platform for future epilepsy treatment development research.

Our results confirm the applicability of *PNPO* mutant mice to human epilepsy patients through demonstration of various behavioral phenotypes, including increased susceptibility to seizures under 2 independent chemoconvulsant models of spontaneous seizures, hyperactivity, and spatial memory and learning deficits. Importantly, the data suggest that *PNPO* mutant mice carrying the D33V and R116Q point mutations exhibit mutation severity-dependent behavioral phenotypes, with mice heterozygote for the severe D33V mutation exhibiting more severe seizure susceptibility and hyperactivity phenotypes compared to homozygote R116Q mutant mice. This could be explained by the mild 16% R116Q enzymatic loss-of-function compared to the severe 56% D33V enzymatic loss-of-function[32] and these findings are consistent with trends from our previously generated fly models carrying the same *PNPO* mutations[114,115]. Interestingly, deficit in spatial learning and memory relearning and PNPO protein localization alteration is unique to the R116Q/R116Q mice, suggesting that the R116Q point mutation has potentially neomorphic effects with altered function outside of only hypomorphic partial loss of *PNPO* enzymatic activity. Previously, these *PNPO* point mutations have only been shown to exhibit reduced

enzymatic activity in human epilepsy patients[32], but our results of mutation-specific loss of protein expression and localization change are consistent with previous studies using *D. melanogaster* models we generated carrying the same *PNPO* mutations[115]. *PNPO* is highly conserved between species, with 89% homology between the mouse and human sequences. Although we knocked-in human *PNPO* containing the D33V and R116Q mutations into our fly models[114] and knocked-in the *PNPO* point mutation into the endogenous mouse gene in these mouse models, the consistency in hyperactivity, altered inhibitory neurotransmission, and altered PNPO protein expression and localization between model organisms suggests strongly conserved mechanisms underlying seizure behavior due to *PNPO* mutation and cross-validates results obtained from both animal models. One difference in the mouse model of *PNPO* mutation from the fly model is the decreased PNPO protein expression level and altered PNPO protein intracellular localization in the R116Q mutant. These changes could potentially arise from the fly models carrying a mutant human *PNPO* gene rather than the endogenous fly *PNPO* gene, whereas the mouse models carry the endogenous mouse *PNPO* gene with a single point mutation. Knocking in the human wild type *PNPO* gene to replace the native *sugarlethal* (*sgll*) analog in fly models has been demonstrated to create mild behavioral changes compared to true 'wild-type' flies[115].

Our *in-vivo* recording and electrophysiology studies reveal the importance of *PNPO* for inhibitory control and provide evidence for a weakening of GABAergic signaling and feedforward inhibition contributing to susceptibility to seizures and increased ictal propagation speed across the cortex in mutant mice. Baseline video-EEG revealed an increased theta frequency power in D33V/+ mice compared to controls, which could be rescued with PLP dietary supplementation. Although the individual significance of the Berger EEG bands is not

well understood, an increase in low frequency EEG rhythms positively correlates with ictal activity in human patients[83,125,130], suggesting the PLP supplement-mediated decrease in theta frequency of D33V/+ mice could have a protective effect on epileptogenesis, which is consistent with our behavioral findings. A decrease in spontaneous inhibitory postsynaptic potential (sIPSP) frequency but not quantal amplitude in D33V/+ compared to controls suggest a presynaptic decrease in GABA neurotransmitter release rather than a decrease in postsynaptic GABA receptor function, and this is supported by a decreased maximum fluorescent signal via extracellular virally encoded GABA sensors following pharmacological block of GABA reuptake via tiagabine administration. This decreased GABA release at baseline may contribute to the faster collapse of GABA fluorescent transients during seizure induction, as evidenced by decreased number and amplitude of interictal and sentinel spiking behavior prior to loss of postural control. These findings are all consistent with a progressive loss of inhibitory control preceding and during ictal activity. This was confirmed via increased ictal propagation speed in D33V/+ mice compared to controls, which could also be rescued by PLP dietary supplementation, consistent with the protective effects of PLP in rescuing D33V/D33V from seizures and decreasing D33V/+ baseline theta frequency power. The weakening of inhibitory restraint leading to failure of feedforward inhibition to prevent propagation of ictal activity has predominantly only been modeled in *in-vitro* and *ex-vivo* experiments using slice preparations[55,57,129] or cell culture models[1,55,57], which have limited applicability due to unphysiological seizure induction methods and constrained sampling of cortical neurons. Additionally, calcium imaging studies are limited by sensor temporal resolution and do not report sub-threshold activity, and recent voltage indicators, despite their dynamic range, have not been leveraged for investigation of ictal mechanisms as of yet[131].

Previous findings in slice preparations have identified that cortical somatosensory neurons exhibit strong IPSPs following EPSPs induced by upstream thalamocortical afferent stimulation suggesting strong inhibitory controls following glutamatergic excitatory signaling[57], which can be recapitulated in the hippocampal slice preparation of the dentate gyrus with granule cell and fast-spiking interneurons[129]. Prior to advancing ictal activity in the brain slice, cortical pyramidal neurons have also been found to receive a barrage of inhibitory inputs which block an intense excitatory drive which would normally exceed the threshold for action potential generation by 10 times[55,67]. Breakdown of this feedforward inhibitory control would therefore allow propagation of ictal activity, which is consistent with our *in-vivo* findings of decreased GABAergic release preceding ictal activity and seizures in mice. Furthermore, the baseline decreased GABAergic release in D33V/+ would further weaken this feedforward inhibitory control mechanism, providing a mechanistic explanation for the increased seizure susceptibility observed in our mutant mice. A recent study using simultaneous recording from fluorescent GABA and glutamate sensors also demonstrated that GABA transients peaked a small distance from pharmacologically-generated seizure foci and propagated toward seizure foci, and that seizure onset is preceded by failure of GABA release with successive interictal spikes[4]. This is also highly consistent with our own findings regarding progressive weakening of inhibitory control contributing to increased propagation of ictal activity.

To obtain homozygote D33V mutant mice, the parent mice had to be continually fed with 150mg/kg/day PLP-supplemented drinking water, based on PLP doses given to human patients with epilepsy[116,117]. Following birth, D33V/D33V mutant mice exhibited severe seizures ~P15, ultimately leading to death if not manually fed every 4h with a combination of formulated rodent milk and 50mg/kg PLP. This feeding dosage was reduced to avoid PLP overdose and potential

development of peripheral neuropathy[132,133] due to the 6 feedings per day. The beginning of these severe seizures coincides with a significant shift during mouse development, wherein activity of inwardly chloride-directing Na-K-2Cl cotransporter 1 (NKCC1) expressed in immature hippocampal and spiny neurons are replaced by activity of outwardly chloride-directing K-Cl cotransporter 2 (KCC2)[134]. This change in chloride concentrations results in a switch in polarity of neuronal membrane's response to GABA-mediated channel opening. During embryonic and early postnatal life, high activity of NKCC1 results in high intracellular chloride ion concentration, and the equilibrium potential of chloride ions (E_{Cl}) is positive relative to neuronal resting membrane potential (V_m). Therefore, GABA-mediated chloride channel opening results in an efflux of chloride ions, leading to neuron membrane depolarization[134]. However, upon maturation, KCC2 activity results in low intracellular chloride ion concentration, leading to lower E_{Cl} relative to V_m, thus leading to chloride ion influx following activation of GABA receptors and membrane hyperpolarization and inhibition of action potential firing[134]. The consistent appearance of lethal seizures in D33V/D33V mice at this developmental timepoint suggests that the shift of GABA neurotransmission from having depolarizing to hyperpolarizing effects on membrane excitability play a large role in development of PNPO deficiency-induced seizures. Further investigations are required to elucidate whether control of intracellular chloride ion concentration can alleviate these early seizures. In humans, this developmental shift of chloride cotransporters occurs at similar times relative to gestation but earlier relative to birth[134], due to mice being born significantly underdeveloped compared to human infants. This could explain the increased survival of humans with D33V/D33V *PNPO* mutations[32] relative to our mouse models and also provide an explanation of how *PNPO* mutations and underlying

deficiencies in GABAergic neurotransmission could contribute to etiologically poorly understood human prenatal and neonatal seizures.

Many current pharmacological treatments focus on decreasing excitatory synaptic transmission through downregulating glutamatergic synaptic release or decreasing sodium channel function to alleviate generation or propagation of ictal activity[135,136]. A small number of pharmacological treatments exist for addressing deficits in inhibitory synaptic transmission, and current available therapeutic treatments focus on upregulation of postsynaptic GABA receptor functionality[71,127,137]. Although these approaches aim to address the imbalance in excitation and inhibition contributing to generation of ictal activity, they do not address the root cause of ictal activity generated by deficits in presynaptic GABA neurotransmission in the case of human patients with PNPO deficiency-induced seizures. This may play a role in the refractory nature of seizures found in patients[32,38] and mice with *PNPO* mutations. Our data provides exciting evidence of dietary PLP supplementation for rescuing seizures and increasing inhibitory control of excitatory activity within *PNPO* mutant mice. Further studies are required to examine whether this PLP supplementation can be combined with existing pharmacological drugs to boost their efficacy in mouse seizure models.

In mice, the *PNPO* point mutation R116Q results in significantly increased seizure susceptibility, spatial learning and memory deficit, unique protein localization alterations, and alterations in downstream *Gad1* and *Gad2* gene expression despite its relatively mild 16% decrease in enzymatic function. This suggests the possibility of the R116Q mutation functioning as a neomorph rather than purely as a hypomorph mutation as previously reported[32,115]. The mild loss-of-function phenotype could influence the relatively high allele frequency of the R116Q mutation in the human general population, where roughly 10% of the population are carriers and

about 1% of the population are homozygotes[32,38]. Due to low genetic penetrance from mild loss-of-function in humans and mild behavioral phenotypes in our mutant mice, the R116Q contribution to human disease could be heavily under-reported and under-studied. However, based on the present findings, R116Q nonetheless has significant effects on seizure susceptibility and possible psychosocial effects including hyperactivity and spatial learning and memory. Although it does not cause the development of spontaneous seizures on its own in our mouse models and likely will not be a monogenic cause for epileptic seizures in human patients, R116Q mutations likely work through gene-gene or gene-environment interactions to contribute to seizure susceptibility. The identification and tailored targeting of treatments to these hidden polygenic risk genes could greatly increase the efficacy of modern treatments in individuals with refractory epilepsies.

One limitation of this study is a lack of cellular specificity for *PNPO* mutation. Previous studies have identified parvalbumin (PV)-expressing interneurons as the predominant mediators of feedforward inhibition to a much greater extent than somatostatin (SST)-expressing and other interneuron subtypes[65,66]. Although the majority of cortical interneurons are PV-expressing[3] and therefore most of our findings may be attributed to failure of GABAergic neurotransmission in PV-expressing interneurons, we cannot rule out the contributions of other SST-expressing and vasoactive intestinal polypeptide (VIP)-expressing interneurons involved in feedforward and recurrent inhibitory microcircuits, respectively[3]. Another caveat of the present study is that seizure induction relied upon use of the acute chemoconvulsants flurothyl and PTZ. Although these two methods were chosen for their relatively high temporal control of seizures, we necessarily were not able to examine long-term inhibitory signaling changes or any neural network alterations due to seizure-induced injury following repeated seizures. Despite these

limitations, we believe the use of acute seizure inductions combined with these *PNPO* mutant mice provide insight into the genesis and propagation of ictal activity and how chronic PLP deficiency can contribute to greater progression of these epileptogenic events.

In conclusion, we generated a novel genetic mouse model with *PNPO* mutations found in human epilepsy patients and characterized behavioral and molecular phenotypes in the mutant mice that can be used to investigate deficits in GABAergic signaling in neuropathological disease, such as epilepsy. Using these mutant mice, we provided evidence for the involvement of weakened feedforward inhibitory control during ictal activity propagation and showed that dietary supplementation of PLP can rescue D33V/+ *PNPO* mutant mice abnormal baseline EEG theta power and increased ictal propagation speed. Additionally, *PNPO* mutant mice exhibit chronic decreased GABA neurotransmitter release, both at baseline and during pre-ictal activity, likely contributing to breakdown of feedforward inhibitory control and onset of seizures. These mutant mice will provide a robust vehicle for further investigations on pathological GABAergic signaling at the single cell and network levels, and how failure of inhibitory control contribute to onset and propagation of seizures.

Chapter 3: Anti-homeostatic excessive alcohol use due to genetic vitamin B6 deficiency

Introduction

Altered GABAergic neurotransmission and specific vitamin deficiencies are both well-documented in human clinical patients and animal models of acute and chronic alcohol abuse[138,139]. However, the neurobiology of how these two effects may be related in exacerbating alcohol toxicity and addictive behavior has never been systematically explored.

Alcohol, or more specifically ethanol, is a known allosteric positive modulator of $GABA_A$ receptors[137,140] and increases the frequency and duration of GABA-gated channel opening within the central nervous system[97]. However, the relationship between alcohol and GABAergic signaling is not one directional, as there have been extensive investigations demonstrating activation of GABAergic signaling via pharmacological manipulation also causing increased alcohol intake in rodents[141,142], whereas decreased GABAergic signaling caused decreased alcohol intake[143]. Quantitative trait locus (QTL) mapping has also identified presynaptic and postsynaptic GABAergic transmission-related candidate genes involved in alcohol use[8,144–147].

Outside of direct effects on GABAergic signaling, chronic alcohol consumption has also been shown to cause vitamin deficiencies, including folate, thiamine, vitamin A, and vitamin B6[138]. In humans, vitamin B6 (VB6) is metabolized by pyridoxal 5'-phosphate oxidase (PNPO) from dietary inactive forms of VB6 (mostly pyridoxine) into pyridoxal 5'-phosphate (PLP)[36,37], a critical cofactor for glutamate decarboxylase (GAD)[148,149]. GAD isoforms GAD67 and GAD65 in turn catalyze GABA production in the soma and nerve terminals, respectively[150,151]. PLP has been found to be reduced in the blood plasma of individuals with AUD[41,42], therefore implicating VB6 as a potential indirect factor through which alcohol can influence GABAergic signaling.

Additionally, a large-scale protein screen in mice revealed *PNPO* to be highly upregulated in the transition to alcohol dependence[152], further implicating VB6 in alcohol dependence. Of clinical relevance is the fact that intravenous injection of metadoxine, a pyridoxine and pyrrolidone carboxylate ion pair salt, is efficacious in treating both acute and chronic alcohol intoxication[153].

PLP is also a cofactor for aromatic amino acid decarboxylase (AADC), a homodimer responsible for production of neurotransmitters dopamine, serotonin and norepinephrine[154], all of which are implicated in reward[155,156] and addiction[157,158]. In mammals, the main targets of dopamine are GABAergic D1 and D2 receptor-expressing neurons in the striatum, providing another potential GABAergic involvement in AUD[159,160].

In human genetic studies, several severe mutations in *PNPO* have been found to cause neonatal encephalopathies as monogenic diseases in patients[32]. In addition, *PNPO* was recently identified as 1 of 16 major risk genes for epilepsy[40], suggesting that mild mutations in *PNPO* can also contribute to epilepsy susceptibility in combination with other genetic and environmental factors. Although there have not yet been any human genetic studies published on the contribution of *PNPO* mutations to AUD or to seizures induced by withdrawal from chronic alcohol use, aldehyde dehydrogenase (ALDH), a family of enzymes known to be involved in alcohol metabolism, is implicated in both pyridoxine-dependent epilepsy and AUD[41,161–163].

All the above data suggest a potential link between PLP and alcohol use. Our group previously generated fly knock-in models in which we replaced the wildtype fly *PNPO* gene with human *PNPO* mutant variants with different severity of enzymatic loss-of-function[114,115]. We reason that these genetic models of PLP deficiency offer a unique angle to investigate the role of PLP and GABAergic signaling in contributing to as well as in response to alcohol use. Drosophila melanogaster has been a powerful model organism for alcohol research. The availability of

genetic manipulations and translatable behavioral phenotypes to humans after alcohol consumption allows for investigations into genetic mechanisms of alcohol metabolism and addictive behaviors driving AUD development. By using flies with human wild-type or mutant *PNPO* knock-in and dietary PLP supplementation, the present study has definitively demonstrated anti-homeostatic changes related to alcohol use: alcohol causes PLP deficiency, PLP deficiency increases alcohol preference and consumption, reduces alcohol clearance, and worsens alcohol toxicity.

Methods

Life span and survival: 15-20 male flies were placed into polypropylene vials filled with 4% sucrose in 1% agar with 16% EtOH (Sigma-Adrich #EX0290) or EtOH-free control. Separate cohorts were also given 0µg/mL, 4µg/mL, 40µg/mL, or 400µg/mL PLP (Sigma-Aldrich #P9255), based on a range of concentrations mimicking and exceeding the maximal doses given in the clinical setting. Survival was recorded each morning over 21 days. Chi-Square tests of independence ($p < .05$) were performed to assess statistical significance. Between-genotype comparisons of each treatment group (Control, 4µg/mL PLP, 40µg/mL PLP, 400µg/mL PLP, 16% EtOH + 4µg/mL PLP, 16% EtOH + 40µg/mL PLP, and 16% EtOH + 400µg/mL PLP) and within-genotype comparisons (Control vs PLP, Control vs 16% EtOH, 16% EtOH vs 16% EtOH + PLP) were all analyzed for significance.

Alcohol consumption: EtOH consumption was assayed using proboscis extension response (PER) and modified fluorometric reading assay of preference primed by alcohol (FRAPPE). PER: 25-30 male mutant and control flies were starved overnight for 16h in an empty vial. Flies were individually picked up via aspirator and inserted head-first into a pipette tip via gentle blowing, such that only the head and forelimbs remained outside of the pipette tip. A 6mm strip of

Kimwipe paper was twisted into a thread and pulled apart into cone-shaped wicks. These wicks were dipped into either 16% EtOH or maltodextrin isocaloric positive control solutions in H_2O, then brought to the sensilla of the Drosophila to assay proboscis extension. To rule out incorrect stimulation of the sensilla, each Drosophila was presented with the EtOH- and maltodextrin-soaked wick up to 3 times. Total number of responsive Drosophila in each genotype for both EtOH and maltodextrin were recorded, and ratios of responsive/nonresponsive animals were calculated. This assay was repeated 3 times with separate batches of male flies, total n=78 flies of each genotype were assayed. Chi-Square tests of independence ($p < .05$) were performed to assess statistical significance. FRAPPE: 16% EtOH or maltodextrin isocaloric (Sigma-Aldrich #419672) controls were mixed with 4% sucrose and 1% dyed blue (FD&C Blue No. 1; #FD110 Spectrum) or red (FD&C Red No. 40; #FD140 Spectrum) color in 3% agar. Alternating foods were placed in each well of a flat bottom polystyrene clear 96 well microplate (Corning, Falcon #353072). 25-30 male mutant and control flies of each genotype were starved overnight for 16h in a 1% agar vial supplied with water only and then allowed to explore the well-plate within a dark chamber for 60min with the well-plate lid preventing escape. Afterward, the number of flies carrying red- or blue-dyed abdomens indicating consumption of corresponding control or EtOH-containing agar was quantified. Flies with purple-dyed abdomens were counted as consuming ½ of each control and EtOH-containing agar food. This assay was repeated 8 times with separate batches of male flies, total n=430 w1118, 423 hWT, 375 hR116Q, 455 hD33V, and 371 sgll95 flies were assayed. Chi-Square tests of independence were performed to assess statistical significance.

Locomotor response to alcohol: fly activity was monitored using the Drosophila activity monitor (LAM25H-3, TriKinetics Inc Waltham, MA) with 7-10 flies in fresh food vials at 23°C,

LD=12:12 (Light on = 09:00 – 21:00). After the flies were acclimated to the vial overnight, 500μL 95% EtOH in H_2O was added to the cotton plug between 15:00 and 15:30 the following day. Activity counts of flies crossing the sensor ring were accumulated every minute and pooled from multiple vials to create a histogram. The activity counter counted the locomotor activity of flies when flies crossed the center position of a vial. Latency and peak counts were calculated based on the running average of 10min. One-way ANOVA ($p < .05$) was used to assess statistical significance between genotypes.

Alcohol sensitivity and tolerance: protocols were performed as previously described[164]. Briefly, 15 male flies, 1-2 days old, were picked into vials filled with modified Bloomington cornmeal-molasses fly food (University of Chicago Fly Kitchen) 24h before the assay, and then transferred into a new empty vial covered with a cotton swab, 3mL of 40% EtOH in H_2O with 1% FD&C Blue No. 1 dye (Spectrum #FD110) was pipetted onto the top of each cotton swab, allowing diffusion of EtOH vapor into the vial. Sedated flies indicated by loss of movement and falling from the vial sides were counted on the bottom of each vial in 6min intervals for 1h. After 1h, all flies were transferred into a new vial for recovery for either 4h or 16h. Flies that remained motionless at the bottom of the vial after the recovery period were assumed to be deceased and were counted and removed. Flies were then re-exposed to 40% blue-dyed EtOH solution, and sedated flies were counted again on the bottom of each vial in 6min intervals for 1.5h. The assay was repeated 4 times for a total of N=60 flies used in each genotype. The time to sedation of 50% (ST50) of flies in each group was calculated for both the first and second alcohol exposures, and the ratio between ST50 of re-exposure compared to ST50 of initial exposure was used as a measurement for tolerance development. Chi-Square tests of independence ($p < .05$) were used to assess statistical significance.

Tissue alcohol content: EtOH metabolism was measured in flies using a modified version of a previously published protocol[165,166]. Briefly, 15 male flies exposed to 1h 40% EtOH from the sensitivity assay described above were homogenized in 75µL 100mM Tris-HCl (Sigma-Aldrich #10812846001), pH 7.5 using a Kontes Microtube Pellet Pestle (DWK Life Sciences #749540-0000) and mixed with 40µL 3.4% perchloric acid (Sigma-Aldrich #244252). Samples were spun at 2000rpm for 6min at 4ºC and 7µL supernatants were mixed with 343µL sample buffer containing 0.5M Tris-HCl pH 8.8, 2.75µg/mL alcohol dehydrogenase (Sigma-Aldrich #A7011), and 0.5mg/mL β-nicotinamide adenine dinucleotide (Sigma-Aldrich #N7132) in duplicate to wells of a flat bottomed polystyrene clear 96 well microplate. 7µL of EtOH standards (200mM, 100mM, 50mM, 25mM, 12.5mM, 6.25mM, 3.13mM, 1.56mM, 0.78mM) treated with perchloric acid and mixed with the same sample buffers were also aliquoted in duplicate into wells adjacent to the samples. The microplate was incubated for 40min at room temperature and absorbance was read at 355nm excitation filter for 500ms using a VICTOR Nivo multimode spectrophotometer (PerkinElmer). EtOH concentration in Drosophila homogenates was calculated from absorbance using the standard curve, then divided by 15 to obtain EtOH concentration per fly. This assay was repeated 4 times with separate batches of male flies, total n=60 for all fly genotypes. Two-way ANOVAs were used to assess the effects of genotype and alcohol exposure time on alcohol content. Post-hoc Tukey HSD tests were conducted following the two-way ANOVAs.

Vitamin B species and neurotransmitter analysis by LC-MS: for vitamin B species analysis, 60 male snap-frozen fly samples of each genotype were collected without alcohol exposure or were collected following 1h 40% EtOH exposure from the sensitivity assay described above. VB6 species and neurotransmitters were extracted with ice-cold 10% trichloroacetic acid (8µL solvent

per mg of flies, LC-MS grade water), homogenized (Omni International, TH115-PCR5H, stainless steel probe), vortexed, sonicated for 3 minutes in an ice-cold water bath, and subsequently vortexed for 5min at 2000rpm and 4°C using a Thermomixer. Samples were incubated on ice for 20min, centrifuged at 20,000g for 25min at 4°C, and 75µL of supernatant was transferred to an LC-MS vial. The pooled sample was generated by combining ~20uL from each sample and was injected every 9 samples to evaluate the reproducibility of the detection. The chromatography separation was performed using the ThermoScientific Vanquish Horizon UHPLC system and cortecs T3 (2.1x100 mm, 2.7µm, Waters Corporation) column. The high-resolution Orbitrap IQ-X Tribrid mass spectrometer (Thermo Scientific) with a H-ESI probe operating in positive mode was used to detect and quantify the metabolite levels. The mobile phase (MPA) was 0.1% Formic acid in water and MPB was 0.1% formic acid in methanol. The column temperature, injection volume, and the flow rate were 30°C, 5µL, and 0.3mL/min, respectively. The chromatographic gradient was 0min: 0% B, 1.5min: 0% B, 7min: 25% B, 8min: 25% B, 9min: 100% B, 10min: 100% B, 10.5min: 0% B, and 18min: 0% B. The global parameters for MS were as follows: spray voltage: 3600V, sheath gas: 40, auxiliary gas: 5, sweep gas: 1, RF lens-60%, ion transfer tube temperature: 250°C and vaporizer temperature: 350°C. We performed simultaneous MS1 acquisition in orbitrap (Scan range of 70-300 m/z at 60K resolution, normalized AGC target-100%, max IT- 118ms) and targeted MS2 acquisition with defined start and end time (isolation width-1.2m/z, fixed HCD-30, MS2 resolution 15K, standard AGC, auto max IT). Data acquisition was done using the Xcalibur software (ThermoScientific) and data analysis was performed using Tracefinder 5.1 (±5ppm) software. Vitamin B species identification was done by matching the retention time and MS/MS fragmentation to the commercially available reference standards.

For neurotransmitter analysis (gamma-aminobutyrate, glutamate, acetylcholine), snap frozen flies samples were extracted with 4/4/2 acetonitrile/methanol/water (20µL solvent per mg of flies, LC-MS grade), homogenized, vortexed, and subjected to 2 times- to freeze in liquid nitrogen for 1min, thaw on ice, sonication for 3min in an ice-cold water bath, and subsequently vortexed for 5min at 2000rpm and 4°C using a Thermomixer. Samples were incubated on ice for 20min, centrifuged at 20,000g for 20min at 4°C, and 300µL of supernatant from each sample was dry-down using the Genevac EZ-2.4 elite evaporator. The pooled sample was generated by combining ~equal volume from each sample and was injected throughout the run to determine the reproducibility of the detection. The dry-down samples were stored at -80°C until the analysis. On the day of analysis, the samples were re-suspended in 140µL of 60/40 acetonitrile/water. The chromatography separation was performed using ThermoScientific Vanquish Horizon UHPLC system and a iHILIC-(P) Classic (2.1x150 mm, 5 µm; part # 160.152.0520; HILICON AB) column. The high-resolution Orbitrap IQ-X Tribrid mass spectrometer (ThermoScientific) with a H-ESI probe operating in switch polarity was used to detect and quantify the metabolite levels. The mobile phase A(MPA) was 20mM ammonium bicarbonate at pH 9.6, adjusted by ammonium hydroxide addition and MPB was acetonitrile. The column temperature, injection volume, and flow rate were 40°C, 2µL, and 0.2mL/min, respectively. The chromatographic gradient was 0min: 85% B, 0.5min: 85% B, 18min: 20% B, 20min: 20% B, 20.5min: 85% B and 28min: 85% B. MS parameters were as follows: acquisition range of 70-1000m/z at 60K resolution, spray voltage: 3600V for positive ionization and 2800V for negative ionization modes, sheath gas: 35, auxiliary gas: 5, sweep gas: 1, ion transfer tube temperature: 250°C, vaporizer temperature: 350°C, AGC target: 100%, and a maximum injection time of 118ms. Targeted MS2 was performed on pooled samples and metabolites were identified

by matching retention time and MS/MS fragmentation to the in-house database generated using the commercially available reference standards. Two-way ANOVAs were used to assess the effects of genotype and alcohol exposure time on vitamin B6 and neurotransmitter content. Post-hoc Tukey HSD tests were conducted following the two-way ANOVAs.

Results

Alcohol exposure causes vitamin B6 deficiency in D. melanogaster

Chronic alcohol consumption has been demonstrated to lead to a variety of vitamin deficiencies, including vitamin B6[138], and PLP has also been found to be reduced in the blood plasma of individuals with chronic alcohol consumption and AUD[41,42]. To examine the effects of acute alcohol exposure on B6 vitamers including PLP, pyridoxal (PL), pyridoxine (PN), and B6 metabolite 4-pyridoxate (PA), we performed mass spectrometry using whole-body homogenates before and after 1h alcohol vapor exposure. We found significantly decreased PLP content following alcohol exposure in the control strain w^{1118}. Since we previously discovered a fly strain with severe PNPO deficiency[114,115] and also generated knock-in strains[115] in which the fly *PNPO* is replaced by human wild type *PNPO* (h^{WT}) and human *PNPO* carrying the R116Q and D33V point mutations (h^{R116Q},16% loss-of-function; h^{D33V}, 56% loss-of-function, based on published *in vitro* assays[32]), we were able to examine both alcohol and genotype effects on PLP, PL, PN, and PA. Consistent with human studies[41,42], all genotypes displayed significantly decreased PLP content following alcohol exposure. $sgll^{95}$ flies, which have the most severe impairment as shown in our previous publications[115], displayed significantly lower baseline PLP content than all other genotypes. There was no significant difference in baseline PLP content among all other genotypes, presumably due to less severe PNPO deficiency.

Changes in pyridoxal content due to alcohol or genotype effects were similar to that of PLP, although the alcohol effect on pyridoxal was less severe whereas the genotype effect was more pronounced than that on PLP. The stronger genotype contributions here are expected as pyridoxal is more directly affected by PNPO activity as it is converted directly from dietary VB6 (pyridoxine and pyridoxamine) by PNPO[36,37].

We also observed an overall decrease in pyridoxine content following alcohol exposure in all strains with varying severities. Interestingly, baseline pyridoxine content was positively correlated with the severity of PNPO loss-of-function, presumably due to reduced conversion of pyridoxine to pyridoxal in PNPO mutants. Meanwhile, there was a general trend that the metabolite 4-pyridoxate content was elevated following alcohol exposure, suggesting increased VB6 degradation following acute alcohol exposure.

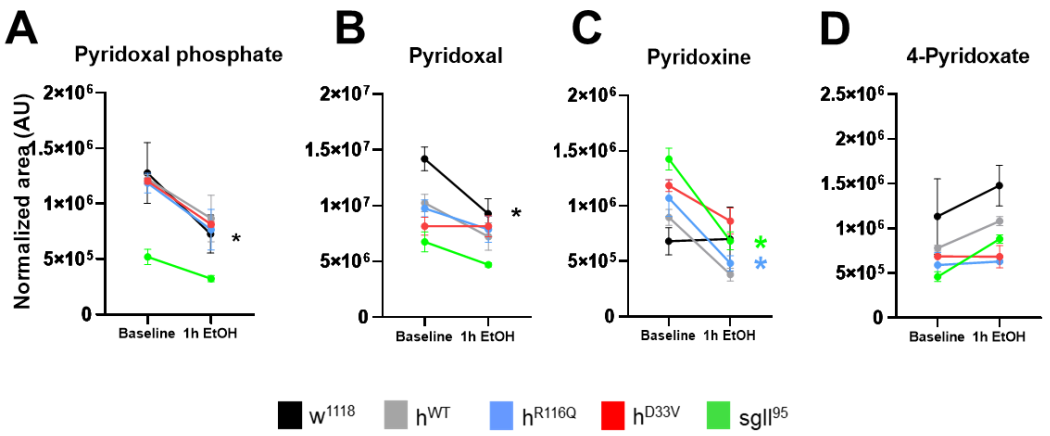

Fig 16: Acute alcohol exposure and mutations in *PNPO* cause PLP deficiency
a-d) Mass spectroscopy quantification of tissue content at baseline and after 1 hour alcohol vapor exposure. A: pyridoxal 5'-phosphate (PLP), B: pyridoxal (PL), C: pyridoxine (PN), and D: 4-pyridoxate (PA). Data is presented as mean and SEM. Genotype x alcohol exposure two-way ANOVAs were performed. Both alcohol exposure and PNPO mutations significantly lowered PLP and PL. See Supplemental Table 1 for all p values in each ANOVA for each B6 vitamer. See Supplemental Table 2 for post-hoc Bonferroni's multiple comparisons test on the comparison between pre- and post-alcohol exposure for each genotype and each B6 vitamer. * denotes $p < .05$ and color denotes genotype.

Mutations in the PNPO gene interact with chronic alcohol consumption to impair survival which can be rescued by PLP supplementation

To examine if PLP deficiency caused by either alcohol exposure or *PNPO* mutations contribute to alcohol toxicity, we investigated the survival of mutant and control fly strains under chronic

alcohol consumption and control conditions with or without PLP supplementation. Flies were introduced into vials and given *ad libitum* access to diet containing or not containing 16% alcohol. We first assessed fly survival without PLP supplementation. We observed lower survival rates in flies carrying more severe *PNPO* mutations over 21 days and alcohol further impaired their survival, indicating a *PNPO* gene x alcohol interaction.

Since both reduced PNPO activity and alcohol use may cause PLP deficiency[36,37,41,42], we therefore investigated whether dietary supplementation with PLP could rescue the reduced survival in *PNPO* mutants and in flies treated with alcohol. Remarkably, PLP dietary supplementation rescued the impaired survival of h^{R116Q}, h^{D33V}, and $sgll^{95}$ mutant flies under chronic alcohol consumption. The most severe loss-of-function $sgll^{95}$ mutants do not exhibit robust survival even under control conditions, and PLP rescued their impaired survival under both control and alcohol conditions. These data suggest that the convergence of PNPO mutations and alcohol consumption worsens PLP deficiency and impairs survival.

Excess PLP has been associated with aldehyde toxicity and neuropathy[132,133] and, unsurprisingly, supplementing food with high concentrations of PLP alone resulted in decreased survival of all flies. Surprisingly, alcohol consumption partially protected flies from this PLP-mediated toxicity. Since it is known that chronic alcohol use is accompanied by low plasma PLP in humans[41,42], we hypothesized that the partial protection from high dose-dependent PLP lethality caused by PLP overdose was mediated by alcohol reduction of PLP. These findings suggest an optimal level of PLP is necessary for survival of flies, and too high concentration via PLP supplementation or too low concentration due to PNPO mutations or alcohol exposure are both lethal. Survival as a function of dietary VB6 amount therefore likely follows a bell curve relationship. Interestingly, alcohol exposure causes a rightward shift of such a bell curve; flies will need more PLP

supplementation for survival but will exhibit increased tolerance for PLP overdose. PNPO mutations also causes a rightward shift of such a bell curve; mutant flies will need more PLP supplementation for survival but will exhibit increased tolerance for PLP overdose.

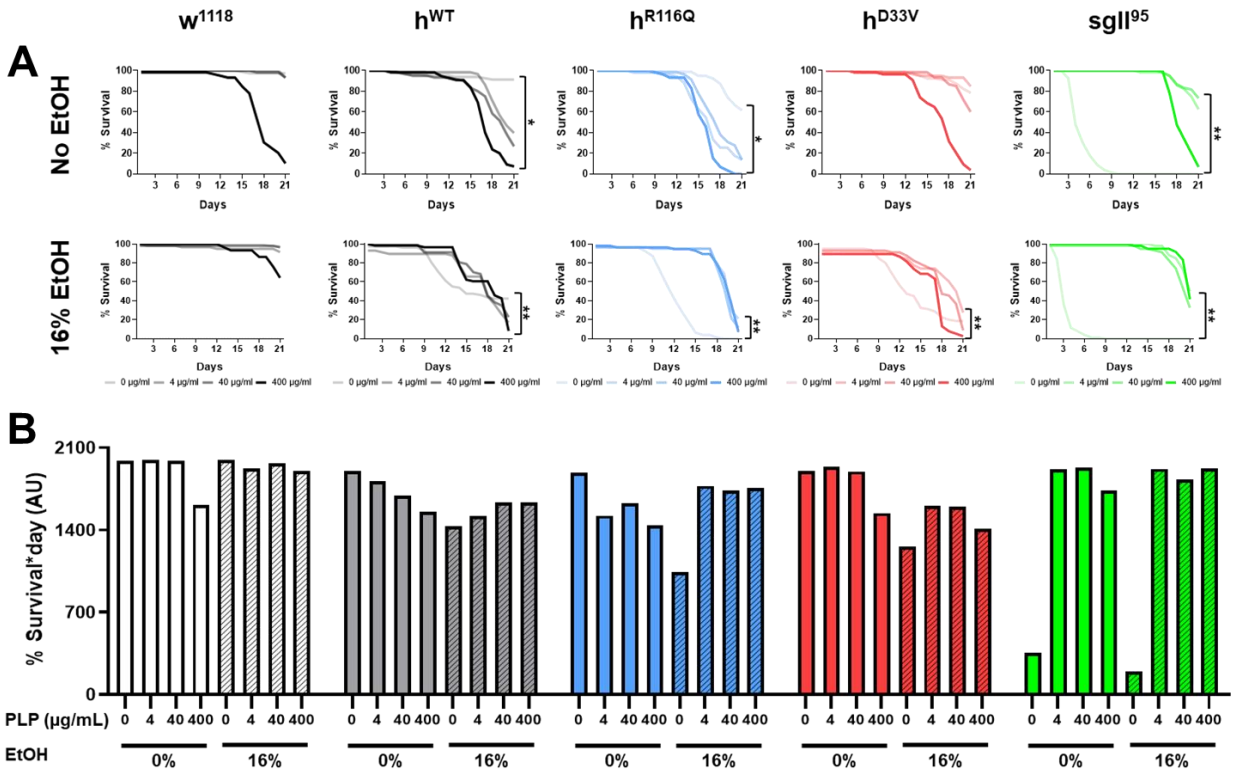

Fig 17: Alcohol interacts with PNPO mutations to affect survival which can be rescued by PLP treatment

a) Survival curves are presented for each genotype on control diet (No EtOH) or 16% alcohol over 21 days (*n*=60 flies/diet treatment) under different PLP treatment doses. Survival is expressed as number of dead flies at the bottom of the food vial divided by the number of total initial flies in the food vial. Survival curve analysis followed by Chi-Square tests of homogeneity were performed to assess genotype effect, alcohol effect, and PLP treatment effect. *PNPO* mutations impaired survival which was worsened by alcohol exposure. PLP treatment rescues both impairments, but very high doses of PLP are toxic.

b) Area under the curve (AU) representation of each survival curve in Panel A. Open bars represent control groups while hatched bars represent 16% alcohol groups. See Supplemental Tables 3-5 for p values in each survival curve comparison.

Mutations in the PNPO gene increase preference and consumption of alcohol

In *Drosophila* as well as other animal models, the sensitivity to nutritional needs and food consumption is often regulated by homeostatic mechanisms[167]. A departure from or impairment of normal homeostatic mechanisms may cause increased intoxication from consumption of excessive amounts of addictive substances such as alcohol[101,109], which may provide additional explanation for mutant flies' decreased survival under the chronic alcohol diet. We therefore examined mutant and control flies' alcohol preference. A proboscis extension reflex (PER) assay was conducted to assess taste behavioral response to alcohol, where an alcohol solution or isocaloric maltodextrin solution droplet was brought to the sensilla of each fly. More than 95% of all flies among each strain exhibited positive feeding responses by extending their proboscis toward an isocaloric maltodextrin droplet positive control and w^{1118} and h^{WT} flies extended their proboscis in response to 16% alcohol at low frequency. However, severe PNPO loss-of-function mutants $sgll^{95}$ and h^{D33V} frequently exhibited proboscis extension upon alcohol solution presentation, with the most severe $sgll^{95}$ mutants exhibiting the greatest frequency of proboscis extension.

To further verify the increased alcohol preference phenotype in mutant flies, flies were given *ad libitum* access to a 96-well plate containing 16% alcohol or isocaloric maltodextrin in agar in alternating wells for 1h in a dark chamber. The alcohol and maltodextrin control foods were dyed blue or red color which allowed determination of food consumption based on colored abdomen, and flies were collected at the end of each 1h session. Since flies may have a natural preference for a particular taste associated with a particular color[168–170], the assay was performed twice with alcohol-containing agar dyed either blue or red. We observed consistently increased alcohol consumption in both dyed colors in flies carrying more severe loss-of-function PNPO mutations, with w^{1118} exhibiting the least consumption whereas $sgll^{95}$ mutants exhibiting the most consumption. These results demonstrate that *PNPO* mutations increase alcohol consumption despite having increased sensitivity to alcohol toxicity.

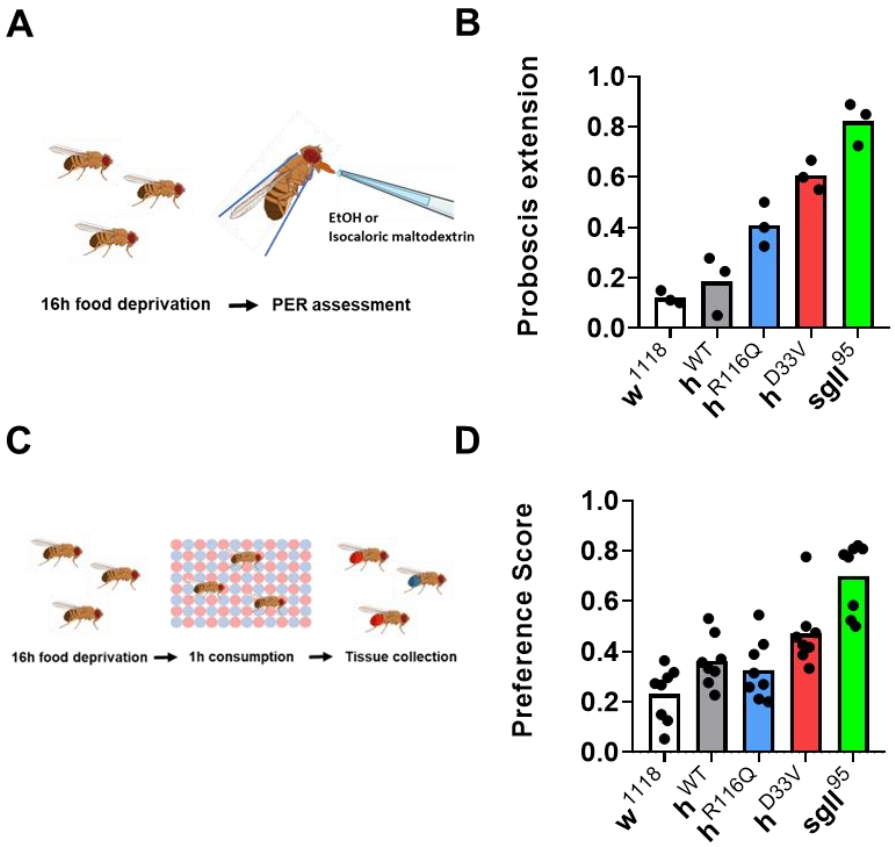

Fig 18: Mutations in the *PNPO* gene increase preference and consumption of alcohol
a) Schematic for proboscis extension reflex assay.
b) Quantification of the ratio of flies with extended proboscis for EtOH from each genotype. Assay was repeated 3 times, *n*=78 flies/genotype. Data is presented as mean. Chi-Square tests of homogeneity was used to compare among different genotypes ($p < 0.001$).
c) Schematic for FRAPPE food preference assay.
d) Quantification of the ratio of flies with alcohol food-colored abdomens compared to total flies. Assay was repeated 8 times for each of EtOH blue and red colors, *n*=430 w^{1118}, 423 h^{WT}, 375 h^{R116Q}, 455 h^{D33V}, and 371 $sgll^{95}$ flies. Data is presented as mean. Chi-Square tests of homogeneity was used to compare among different genotypes ($p < 0.001$).

Alcohol exposure increases inhibitory neurotransmission and decreases excitatory neurotransmission

Alcohol is known to affect neuronal functions through a multitude of mechanisms[138–140,144]. Additionally, PLP is a critical coenzyme for synthesis of the primary inhibitory neurotransmitter GABA, through which an animal's alcohol consumption may be affected. To examine consequences of alcohol exposure on neuronal chemical signaling in *PNPO* mutants, we assayed PLP-dependent and other neurotransmitter levels in whole-body homogenates before and after 1h 40% alcohol vapor exposure using mass spectrometry. GABA content increased following acute alcohol exposure in all strains, even though the same alcohol exposure decreased tissue PLP level, suggesting that these changes were likely due to effects of alcohol on other aspects of GABA synthesis and/or metabolism rather than through changes in PLP content. There was no dramatic genotype effect on baseline levels of GABA. Contrary to changes in GABA, we observed neuromuscular junction excitatory neurotransmitter glutamate and central nervous system excitatory neurotransmitter acetylcholine content decrease following alcohol exposure in all strains. There was no genotype effect on glutamate or acetylcholine levels. Overall, acute alcohol in flies seems to increase inhibitory neurotransmission and decrease excitatory neurotransmission.

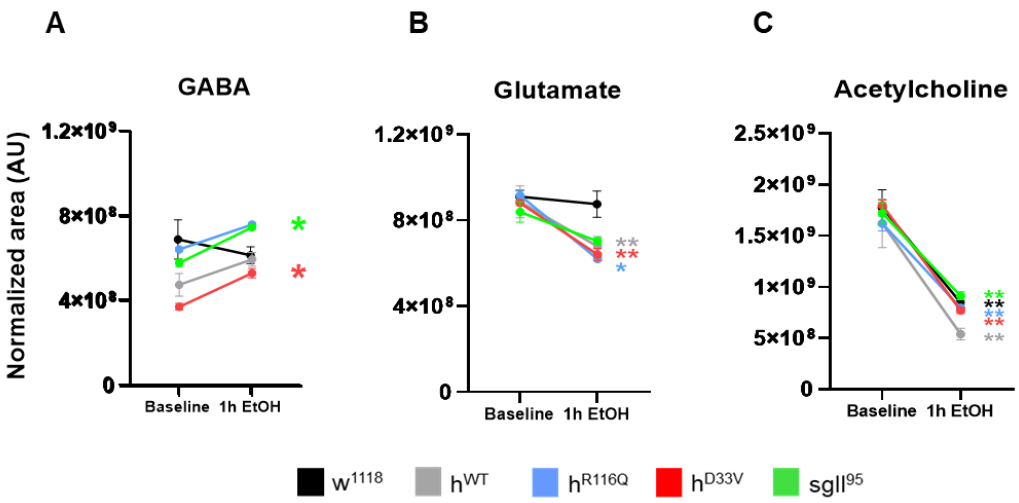

Fig 19: Acute alcohol exposure affects tissue neurotransmitter content
a-c) Mass spectrometry quantification of tissue A: GABA, B: glutamate, and C: acetylcholine content at baseline and after 1h alcohol exposure. Data is presented as mean and SEM. Alcohol exposure significantly increased GABA and decreased glutamate and acetylcholine content. There are mild genotype effects and genotype x alcohol exposure interaction (See Supplemental Table 6 and 7). * denotes $p < .05$, ** denotes $p < .001$, and color denotes genotype.

Mutations in the PNPO gene affect the biphasic response to alcohol

Alcohol induces complex behavioral responses through widely diverse targets, including ion channel receptor-mediated and intracellular signaling pathways, which are reflected in its well characterized biphasic effect on both mood and motor control[101,107,171,172]. Since we observed PLP-dependent changes in sensitivity to alcohol toxicity and consumption, we assessed locomotor activity in *PNPO* mutant flies immediately following alcohol vapor exposure. We observed biphasic responses in all genotypes: increased activity for 30min after alcohol exposure followed by decreased activity over the remaining 1.5h. We quantified locomotor activity through summation of activity over 3h after EtOH exposure, peak activity counts, and latency to 90% peak activity. h^{R116Q} and h^{D33V} flies consistently displayed higher activity compared to h^{WT},

whereas flies carrying the fly *sgll*^{95} mutation had activity similar to w^{1118} controls. In all strains, activity fell below pretreatment levels 2h after alcohol administration.

We further probed alcohol-induced sedation and development of tolerance to alcohol in our mutant flies using a previously described repeated exposure paradigm[164]. Cohorts from each genotype were exposed to 40% alcohol vapor in a clear vial for 1h and the time to reach 50% of flies sedated in the vial was used as a measure of alcohol sensitivity (ST50). Upon initial exposure to alcohol, w^{1118} flies showed stronger sensitivity to alcohol sedation, indicated by shorter sedation time compared to all other genotypes (ST50 = 19.5). h^{WT} and h^{D33V} mutants were least sensitive to alcohol sedation (ST50 = 46.82 and 48.48, respectively), whereas h^{R116Q} and *sgll*^{95} mutants exhibited moderate sensitivity to alcohol sedation.

In order to evaluate responses to repeated alcohol exposure, flies received a second 40% alcohol exposure after 4h or 16h. All fly genotypes that received the second alcohol exposure after 4h recovery reached similar levels of reduced sedation indicating significant tolerance development in all genotypes, potentially due to reaching the maximum level of tolerance. In flies receiving a second alcohol exposure after 16 hours, significant tolerance was also observed in all genotypes but to a lesser extent compared to the 4h recovery groups. The ratio of the second exposure ST50 to the first exposure ST50 was used as a measurement of tolerance development. The level of tolerance upon re-exposure following 16h recovery was similar among all genotypes.

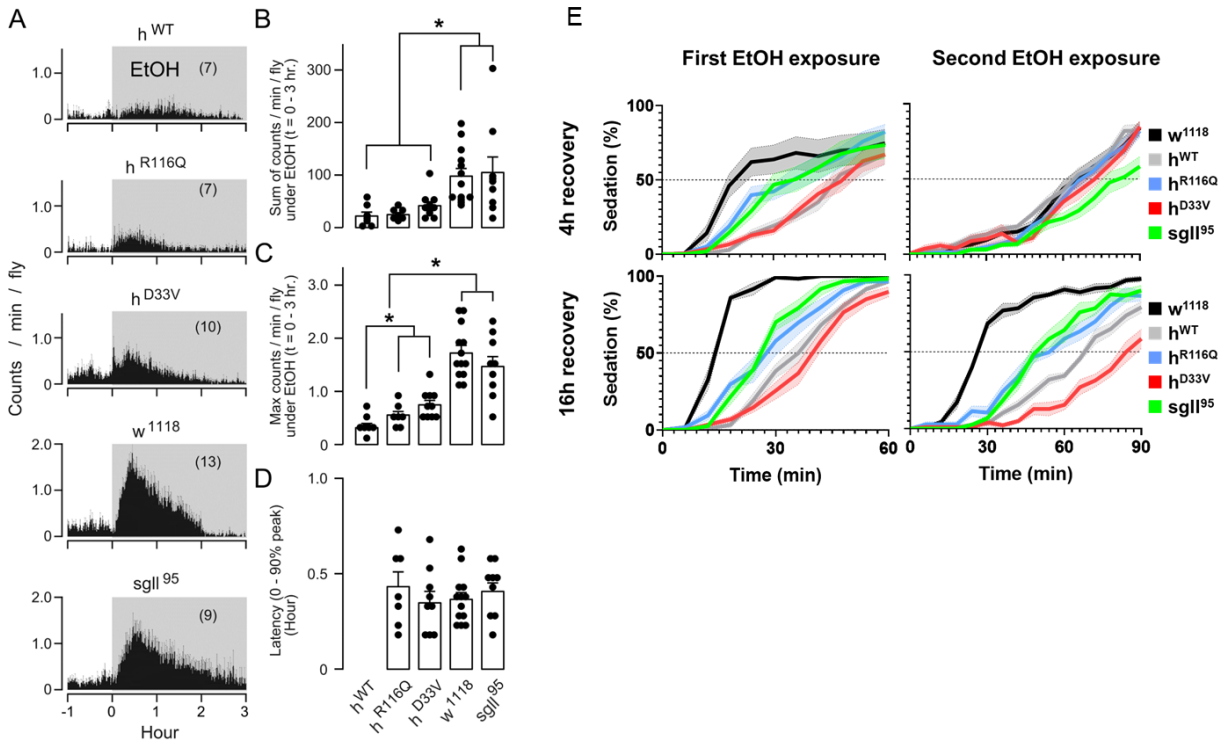

Fig 20: *PNPO* mutations affect the biphasic alcohol response and sedation
a) Representative locomotor counts for 10 flies exposed to 500µl of 95% EtOH.
b) Summation of activities over 3h after EtOH application.
c) Peak activity counts after EtOH application.
d) Latency to 90% of peak activity. * denotes $p < .05$ between genotypes. Each dot indicates a vial containing 7-10 flies. Error bars indicate SEM. Activity counts were measured every minute. Latency and peak counts were calculated based on the running average of 10min.
e) Quantification of sedated flies of each genotype over time of EtOH exposure. Flies were exposed to 40% EtOH vapor for 1h and given a 4h (top) or 16h (bottom) recovery period before re-exposure to 40% EtOH vapor for 1.5h. Dotted line represents 50% sedation. Total of $N=60$ flies of each genotype used. See Supplemental Table 8 for the exact time to reach 50% sedation (ST50) for each genotype under each condition. Tolerance is expressed as the ratio of ST50 between second EtOH exposure and first EtOH exposure. Statistics for tolerance are displayed in Supplemental Table 9.

PNPO mutant flies have higher tissue alcohol content after acute alcohol exposure

A small number of flies died after the initial alcohol sedation. We observed a *PNPO* mutation severity-dependent increase in death in the h^{D33V} (17.7%) and h^{R116Q} (9.9%) groups compared to w^{1118} (4%) and h^{WT} (2%) controls.

Following the tolerance study, we pooled flies from each strain and experimental timepoint and measured whole body tissue alcohol content to assess whether tolerance and mortality were impacted by alcohol metabolism. We used a fluorescence-based detection method at timepoints immediately following 1h alcohol exposure, after 4h or 16h recovery, and after 1.5h re-exposure following 4h and 16h recovery. After initial 1h exposure to 40% alcohol vapor, the h^{R116Q} and h^{D33V} flies exhibited the highest body alcohol content, followed by the h^{WT}, $sgll^{95}$, and w^{1118} flies. Interestingly, higher tissue alcohol content among strains are consistent with higher rate of death following exposure to alcohol as described above.

After 4h or 16h recovery from initial alcohol exposure, all genotypes exhibited significantly reduced alcohol content. Following 1.5h re-exposure to alcohol after 4h or 16h recovery, h^{R116Q} and h^{D33V} flies once again exhibited much higher alcohol tissue content than h^{WT}, w^{1118}, and $sgll^{95}$ flies, suggesting reduced metabolic alcohol clearance in the h^{R116Q} and h^{D33V} mutant flies although it will be difficult to completely rule out the possibility of differences in alcohol inhalation and transport inside the fly body.

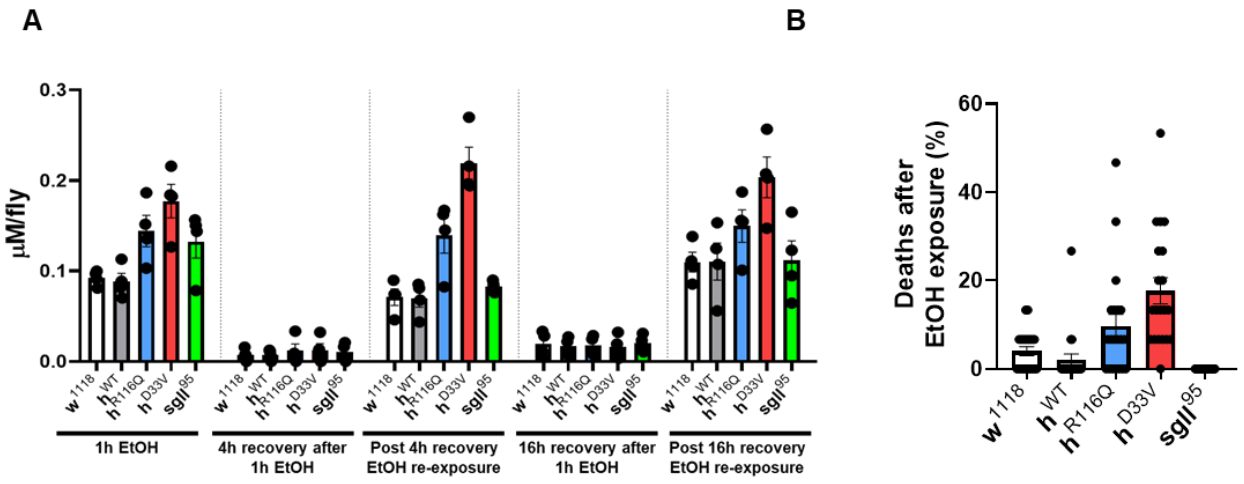

Fig 21: *PNPO* mutants have higher tissue alcohol content after acute alcohol exposure
a) Quantification of whole-body alcohol tissue content in each genotype using biochemical alcohol dehydrogenase luminescence assay. Data is presented as mean and SEM. Genotype x alcohol exposure two-way ANOVA was performed to assess statistical significance. There was significant genotype effect ($p < .0001$), alcohol exposure effect ($p < .0001$), and genotype x alcohol exposure interaction ($p < .0001$). Assay was repeated 4 times and fly alcohol content was calculated from 15 flies per batch, N=60 total flies for each genotype.
b) Death rate following acute 1h exposure to alcohol.

Discussion

PLP deficiency can cause profound impacts on organismal physiology and behavior, as it is a cofactor for more than 140 enzymes in mammals[39]. The present study clearly demonstrates that PLP deficiency plays a highly significant role in both acute and chronic alcohol exposure. Our findings reveal that 1) consistent with existing literature[41,42], alcohol consumption leads to PLP deficiency; 2) PLP deficiency increases alcohol consumption, contributing to a vicious cycle of increasing alcohol consumption; 3) PLP deficiency impairs alcohol clearance, contributing to a vicious cycle of further PLP deficiency; and 4) PLP deficiency itself has potentially lethal consequences which are worsened by alcohol and rescued with PLP supplementation.

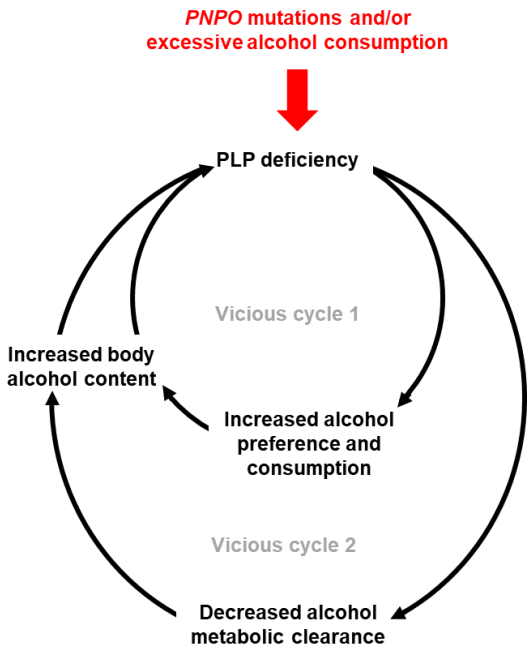

Fig 22: A hypothetical model describing vicious cycles in which PNPO mutations and PLP deficiency may contribution to increased alcohol consumption and increased sensitivity to alcohol toxicity

Drosophila mutants with PLP deficiency have demonstrated a genetic predisposition toward alcohol consumption and mortality. *PNPO* mutations cause increased alcohol consumption, which can further decrease endogenous PLP content. Decreased PLP in turn exacerbates alcohol preference and consumption. Thus, PNPO mutations may mediate a genetic predisposition toward vicious cycles that increase alcohol consumption and increase sensitivity to alcohol toxicity.

PNPO is an indispensable enzyme that converts dietary VB6 to its active form PLP[35,36]. Therefore, partial loss-of-function mutations in *PNPO* could potentially initiate and/or worsen the vicious cycles leading to ever-increasing consumption of alcohol and ever-increasing PLP deficiency. Various loss-of-function mutations in *PNPO* of different degrees of severity have been discovered in human patients[32], potentially contributing to the heterogeneity of human response to alcohol consumption. We also found significant *PNPO* gene-alcohol interactions for *Drosophila* survival, in which survival is positively correlated to PNPO enzymatic activity (more severe *PNPO* mutations have increasing consequences for survival), and alcohol dose is negatively correlated with survival. As expected, dietary PLP supplementation is effective in improving survival under chronic alcohol consumption and/or under *PNPO* mutations. However, extremely high concentrations of PLP are also toxic for *Drosophila* in a dose-dependent manner. This is consistent with human literature demonstrating that both VB6 deficiency and excessive VB6 can have severe physiological consequences, such as peripheral neuropathy[132,133]. Therefore, the impact of dietary PLP supplementation on survival may be thought of as a bell-curve, with an

optimal concentration required for survival. Since *PNPO* mutations lower body PLP content, they shift the bell curve to the right, i.e., high concentrations of dietary PLP supplementation are less toxic in *PNPO* mutant flies. Similarly, alcohol also lowers body PLP content, as indicted by our data here and published studies by others[41,42]. Therefore, alcohol also shifts the bell curve to the right, i.e., high concentrations of dietary PLP concentration are actually less toxic in flies treated with alcohol.

Since chronic alcohol consumption has been demonstrated to reduce PLP content and our results indicate reduced PLP content can increase consumption of alcohol, disentangling cause from consequence would normally provide a significant challenge due to the cyclical nature of this relationship. By using loss-of-function *PNPO* mutant flies and dietary PLP supplementation, we were able to definitively demonstrate that PLP deficiency caused increased alcohol consumption and reduced alcohol clearance. Such an approach also allowed us to examine beneficial and toxic effects of PLP dose-response both independent of and in combination with alcohol consumption.

Although previous studies have demonstrated that chronic alcohol consumption in humans decreases plasma PLP levels[41,42], no studies have examined PLP body content following acute alcohol exposure. Our data revealed significantly decreased PLP and other B6 vitamers in tissues of all fly genotypes following acute 1h exposure to 40% alcohol vapor. The consistent decreases in both PLP and PLP precursors suggest that alcohol-induced PLP deficiency is caused by accelerated VB6 metabolism rather than by slower conversion of PLP precursors to PLP. In contrast, PLP deficiency caused by loss-of-function mutations in *PNPO* increased the PLP precursor PN, likely due to slower enzymatic consumption for PLP production. Although alcohol has many targets, PNPO is unlikely to be one based on the above.

Drosophila exhibit an innate preference for alcohol-containing food under the proboscis extension assay[173] and develop increased alcohol consumption upon consecutive exposures to alcohol[174], possibly due to the presence of alcohol on rotting fruit signaling an abundance of food[175]. Furthermore, female *D. melanogaster* prefer laying eggs on 9% alcohol-containing food but not 15% alcohol-containing food[176,177], suggesting an alcohol dose-sensitive attraction. *PNPO* mutant *Drosophila* prefer to consume alcohol-containing food beyond the level exhibited by control flies in a mutation severity-dependent manner despite the negative effects for survival, suggesting a strong drive for alcohol consumption that overwrites homeostatic mechanisms. Our data also demonstrates that h^{R116Q} and h^{D33V} flies exhibit a mutation severity-dependent decrease in ability to metabolize and eliminate alcohol following exposure to alcohol vapor. This could 1) contribute to the increased lethality to alcohol consumption observed in mutant *PNPO* flies; and 2) suggest that the mutant *Drosophila* do not consume more alcohol to address an innate biological deficiency. Further investigation is required to confirm whether this increased consumption is due to altered ability to sense alcohol consumption or altered behavioral preference for alcohol.

The prevailing model for development of addictive behaviors suggests addiction stems not from homeostatic adaptations but through allostatic maladaptation to maintain a new stability outside of the normal homeostatic range[101,108], including changes in hormones and neurotransmitters[109]. As PLP is a cofactor for GABA synthesis[37,39,113], we would expect a decrease in GABA content following alcohol exposure, yet we found increased GABA content in alcohol-exposed fly tissues. It is possible that the time required to observe changes in GABA content due to PLP deficiency occurs on a longer time scale than assayed. Alternatively, acute alcohol consumption in humans has been shown to increase GABAergic signaling through allosteric upregulation of

$GABA_A$ receptor activity[97,98]. Our data suggest that alcohol also increases total GABA content in *Drosophila* in addition to its enhancement of GABAergic signaling post-synaptic effects. We also found that glutamate and primary *Drosophila* excitatory neurotransmitter acetylcholine were decreased following acute alcohol exposure, which is consistent with previously observed decreased glutamatergic excitatory signaling following alcohol consumption[99,100]. All these lead to tipping of the brain excitation/inhibition (E/I) balance toward inhibition. Whether the combined pre-synaptic and post-synaptic effects from acute alcohol exposure on enhancing GABAergic signaling and reducing excitatory neurotransmission are responsible for development of addictive behaviors and the increased alcohol consumption exhibited by mutant *Drosophila* in our data remains to be seen, although the well-documented addictive properties of GABA receptor agonists such as benzodiazepines[178,179] and glutamate receptor antagonists such as PCP[180,181] and ketamine[182] suggest potential links. While we observed a significant alcohol effect on neurotransmitter levels, we did not observe a large genotype effect except for the overall reduced GABA content in flies carrying the severe loss-of-function D33V mutation.

Genetic contributions toward alcohol use disorder (AUD) vulnerability have long been hypothesized based on twin studies with adoption[110,111]. Our data suggests that *PNPO* could be a genetic risk factor for AUD and that there are complex gene-environment interactions. The R116Q *PNPO* point mutation was initially identified in human neonatal epilepsy patients[32,38] and results in a mere 16% loss-of-function enzymatic activity. Its relatively mild effect on PNPO function could influence its relatively high allele frequency, with about 10% of the general population carrying at least one copy of the R116Q allele, and about 1% of the general population being homozygotes[32]. Due to low genetic penetrance from mild loss-of-function combined with relatively high allele frequency, the R116Q contribution to gene-environment or

gene-diet interactions may be highly under-reported and under-studied. Our present data has demonstrated that even the mild *PNPO* loss-of-function caused by R116Q can result in significantly increased alcohol consumption, decreased metabolic clearing of consumed alcohol, and increased alcohol toxicity as assessed by survival. Alcohol-use disorder and alcohol withdrawal are highly linked with new onset of convulsive seizures[43,183], and *PNPO* partial loss-of-function mutations have also been linked to human neonatal encephalopathy[32]. Although no human genetic studies have implicated the *PNPO* R116Q mutation in AUD or alcohol toxicity, its effects on addictive behavior development to alcohol and gene-diet interactions warrant further study.

The mutant fly strains used in our study have different degrees of impaired PNPO activity, with their PNPO activity in the following descending order: w^{1118}, h^{WT}, h^{R116Q}, h^{D33V}, $sgll^{95}$, based on our previously published studies and the human literature[38,114,115]. The *Drosophila* survival, alcohol consumption, and VB6 tissue content findings in the present study are consistent with previous observations. However, our other findings regarding hyperactivity, alcohol clearance and mortality following acute alcohol exposure are mutation severity-dependent only among the human *PNPO* knock-in strains (h^{WT}, h^{R116Q}, h^{D33V}), suggesting potential cell-type specific differences between human PNPO and fly PNPO proteins despite sharing 45% identity and 75% similarity[115]. Moreover, rather than observing reduced GABA neurotransmitter synthesis due to alcohol exposure-induced reduction in PLP content, we discovered that all fly genotypes exhibited both pre- and post-synaptically enhanced GABA neurotransmission following alcohol exposure. These fascinating discoveries are indicative of the complex pharmacology of alcohol, and evidence that its impact on behavior cannot be easily explained by a single target.

Despite causing significant medical, social, and economic burdens for 10-15% of the global population[184], many of the specific molecular mechanisms underlying AUD that could lead to therapeutic strategies remain poorly understood. The present study unambiguously demonstrates that PLP deficiency plays a highly significant role in alcohol toxicity both acutely and chronically and potentially contributes to vicious cycles leading to increased alcohol consumption. As the amino acid sequence and structure of PNPO protein is evolutionarily conserved ranging from *E. coli* to humans and our mutant flies are modeled after human *PNPO* mutations, these results have important implications for public health and the role of *PNPO* mutations in addictive behavior development, alcohol metabolism, and neurotransmitter content.

Conclusions

Genetic deficiencies in GABAergic signaling have been correlated with a variety of neurological disorders in human patients including epilepsy[185], autism[186], and schizophrenia[187]. Among these conditions, seizures[3,54,57], and cognitive decline[188,189] have been especially common observations in animal models with genetic[83,144], electrophysiological[57,67], or pharmacological[80,81] manipulation of GABAergic inhibitory signaling.

GABA synthesis is predominantly mediated through the activity of GAD and PLP, the active form of vitamin B6. PLP acts as a cofactor in a vast number of catalytic processes, and excessive scarcity has been shown to lead to a variety of diseases, including neonatal encephalopathies caused by genetic mutation and compromise of PNPO enzymatic activity[32,38] and hyperprolinaemia type II caused by ALDH7A1 deficiency and chemical depletion through Knoevenagel condensation[39].

In the *M. musculus* models containing mild R116Q and severe D33V point mutations isolated from human patients (16% and 56% enzymatic loss-of-function, respectively[32]), we observed lethality of D33V homozygous mice due to seizures and were able to obtain surviving mice through dietary 150mg/kg PLP supplementation to the heterozygote parents and 50mg/kg PLP supplementation to the homozygote pups. Mice homozygous for the mild R116Q mutation did not exhibit spontaneous seizures, however. Among the D33V heterozygotes and R116Q mutant mice that did not exhibit spontaneous seizures and lethality, we observed increased seizure susceptibility upon flurothyl and pentylenetetrazole competitive $GABA_A$ receptor antagonist exposure. The severe mutation D33V heterozygote mutant mice exhibited hyperactivity and spatial learning and memory deficits during open field locomotor assay and Morris water maze behavioral assays, respectively. Meanwhile, the mutant mice homozygote for the mild R116Q

mutation did not exhibit hyperactivity during the open field locomotor assay and exhibited distinct spatial learning and memory deficits from the D33V mutants in the Morris water maze assay. These results suggest that, although both D33V and R116Q mutant mice recapitulate seizure and behavioral phenotypes found in human epilepsy patients carrying these *PNPO* mutations, the mechanisms through which these mutations induce epilepsy and associated phenotypes may differ outside of varying degrees of enzymatic loss-of-function.

To further probe these differential phenotypes between D33V and R116Q mutant mice, we used molecular assays and found decreased PNPO protein expression among both D33V and R116Q mutant mice and protein localization alterations in R116Q mutant mice. RT-PCR revealed similarly decreased mRNA expression in D33V mice, although no significant mRNA expression changes in R116Q mice. Interestingly, R116Q mutant mice also exhibited significant reductions in GAD67 and GAD65 mRNA expression. Using *in-vivo* continuous wireless EEG recordings, we identified increased baseline theta power in D33V/+ mutant mice, which is used as a marker for seizure activity and epileptogenesis in human patients and mice[125,190,191] and theorized to originate from decentralization and desynchronization of thalamic theta rhythms spreading to cortical regions captured in intracranial and scalp EEG[83,125]. Interestingly, the increased theta power was rescued in mutant mice treated with dietary 150mg/kg PLP supplementation, which correlated with decreased seizure susceptibility. Furthermore, measurement of the speed of ictal wavefront spread across the cortex during seizures was decreased in D33V/+ mutant mice, suggesting decreased strength of inhibitory feedforward control mechanisms, and this phenomenon could also be rescued using dietary PLP supplementation. To further investigate the strength of inhibitory control in mutant mice and to examine possible mechanisms underlying the observed spatial learning and memory deficits, we utilized an *in-vivo* virally-expressed

fluorescent GABA sensor[192] and discovered decreased maximal GABA release in the D33V/+ mice hippocampal CA1 region compared to wild type following administration of tiagabine, a competitive GAT-1 GABA reuptake inhibitor. Furthermore, seizure induction revealed severely decreased GABA release in mutant mice immediately preceding collapse of GABAergic inhibitory control during seizure onset, which is consistent with previous findings in brain slice preparations and early theorized mechanisms of ictal spread following breakdown of inhibitory control[4,64]. Patch clamp experiments using slice preparations also revealed decreased mIPSP frequency and unchanged mIPSP amplitude and event decay time in D33V/+ mice hippocampal neurons. Together, these results suggest the weakened inhibitory control was mediated by reduced presynaptic GABA release, and that the reduced presynaptic release could contribute both to reduced inhibitory control leading to seizure onset as well as to the increased speed of ictal propagation over the cortex in *PNPO* D33V mutant mice.

In the *D. melanogaster* models containing mutations in the endogenous fly *PNPO* gene, *sugarlethal (sgll)*, and knocked-in human *PNPO* mutations, we discovered that acute alcohol consumption could decrease fly body PLP, vitamin B6 vitamer concentrations, and alter neurotransmitter content. Mutant flies demonstrated PNPO mutation severity-dependent lethality, which was exacerbated by alcohol consumption and rescued with PLP dietary supplementation. However, excessive PLP consumption also had deleterious effects on survival, and PNPO mutations and alcohol consumption could blunt the effects of excessive PLP. This suggested an optimal bell-curve model of survival, where too little and too much PLP could both negatively impact survival in flies, and that PNPO mutations and alcohol consumption could both induce a rightward shift of this bell-curve. Mutant *Drosophila* strains with *PNPO* mutations exhibited increased alcohol consumption compared to controls in a mutation severity-dependent manner

and displayed altered biphasic alcohol locomotor response. Sedation and tolerance development upon repeated alcohol exposures were similar between strains, although h^{R116Q} and h^{D33V} mutant fly strains exhibited remarkably increased body alcohol content following acute alcohol vapor exposure, and these trends had high correlation with mortality following the acute exposure. Of particular interest among these results is that 1) an optimal amount of PLP is required for *Drosophila* survival, and *PNPO* mutations and alcohol consumption can both shift this curve rightward; 2) acute alcohol exposure can decrease *Drosophila* body PLP and vitamin B6 vitamer content; and 3) PLP deficiency can cause increased alcohol consumption and decreased alcohol clearance following acute exposure. These findings suggest the existence of two separate vicious cycles promoting continual anti-homeostatic alcohol consumption due to decreased PLP. Genetic *PNPO* mutations and chronic alcohol consumption can both serve as drivers for decreased PLP, thus suggesting a predisposition of subsets of the general human population to falling into one or both of these vicious cycles.

In this thesis, we discovered separate neurophysiological and behavioral consequences of the effects of PLP deficiency on GABA neurotransmission in *M. musculus* and *D. melanogaster* models related to epilepsy and alcohol consumption. Despite the high correlation of new-onset epilepsy in individuals with chronic alcohol consumption and AUD, no studies have systematically examined potential genetic contributors leading to increased simultaneous risk of neonatal epilepsy development and later alcohol addictive behavior development. As altered GABA neurotransmission is well-known to be involved in both these pathological states, examining *PNPO* mutations covering a span of loss-of-function phenotypes found in the general human population presents an attractive genetic target for research. The fact that *PNPO* mutations can both directly cause neonatal encephalopathy development[38] and also indirectly

influence epilepsy development through gene-gene or gene-environment interactions[40] suggests this gene can provide a fascinating spectrum of loss-of-function phenotypes for understanding GABAergic signaling during epilepsy, alcohol addiction, and other neuropathological states. Although these two animal models were used to examine either PLP deficiency-induced epilepsy or alcohol addiction development, a few common threads among our findings warrant further discussion.

As critical enzymes for GABA synthesis, glutamate decarboxylase (GAD) isoforms 67 (GAD67) and 65 (GAD65) are highly regulated and localized to spatially distinct regions of the neuron. Encoded by the *Gad1* gene, GAD67 is expressed throughout the neuron soma and dendrites and is almost constitutively active (92% active[28] through binding to cofactor PLP, allowing for constant GABA production which is essential for neuronal development and function[26,149,151]. Meanwhile, GAD65 is encoded by the *Gad2* gene and is expressed predominantly in axon terminals. GAD65 enzymatic activity also requires PLP cofactor binding, is predominantly inactivated (28% active[28]), and is responsive to synaptic activity and produces GABA for neurotransmission[26,149,151,193]. Animal models have shown that GAD65 and GAD67 dysfunction play distinct roles in neurological disease and disrupted neurotransmission. Genetic knockout of GAD65 resulted in higher susceptibility to chemoconvulsant-induced seizures despite physiologically normal GABA neurotransmitter levels in mice[194] and spontaneous seizures in rats[195]. Meanwhile mice with genetic knockout of GAD67 exhibited severe neonatal survival deficit, cleft palate, respiratory failure, spontaneous seizures, and reduced GABA neurotransmitter concentration[193], while viral-induced overexpression of GAD67 in a multifactorial temporal lobe epilepsy mouse model also reduced spontaneous EEG seizure activity[196]. In humans, bi-allelic mutations in the *Gad1* gene have also been isolated in patients

with developmental encephalopathies, hypotonia, and dysmorphic features[197]. We observed significantly reduced GAD67 and GAD65 mRNA expression in R116Q/R116Q mutant mice which could have contributed to the seizure and spatial learning and memory phenotypes. The absence of these mRNA expression changes in D33V mutant mice coupled with the distinct spatial learning and memory phenotypes between D33V and R116Q mutant mice could also suggest the R116Q mutation alters activity of the PNPO protein outside of mere partial loss of enzymatic function, which would be in line with our previous findings in *Drosophila* models[32,115]. If the h^{R116Q} *Drosophila* strain were to also exhibit the decreased GAD mRNA expression, then it's possible long-term decreased GAD activity could contribute to the observed vulnerability to excessive alcohol consumption. Indeed, human communities with mutations in *Gad1* have been noted to exhibit increased initial alcohol sensitivity[198] and increased risk of alcohol dependence[199] and alcohol use disorder development[200]. Future studies into GAD activity in *Drosophila* strains carrying the mutant *PNPO* gene would be invaluable in confirming the possibility of PNPO deficiency affecting GAD expression and the subsequent consequences on addictive behavior development.

The effect of genetic determinants on previously idiopathic epilepsies and addictive behavior development has become a highly diverse field of study with the creation of accessible and accurate genetic sequencing technology in recent years[40,144,152,201]. Despite the relatively mild reported loss-of-function phenotype in humans carrying the *PNPO* R116Q point mutation, our results have consistently demonstrated that the R116Q mutation may cause additional neomorphic effects, such as novel deficits in spatial learning and memory, or regulation of GAD expression and PNPO protein localization in mice. In fruit flies, strains carrying the R116Q mutation also exhibit strong alcohol consumption likelihood, decreased alcohol clearance

following acute exposure, altered tolerance development, and altered neurotransmitter content following alcohol exposure, to a larger degree than what would be expected, given its mild enzymatic loss-of-function. All these findings make the mechanisms underlying *PNPO* R116Q point mutation-mediated effects on epileptogenesis and addictive behavior development more multifaceted and interesting for future investigations. Additionally, R116Q has been shown to be relatively common among the human population of genetic epilepsies, with up to 10% of the general population being carriers and 1% of the general population being homozygotes[32]. This is much higher than the prevalence of genetic seizures among the general population[40,48], suggesting that the R116Q point mutation interacts with additional gene-gene or gene-environment factors to mediate its effects on seizure development. Similarly, the highly heterogeneous response to alcohol and development of tolerance would suggest that addictive behavior development is also influenced by many factors, with genetics being merely one of them[144,152]. In our data, despite lacking severe phenotypes such as survival deficit or spontaneous seizures, both the *PNPO* R116Q mouse model and the h^{R116Q} fruit fly strain exhibited significant seizure susceptibility, behavioral deficit, increased alcohol consumption, and decreased alcohol clearance. Although individuals in the human population carrying the R116Q point mutation may appear similarly phenotypically normal, these individuals could be at risk of increased epileptogenesis and vulnerable to addictive behavior development. All these factors would suggest that the effect of R116Q on epileptogenesis and addictive behaviors is both underreported and understudied. It is likely that this point mutation is not the last nor the least genetic mutation contributing to human disease in such a manner. Although much of both current epilepsy and addictions research focuses on direct correlates and causal genes with strong phenotypes[83,87,110,144,177] and such an approach has strong advantages in replicability of findings

and ease of discerning between wild type- and mutant-driven phenotypes, monogenic genetic drivers of disease are relatively rare and far outnumbered by polygenic genetic drivers[202–205]. As such, the future of personalized healthcare and understanding of human disease conditions would benefit greatly from further study and investigation of these milder, more common genetic drivers of disease. Additionally, further investigations of these kinds of mutations could serve to identify new personalized therapies and quality of life improvements for a broader patient population.

The generation of novel mouse and fruit fly models containing *PNPO* mutations has allowed us to tease apart neural mechanisms and processes underlying seizures and addictive behavior development. Using these genetically tractable model organisms and the diverse behavioral, molecular, and neural imaging tools available to them, we have demonstrated the importance of *PNPO* and PLP in GABAergic neurotransmission and contributions of *PNPO* mutations to pathological states. The development of new treatment strategies for human disease is predicated on the understanding of disease mechanisms. As such, the findings in this thesis may contribute to future treatment development by advancing our understanding of genetic epilepsies and maladaptive addictive behavior development, and these novel model organisms also have applicability in a broad range of neuroscience research due to their unique genetic GABA deficiency. It is the hope of this thesis that one day these novel findings will lead to new therapies and the betterment of lives.

Supplemental Tables

Table 1: P values from two-way ANOVA for genotype and EtOH exposure effect in vitamin B6 vitamer concentration analysis

	Genotype effect	EtOH exposure effect	Interaction
PLP	0.0002	0.0006	0.71
PL	0.0009	0.0001	0.19
PN	0.01	<0.0001	0.080
PA	0.0023	0.047	0.62

Table 2: P values from post-hoc Bonferroni's multiple comparisons test for genotype and EtOH exposure effect in vitamin B6 vitamer concentration analysis

PLP	**Baseline – 1h EtOH**
w^{1118}	0.03
h^{WT}	0.39
h^{R116Q}	0.20
h^{D33V}	0.27
$sgll^{95}$	>0.99
PL	
w^{1118}	0.009
h^{WT}	0.20
h^{R116Q}	0.91
h^{D33V}	>0.99
$sgll^{95}$	0.74
PN	
w^{1118}	>0.99
h^{WT}	0.058
h^{R116Q}	0.024
h^{D33V}	0.49
$sgll^{95}$	0.004
PA	
w^{1118}	0.77
h^{WT}	>0.99
h^{R116Q}	>0.99
h^{D33V}	>0.99
$sgll^{95}$	0.43

Table 3: P values from Chi-Square tests of homogeneity for genotype effect on Drosophila survival curves

Genotype effect	No EtOH	16% EtOH
0µg/mL PLP	<0.001	<0.001
4µg/mL PLP	0.13	<0.001
40µg/mL PLP	0.99	0.12
400µg/mL PLP	<0.001	<0.001

Table 4: P values from Chi-Square tests of homogeneity for alcohol effect on Drosophila survival curves

Alcohol effect	0µg/mL PLP	4µg/mL PLP	40µg/mL PLP	400µg/mL PLP
w^{1118}	0.99	0.99	0.99	0.075
h^{WT}	0.34	0.11	0.36	<0.001
h^{R116Q}	<0.001	<0.001	<0.001	<0.001
h^{D33V}	0.035	0.93	0.66	0.42
$sgll^{95}$	<0.001	0.99	0.99	0.001

Table 5: P values from Chi-Square tests of homogeneity for PLP effect on *Drosophila* survival curves

PLP effect	No EtOH	16% EtOH
w^{1118}	0.99	0.82
h^{WT}	0.002	<0.001
h^{R116Q}	0.006	<0.001
h^{D33V}	0.18	<0.001
$sgll^{95}$	<0.001	<0.001

Table 6: P values from two-way ANOVA for genotype and EtOH exposure effect on neurotransmitter content

	Genotype effect	EtOH exposure effect	Interaction
GABA	<0.0001	0.0008	0.03
Glutamate	0.03	<0.0001	0.04
Acetylcholine	0.20	<0.0001	0.65

Table 7: P values from post-hoc Bonferroni's multiple comparisons test for genotype and EtOH exposure effect on neurotransmitter content

GABA	Baseline – 1h EtOH
w^{1118}	0.97
h^{WT}	0.21
h^{R116Q}	0.24
h^{D33V}	0.04
$sgll^{95}$	0.03
Glutamate	
w^{1118}	>0.99
h^{WT}	0.005
h^{R116Q}	0.0001
h^{D33V}	0.001
$sgll^{95}$	0.10
Acetylcholine	
w^{1118}	0.0002
h^{WT}	<0.0001
h^{R116Q}	0.0002
h^{D33V}	<0.0001
$sgll^{95}$	0.0002

Table 8: ST50 values from first and second EtOH exposures for each genotype

Recovery time	Genotype	ST50 – 1st EtOH exposure (s)	ST50 – 2nd EtOH exposure (s)	Tolerance
4h recovery	w^{1118}	19.50	65.41	3.35
	h^{WT}	46.82	64.28	1.37
	h^{R116Q}	35.22	67.19	1.91
	h^{D33V}	48.48	72.27	1.49
	$sgll^{95}$	35.20	81.74	2.32
16h recovery	w^{1118}	13.97	26.10	1.87
	h^{WT}	36.00	67.94	1.89
	h^{R116Q}	27.52	54.22	1.97
	h^{D33V}	39.77	84.11	2.12
	$sgll^{95}$	26.11	49.00	1.88

Table 9: P values from Chi-Square tests of homogeneity for within-genotype comparison between first and second EtOH exposure

	4h recovery between EtOH exposures	16h recovery between EtOH exposures
w^{1118}	<0.001	<0.001
h^{WT}	<0.001	0.09
h^{R116Q}	<0.001	<0.001
h^{D33V}	<0.001	<0.001
$sgll^{95}$	<0.001	<0.001

Bibliography

1. Curtis DR, Duggan AW, Felix D, Johnston G a. R. GABA, Bicuculline and Central Inhibition. *Nature*. 1970;226(5252):1222-1224. doi:10.1038/2261222a0

2. Treiman DM. GABAergic Mechanisms in Epilepsy. *Epilepsia*. 2001;42:8-12.

3. Paz JT, Huguenard JR. Microcircuits and their interactions in epilepsy: Is the focus out of focus? *Nat Neurosci*. 2015;18(3):351-359. doi:10.1038/nn.3950

4. Shimoda Y, Leite M, Graham RT, et al. Extracellular glutamate and GABA transients at the transition from interictal spiking to seizures. *Brain J Neurol*. 2024;147(3):1011-1024. doi:10.1093/brain/awad336

5. Roberts E, Frankel S. γ-AMINOBUTYRIC ACID IN BRAIN: ITS FORMATION FROM GLUTAMIC ACID. *J Biol Chem*. 1950;187(1):55-63. doi:10.1016/S0021-9258(19)50929-2

6. Bazemore AW, Elliott K a. C, Florey E. Isolation of Factor I. *J Neurochem*. 1957;1(4):334-339. doi:10.1111/j.1471-4159.1957.tb12090.x

7. Hansen SL, Sperling BB, Sánchez C. Anticonvulsant and antiepileptogenic effects of GABAA receptor ligands in pentylenetetrazole-kindled mice. *Prog Neuropsychopharmacol Biol Psychiatry*. 2004;28(1):105-113. doi:10.1016/j.pnpbp.2003.09.026

8. Boehm SL, Ponomarev I, Blednov YA, Harris RA. From gene to behavior and back again: new perspectives on GABAA receptor subunit selectivity of alcohol actions. *Adv Pharmacol San Diego Calif*. 2006;54:171-203. doi:10.1016/s1054-3589(06)54008-6

9. Nicoll RA, Malenka RC, Kauer JA. Functional comparison of neurotransmitter receptor subtypes in mammalian central nervous system. *Physiol Rev*. 1990;70(2):513-565. doi:10.1152/physrev.1990.70.2.513

10. Fatt P, Katz B. The effect of inhibitory nerve impulses on a crustacean muscle fibre. *J Physiol*. 1953;121(2):374-389.

11. Staley KJ, Mody I. Shunting of excitatory input to dentate gyrus granule cells by a depolarizing GABAA receptor-mediated postsynaptic conductance. *J Neurophysiol*. 1992;68(1):197-212. doi:10.1152/jn.1992.68.1.197

12. Blomfield S. Arithmetical operations performed by nerve cells. *Brain Res*. 1974;69(1):115-124. doi:10.1016/0006-8993(74)90375-8

13. Mitchell SJ, Silver RA. Shunting Inhibition Modulates Neuronal Gain during Synaptic Excitation. *Neuron*. 2003;38(3):433-445. doi:10.1016/S0896-6273(03)00200-9

14. Gulledge AT, Stuart GJ. Excitatory Actions of GABA in the Cortex. *Neuron*. 2003;37(2):299-309. doi:10.1016/S0896-6273(02)01146-7

15. Kaupmann K, Huggel K, Heid J, et al. Expression cloning of GABAB receptors uncovers similarity to metabotropic glutamate receptors. *Nature*. 1997;386(6622):239-246. doi:10.1038/386239a0

16. Padgett CL, Slesinger PA. GABAB Receptor Coupling to G-proteins and Ion Channels. In: Blackburn TP, ed. *Advances in Pharmacology*. Vol 58. GABAReceptor Pharmacology. Academic Press; 2010:123-147. doi:10.1016/S1054-3589(10)58006-2

17. Buzsáki G, Chrobak JJ. Temporal structure in spatially organized neuronal ensembles: a role for interneuronal networks. *Curr Opin Neurobiol*. 1995;5(4):504-510. doi:10.1016/0959-4388(95)80012-3

18. Singer W. Neurophysiology: The changing face of inhibition. *Curr Biol*. 1996;6(4):395-397. doi:10.1016/S0960-9822(02)00505-5

19. Jonas P, Bischofberger J, Fricker D, Miles R. *Interneuron Diversity series*: Fast in, fast out – temporal and spatial signal processing in hippocampal interneurons. *Trends Neurosci*. 2004;27(1):30-40. doi:10.1016/j.tins.2003.10.010

20. Cobb SR, Buhl EH, Halasy K, Paulsen O, Somogyi P. Synchronization of neuronal activity in hippocampus by individual GABAergic interneurons. *Nature*. 1995;378(6552):75-78. doi:10.1038/378075a0

21. Huntsman MM, Porcello DM, Homanics GE, DeLorey TM, Huguenard JR. Reciprocal Inhibitory Connections and Network Synchrony in the Mammalian Thalamus. *Science*. 1999;283(5401):541-543. doi:10.1126/science.283.5401.541

22. Clayton PT, Surtees RAH, DeVile C, Hyland K, Heales SJR. Neonatal epileptic encephalopathy. *Lancet*. 2003;361(9369):1614. doi:10.1016/S0140-6736(03)13312-0

23. Engel J. Approaches to refractory epilepsy. *Ann Indian Acad Neurol*. 2014;17(SUPPL. 1). doi:10.4103/0972-2327.128644

24. Chaudhry FA, Reimer RJ, Bellocchio EE, et al. The Vesicular GABA Transporter, VGAT, Localizes to Synaptic Vesicles in Sets of Glycinergic as Well as GABAergic Neurons. *J Neurosci*. 1998;18(23):9733-9750. doi:10.1523/JNEUROSCI.18-23-09733.1998

25. Balázs R, Machiyama Y, Hammond BJ, Julian T, Richter D. The operation of the gamma-aminobutyrate bypath of the tricarboxylic acid cycle in brain tissue in vitro. *Biochem J*. 1970;116(3):445-461. doi:10.1042/bj1160445

26. Kaufman DL, Houser CR, Tobin AJ. Two Forms of the γ-Aminobutyric Acid Synthetic Enzyme Glutamate Decarboxylase Have Distinct Intraneuronal Distributions and Cofactor Interactions. *J Neurochem*. 1991;56(2):720-723. doi:10.1111/j.1471-4159.1991.tb08211.x

27. Kanaani J, Cianciaruso C, Phelps EA, et al. Compartmentalization of GABA Synthesis by GAD67 Differs between Pancreatic Beta Cells and Neurons. *PLoS ONE*. 2015;10(2):e0117130. doi:10.1371/journal.pone.0117130

28. Battaglioli G, Liu H, Martin DL. Kinetic differences between the isoforms of glutamate decarboxylase: implications for the regulation of GABA synthesis. *J Neurochem*. 2003;86(4):879-887. doi:10.1046/j.1471-4159.2003.01910.x

29. Wei J, Davis KM, Wu H, Wu JY. Protein Phosphorylation of Human Brain Glutamic Acid Decarboxylase (GAD)65 and GAD67 and Its Physiological Implications. *Biochemistry*. 2004;43(20):6182-6189. doi:10.1021/bi0496992

30. György P, Eckardt RE. Further investigations on vitamin B6 and related factors of the vitamin B2 complex in rats. Parts I and II. *Biochem J*. 1940;34(8-9):1143-1154.

31. Rosenberg IH. A History of the Isolation and Identification of Vitamin B6. *Ann Nutr Metab*. 2012;61(3):236-238. doi:10.1159/000343113

32. Mills PB, Camuzeaux SSM, Footitt EJ, et al. Epilepsy due to PNPO mutations: Genotype, environment and treatment affect presentation and outcome. *Brain*. 2014;137(5):1350-1360. doi:10.1093/brain/awu051

33. Ghatge MS, Al Mughram M, Omar AM, Safo MK. Inborn errors in the vitamin B6 salvage enzymes associated with neonatal epileptic encephalopathy and other pathologies. *Biochimie*. 2021;183:18-29. doi:10.1016/j.biochi.2020.12.025

34. Hellmann H, Mooney S. Vitamin B6: a molecule for human health? *Mol Basel Switz*. 2010;15(1):442-459. doi:10.3390/molecules15010442

35. Percudani R, Peracchi A. A genomic overview of pyridoxal-phosphate-dependent enzymes. *EMBO Rep*. 2003;4(9):850-854. doi:10.1038/sj.embor.embor914

36. Barile A, Nogués I, di Salvo ML, Bunik V, Contestabile R, Tramonti A. Molecular characterization of pyridoxine 5′-phosphate oxidase and its pathogenic forms associated with neonatal epileptic encephalopathy. *Sci Rep*. 2020;10(1). doi:10.1038/s41598-020-70598-7

37. Kang JH, Hong ML, Kim DW, et al. Genomic organization, tissue distribution and deletion mutation of human pyridoxine 5′-phosphate oxidase. *Eur J Biochem*. 2004;271(12):2452-2461. doi:10.1111/j.1432-1033.2004.04175.x

38. Mills PB, Surtees RAH, Champion MP, et al. Neonatal epileptic encephalopathy caused by mutations in the PNPO gene encoding pyridox(am)ine 5′-phosphate oxidase. *Hum Mol Genet*. 2005;14(8):1077-1086. doi:10.1093/hmg/ddi120

39. Wilson MP, Plecko B, Mills PB, Clayton PT. Disorders affecting vitamin B6 metabolism. *J Inherit Metab Dis*. 2019;42(4):629-646. doi:10.1002/jimd.12060

40. Fisher RS, Acevedo C, Arzimanoglou A, et al. ILAE Official Report: A practical clinical definition of epilepsy. *Epilepsia*. 2014;55(4):475-482. doi:10.1111/epi.12550

41. Lumeng L, Li TK. Vitamin B6 Metabolism in Chronic Alcohol Abuse. *J Clin Invest*. 1974;53(3):693-704. doi:10.1172/JCI107607

42. Diehl AM, Potter J, Boitnott J, Van Duyn MA, Herlong HF, Mezey E. Relationship between pyridoxal 5'-phosphate deficiency and aminotransferase levels in alcoholic hepatitis. *Gastroenterology*. 1984;86(4):632-636.

43. Hillbom M, Pieninkeroinen I, Leone M. Seizures in Alcohol-Dependent Patients. *CNS Drugs*. 2003;17(14):1013-1030. doi:10.2165/00023210-200317140-00002

44. Magiorkinis E, Sidiropoulou K, Diamantis A. Hallmarks in the history of epilepsy: Epilepsy in antiquity. *Epilepsy Behav*. 2010;17(1):103-108. doi:10.1016/j.yebeh.2009.10.023

45. Eadie MJ. The origin of the concept of partial epilepsy. *J Clin Neurosci Off J Neurosurg Soc Australas*. 1999;6(2):103-105. doi:10.1054/jocn.1998.0001

46. Ahmed OJ, Cash SS. Finding synchrony in the desynchronized EEG: the history and interpretation of gamma rhythms. *Front Integr Neurosci*. 2013;7. doi:10.3389/fnint.2013.00058

47. Remy S, Beck H. Molecular and cellular mechanisms of pharmacoresistance in epilepsy. *Brain*. 2006;129(1):18-35. doi:10.1093/brain/awh682

48. Thijs RD, Surges R, O'Brien TJ, Sander JW. Epilepsy in adults. *The Lancet*. 2019;393(10172):689-701. doi:10.1016/S0140-6736(18)32596-0

49. Scheffer IE, Berkovic S, Capovilla G, et al. ILAE Classification of the Epilepsies Position Paper of the ILAE Commission for Classification and Terminology. *Epilepsia*. 2017;58(4):512-521. doi:10.1111/epi.13709

50. Wang J, Lin ZJ, Liu L, et al. Epilepsy-associated genes. *Seizure*. 2017;44:11-20. doi:10.1016/j.seizure.2016.11.030

51. Steinlein OK, Mulley2 JC, Propping P, et al. A missense mutation in the neuronal nicotinic acetylcholine receptor a4 subunit is associated with autosomal dominant nocturnal frontal lobe epilepsy. *Nat Genet*. Published online 1995. http://www.nature.com/naturegenetics

52. Jones EG. Viewpoint: the core and matrix of thalamic organization. *Neuroscience*. 1998;85(2):331-345. doi:10.1016/S0306-4522(97)00581-2

53. Douglas RJ, Martin KA. A functional microcircuit for cat visual cortex. *J Physiol*. 1991;440:735-769.

54. Schevon CA, Weiss SA, McKhann G, et al. Evidence of an inhibitory restraint of seizure activity in humans. *Nat Commun*. 2012;3:1060. doi:10.1038/ncomms2056

55. Trevelyan AJ, Sussillo D, Watson BO, Yuste R. Modular Propagation of Epileptiform Activity: Evidence for an Inhibitory Veto in Neocortex. *J Neurosci*. 2006;26(48):12447-12455. doi:10.1523/JNEUROSCI.2787-06.2006

56. Gabernet L, Jadhav SP, Feldman DE, Carandini M, Scanziani M. Somatosensory Integration Controlled by Dynamic Thalamocortical Feed-Forward Inhibition. *Neuron*. 2005;48(2):315-327. doi:10.1016/j.neuron.2005.09.022

57. Sun QQ, Huguenard JR, Prince DA. Barrel Cortex Microcircuits: Thalamocortical Feedforward Inhibition in Spiny Stellate Cells Is Mediated by a Small Number of Fast-Spiking Interneurons. *J Neurosci*. 2006;26(4):1219-1230. doi:10.1523/JNEUROSCI.4727-04.2006

58. Bagnall MW, Hull C, Bushong EA, Ellisman MH, Scanziani M. Multiple clusters of release sites formed by individual thalamic afferents onto cortical interneurons ensure reliable transmission. *Neuron*. 2011;71(1):180-194. doi:10.1016/j.neuron.2011.05.032

59. Inoue T, Imoto K. Feedforward inhibitory connections from multiple thalamic cells to multiple regular-spiking cells in layer 4 of the somatosensory cortex. *J Neurophysiol*. 2006;96(4):1746-1754. doi:10.1152/jn.00301.2006

60. Lee SH, Marchionni I, Bezaire M, et al. Parvalbumin-Positive Basket Cells Differentiate Among Hippocampal Pyramidal Cells. *Neuron*. 2014;82(5):1129-1144. doi:10.1016/j.neuron.2014.03.034

61. Miles R. Synaptic excitation of inhibitory cells by single CA3 hippocampal pyramidal cells of the guinea-pig in vitro. *J Physiol*. 1990;428:61-77.

62. Kee T, Sanda P, Gupta N, Stopfer M, Bazhenov M. Feed-Forward versus Feedback Inhibition in a Basic Olfactory Circuit. *PLoS Comput Biol*. 2015;11(10):e1004531. doi:10.1371/journal.pcbi.1004531

63. Roux L, Buzsáki G. Tasks for inhibitory interneurons in intact brain circuits. *Neuropharmacology*. 2015;0:10-23. doi:10.1016/j.neuropharm.2014.09.011

64. Zhang ZJ, Koifman J, Shin DS, et al. Transition to Seizure: Ictal Discharge Is Preceded by Exhausted Presynaptic GABA Release in the Hippocampal CA3 Region. *J Neurosci*. 2012;32(7):2499-2512. doi:10.1523/JNEUROSCI.4247-11.2012

65. Călin A, Ilie AS, Akerman CJ. Disrupting Epileptiform Activity by Preventing Parvalbumin Interneuron Depolarization Block. *J Neurosci*. 2021;41(45):9452-9465. doi:10.1523/JNEUROSCI.1002-20.2021

66. Cammarota M, Losi G, Chiavegato A, Zonta M, Carmignoto G. Fast spiking interneuron control of seizure propagation in a cortical slice model of focal epilepsy. *J Physiol*. 2013;591(Pt 4):807-822. doi:10.1113/jphysiol.2012.238154

67. Trevelyan AJ, Sussillo D, Yuste R. Feedforward Inhibition Contributes to the Control of Epileptiform Propagation Speed. *J Neurosci*. 2007;27(13):3383-3387. doi:10.1523/JNEUROSCI.0145-07.2007

68. Alarcon G, Garcia Seoane JJ, Binnie CD, et al. Origin and propagation of interictal discharges in the acute electrocorticogram. Implications for pathophysiology and surgical treatment of temporal lobe epilepsy. *Brain J Neurol*. 1997;120 (Pt 12):2259-2282. doi:10.1093/brain/120.12.2259

69. Smith EH, Liou J you, Merricks EM, et al. Human interictal epileptiform discharges are bidirectional traveling waves echoing ictal discharges. *eLife*. 2022;11:e73541. doi:10.7554/eLife.73541

70. Kwan P, Brodie MJ. Early identification of refractory epilepsy. *N Engl J Med*. Published online 2000.

71. Löscher W. Critical review of current animal models of seizures and epilepsy used in the discovery and development of new antiepileptic drugs. *Seizure*. 2011;20(5):359-368. doi:10.1016/j.seizure.2011.01.003

72. Löscher W. Animal Models of Seizures and Epilepsy: Past, Present, and Future Role for the Discovery of Antiseizure Drugs. *Neurochem Res*. 2017;42(7):1873-1888. doi:10.1007/s11064-017-2222-z

73. Birbeck GL, Hays RD, Cui X, Vickrey BG. Seizure Reduction and Quality of Life Improvements in People with Epilepsy. *Epilepsia*. 2002;43(5):535-538. doi:10.1046/j.1528-1157.2002.32201.x

74. Ruan Y, Chen L, She D, Chung Y, Ge L, Han L. Ketogenic diet for epilepsy: an overview of systematic review and meta-analysis. *Eur J Clin Nutr*. 2022;76(9):1234-1244. doi:10.1038/s41430-021-01060-8

75. Ko A, Kwon HE, Kim HD. Updates on the ketogenic diet therapy for pediatric epilepsy. *Biomed J*. 2022;45(1):19-26. doi:10.1016/j.bj.2021.11.003

76. Dyńka D, Kowalcze K, Paziewska A. The Role of Ketogenic Diet in the Treatment of Neurological Diseases. *Nutrients*. 2022;14(23):5003. doi:10.3390/nu14235003

77. Putnam TJ, Merritt HH. EXPERIMENTAL DETERMINATION OF THE ANTICONVULSANT PROPERTIES OF SOME PHENYL DERIVATIVES. *Science*. 1937;85(2213):525-526. doi:10.1126/science.85.2213.525

78. Toman JEP, Swinyard EA, Goodman LS. Properties of maximal seizures, and their alteration by anticonvulsant drugs and other agents. *J Neurophysiol*. 1946;9(3):231-239. doi:10.1152/jn.1946.9.3.231

79. Everett GM, Richards RK. Comparative Anticonvulsive Action of 3,5,5-Trimethyloxazolidine-2,4-Dione (tridione), Dilantin and Phenobarbital. *J Pharmacol Exp Ther*. 1944;81(4):402-407.

80. Ferland R. The Repeated Flurothyl Seizure Model in Mice. *Bio-Protoc*. 2017;7(11):1-12. doi:10.21769/bioprotoc.2309

81. Shimada T, Yamagata K. Pentylenetetrazole-Induced Kindling Mouse Model. *J Vis Exp JoVE*. 2018;(136):56573. doi:10.3791/56573

82. Curia G, Longo D, Biagini G, Jones RSG, Avoli M. The pilocarpine model of temporal lobe epilepsy. *J Neurosci Methods*. 2008;172(2-4):143-157. doi:10.1016/j.jneumeth.2008.04.019

83. Catron MA, Howe RK, Besing GLK, et al. Sleep slow-wave oscillations trigger seizures in a genetic epilepsy model of Dravet syndrome. *Brain Commun*. 2022;5(1):fcac332. doi:10.1093/braincomms/fcac332

84. Rubinstein M, Westenbroek RE, Yu FH, Jones CJ, Scheuer T, Catterall WA. Genetic Background Modulates Impaired Excitability of Inhibitory Neurons in a Mouse Model of Dravet Syndrome. *Neurobiol Dis*. 2015;73:106-117. doi:10.1016/j.nbd.2014.09.017

85. Liu J, Gao C, Chen W, et al. CRISPR/Cas9 facilitates investigation of neural circuit disease using human iPSCs: mechanism of epilepsy caused by an SCN1A loss-of-function mutation. *Transl Psychiatry*. 2016;6(1):e703-e703. doi:10.1038/tp.2015.203

86. Serikawa T, Mashimo T, Kuramoto T, Voigt B, Ohno Y, Sasa M. Advances on genetic rat models of epilepsy. *Exp Anim*. 2015;64(1):1-7. doi:10.1538/expanim.14-0066

87. Mistry AM, Thompson CH, Miller AR, Vanoye CG, George AL, Kearney JA. Strain- and age-dependent hippocampal neuron sodium currents correlate with epilepsy severity in Dravet syndrome mice. *Neurobiol Dis*. 2014;65:1-11. doi:10.1016/j.nbd.2014.01.006

88. Kang JQ, Macdonald RL. GABRG2 Mutations Associated with a spectrum of epilepsy syndromes from Generalized Absence Epilepsy to Dravet syndrome. *JAMA Neurol*. 2016;73(8):1009-1016. doi:10.1001/jamaneurol.2016.0449

89. Vergnes M, Marescaux Ch, Micheletti G, et al. Spontaneous paroxysmal electroclinical patterns in rat: A model of generalized non-convulsive epilepsy. *Neurosci Lett*. 1982;33(1):97-101. doi:10.1016/0304-3940(82)90136-7

90. Yu FH, Mantegazza M, Westenbroek RE, et al. Reduced sodium current in GABAergic interneurons in a mouse model of severe myoclonic epilepsy in infancy. *Nat Neurosci*. 2006;9(9):1142-1149. doi:10.1038/nn1754

91. 2018 National Survey on Drug Use and Health (NSDUH) Releases. Accessed May 21, 2024. https://www.samhsa.gov/data/release/2018-national-survey-drug-use-and-health-nsduh-releases

92. American Psychiatric Association. *Diagnostic and Statistical Manual of Mental Disorders*. 5th ed.

93. Sacks JJ, Gonzales KR, Bouchery EE, Tomedi LE, Brewer RD. 2010 National and State Costs of Excessive Alcohol Consumption. *Am J Prev Med*. 2015;49(5):e73-e79. doi:10.1016/j.amepre.2015.05.031

94. Burnette EM, Nieto SJ, Grodin EN, et al. Novel Agents for the Pharmacological Treatment of Alcohol Use Disorder. *Drugs*. 2022;82(3):251-274. doi:10.1007/s40265-021-01670-3

95. Kranzler HR, Leong SH, Naps M, Hartwell EE, Fiellin DA, Rentsch CT. Association of topiramate prescribed for any indication with reduced alcohol consumption in electronic health record data. *Addiction*. 2022;117(11):2826-2836. doi:10.1111/add.15980

96. Collins SE. Associations Between Socioeconomic Factors and Alcohol Outcomes. *Alcohol Res Curr Rev*. 2016;38(1):83-94.

97. Tatebayashi H, Motomura H, Narahashi T. Alcohol modulation of single GABA(A) receptor-channel kinetics. *Neuroreport*. 1998;9(8):1769-1775. doi:10.1097/00001756-199806010-00018

98. Davies M. The role of GABAA receptors in mediating the effects of alcohol in the central nervous system. *J Psychiatry Neurosci*. 2003;28(4):263-274.

99. Kumar S, Porcu P, Werner DF, et al. The role of GABAA receptors in the acute and chronic effects of ethanol: a decade of progress. *Psychopharmacology (Berl)*. 2009;205(4):529. doi:10.1007/s00213-009-1562-z

100. Vengeliene V, Bilbao A, Molander A, Spanagel R. Neuropharmacology of alcohol addiction. *Br J Pharmacol*. 2008;154(2):299-315. doi:10.1038/bjp.2008.30

101. Koob GF, Le Moal M. Plasticity of reward neurocircuitry and the "dark side" of drug addiction. *Nat Neurosci*. 2005;8(11):1442-1444. doi:10.1038/nn1105-1442

102. Samokhvalov AV, Irving H, Mohapatra S, Rehm J. Alcohol consumption, unprovoked seizures, and epilepsy: A systematic review and meta-analysis. *Epilepsia*. 2010;51(7):1177-1184. doi:10.1111/j.1528-1167.2009.02426.x

103. Chan AWK. Alcoholism and Epilepsy. *Epilepsia*. 1985;26(4):323-333. doi:10.1111/j.1528-1157.1985.tb05658.x

104. Hauser WA, Ng SKC, Brust JCM. Alcohol, Seizures, and Epilepsy. *Epilepsia*. 1988;29(s2):S66-S78. doi:10.1111/j.1528-1157.1988.tb05800.x

105. Dam AM, Fuglsang-Frederiksen A, Svarre-Olsen U, Dam M. Late-Onset Epilepsy: Etiologies, Types of Seizure, and Value of Clinical Investigation, EEG, and Computerized Tomography Scan. *Epilepsia*. 1985;26(3):227-231. doi:10.1111/j.1528-1157.1985.tb05410.x

106. Rathlev NK, Ulrich AS, Delanty N, D'Onofrio G. Alcohol-related seizures. *J Emerg Med*. 2006;31(2):157-163. doi:10.1016/j.jemermed.2005.09.012

107. Pandey SC, Ugale R, Zhang H, Tang L, Prakash A. Brain chromatin remodeling: a novel mechanism of alcoholism. *J Neurosci Off J Soc Neurosci*. 2008;28(14):3729-3737. doi:10.1523/JNEUROSCI.5731-07.2008

108. Koob GF. The neurobiology of addiction: a neuroadaptational view relevant for diagnosis. *Addiction*. 2006;101(s1):23-30. doi:10.1111/j.1360-0443.2006.01586.x

109. Sterling P, Eyer J. Allostasis: A new paradigm to explain arousal pathology. In: *Handbook of Life Stress, Cognition and Health*. John Wiley & Sons; 1988:629-649.

110. Heath AC. Genetic Influences on Alcoholism Risk. *Alcohol Health Res World*. 1995;19(3):166-171.

111. Heath AC, Bucholz KK, Madden PA, et al. Genetic and environmental contributions to alcohol dependence risk in a national twin sample: consistency of findings in women and men. *Psychol Med*. 1997;27(6):1381-1396. doi:10.1017/s0033291797005643

112. Verhulst B, Neale MC, Kendler KS. The heritability of alcohol use disorders: a meta-analysis of twin and adoption studies. *Psychol Med*. 2015;45(5):1061-1072. doi:10.1017/S0033291714002165

113. Stover PJ, Field MS. Vitamin B-61. *Adv Nutr*. 2015;6(1):132-133. doi:10.3945/an.113.005207

114. Chi W, Iyengar ASR, Albersen M, et al. Pyridox (am) ine 5'-phosphate oxidase deficiency induces seizures in Drosophila melanogaster. *Hum Mol Genet*. 2019;28(18):3126-3136. doi:10.1093/hmg/ddz143

115. Chi W, Iyengar ASR, Fu W, et al. Drosophila carrying epilepsy-associated variants in the vitamin B6 metabolism gene PNPO display allele- and diet-dependent phenotypes. *Proc Natl Acad Sci*. 2022;119(9). doi:10.1073/pnas.2115524119/-/DCSupplemental

116. Stockler S, Plecko B, Gospe SM, et al. Pyridoxine dependent epilepsy and antiquitin deficiency: clinical and molecular characteristics and recommendations for diagnosis, treatment and follow-up. *Mol Genet Metab*. 2011;104(1-2):48-60. doi:10.1016/j.ymgme.2011.05.014

117. Karnebeek CDM van, Tiebout SA, Niermeijer J, et al. Pyridoxine-Dependent Epilepsy: An Expanding Clinical Spectrum. *Pediatr Neurol*. 2016;59:6-12. doi:10.1016/j.pediatrneurol.2015.12.013

118. Dolenz BJ. Flurothyl (Indoklon) Side Effects. *Am J Psychiatry*. 1967;123(11):1453-1455. doi:10.1521/00332747.1961.11023285

119. Van Erum J, Van Dam D, De Deyn PP. PTZ-induced seizures in mice require a revised Racine scale. *Epilepsy Behav*. 2019;95:51-55. doi:10.1016/j.yebeh.2019.02.029

120. Vorhees CV, Williams MT. Morris water maze: Procedures for assessing spatial and related forms of learning and memory. *Nat Protoc*. 2006;1(2):848-858. doi:10.1038/nprot.2006.116

121. Kaminiów K, Pająk M, Pająk R, Paprocka J. Pyridoxine-Dependent Epilepsy and Antiquitin Deficiency Resulting in Neonatal-Onset Refractory Seizures. *Brain Sci*. 2021;12(1):65. doi:10.3390/brainsci12010065

122. Beghi E, Giussani G, Sander JW. The natural history and prognosis of epilepsy. *Epileptic Disord*. 2015;17(3):243-253. doi:10.1684/epd.2015.0751

123. Chi W, Zhang L, Du W, Zhuang X. A Nutritional Conditional Lethal Mutant Due to Pyridoxine 5′-Phosphate Oxidase Deficiency in Drosophila melanogaster. *G3 GenesGenomesGenetics*. 2014;4(6):1147-1154. doi:10.1534/g3.114.011130

124. Hanno-Iijima Y, Tanaka M, Iijima T. Activity-dependent bidirectional regulation of GAD expression in a homeostatic fashion is mediated by BDNF-dependent and independent pathways. *PLoS ONE*. 2015;10(8):1-18. doi:10.1371/journal.pone.0134296

125. Chauvière L, Rafrafi N, Thinus-Blanc C, Bartolomei F, Esclapez M, Bernard C. Early Deficits in Spatial Memory and Theta Rhythm in Experimental Temporal Lobe Epilepsy. *J Neurosci*. 2009;29(17):5402-5410. doi:10.1523/JNEUROSCI.4699-08.2009

126. Deshpande LS, DeLorenzo RJ. Mechanisms of levetiracetam in the control of status epilepticus and epilepsy. *Front Neurol*. 2014;5 JAN. doi:10.3389/fneur.2014.00011

127. Meldrum BS, Chapman AG. Basic mechanisms of gabitril (tiagabine) and future potential developments. *Epilepsia*. 1999;40 Suppl 9:S2-6. doi:10.1111/j.1528-1157.1999.tb02087.x

128. Prince DA, Wilder BJ. Control mechanisms in cortical epileptogenic foci. "Surround" inhibition. *Arch Neurol*. 1967;16(2):194-202. doi:10.1001/archneur.1967.00470200082007

129. Ewell LA, Jones MV. Frequency-Tuned Distribution of Inhibition in the Dentate Gyrus. *J Neurosci*. 2010;30(38):12597-12607. doi:10.1523/JNEUROSCI.1854-10.2010

130. De Stefano P, Carboni M, Marquis R, Spinelli L, Seeck M, Vulliemoz S. Increased delta power as a scalp marker of epileptic activity: a simultaneous scalp and intracranial electroencephalography study. *Eur J Neurol*. 2022;29(1):26-35. doi:10.1111/ene.15106

131. Fan LZ, Kim DK, Jennings JH, et al. All-optical physiology resolves a synaptic basis for behavioral timescale plasticity. *Cell*. 2023;186(3):543-559.e19. doi:10.1016/j.cell.2022.12.035

132. Hadtstein F, Vrolijk M. Vitamin B-6-Induced Neuropathy: Exploring the Mechanisms of Pyridoxine Toxicity. *Adv Nutr*. 2021;12(5):1911-1929. doi:10.1093/advances/nmab033

133. Schaumburg Herbert, Kaplan Jerry, Windebank Anthony, et al. Sensory Neuropathy from Pyridoxine Abuse. *N Engl J Med*. 1983;309(8):445-448. doi:10.1056/NEJM198308253090801

134. Kahle KT, Staley KJ, Nahed BV, et al. Roles of the cation–chloride cotransporters in neurological disease. *Nat Clin Pract Neurol*. 2008;4(9):490-503. doi:10.1038/ncpneuro0883

135. Wierenga CJ, Wadman WJ. Miniature Inhibitory Postsynaptic Currents in CA1 Pyramidal Neurons After Kindling Epileptogenesis. *J Neurophysiol*. 1999;82(3):1352-1362.

136. Liljelund P, Ferguson C, Homanics G, Olsen RW. Long-term effects of diazepam treatment of epileptic GABAA receptor beta3 subunit knockout mouse in early life. *Epilepsy Res*. 2005;66(1-3):99-115. doi:10.1016/j.eplepsyres.2005.07.005

137. Fink-Jensen A, Suzdak PD, Swedberg MDB, Judge ME, Hansen L, Nielsen PG. The γ-aminobutyric acid (GABA) uptake inhibitor, tiagabine, increases extracellular brain levels of GABA in awake rats. *Eur J Pharmacol*. 1992;220(2-3):197-201. doi:10.1016/0014-2999(92)90748-S

138. Hoyumpa AM. Mechanisms of Vitamin Deficiencies in Alcoholism. *Alcohol Clin Exp Res*. 1986;10(6):573-581. doi:10.1111/j.1530-0277.1986.tb05147.x

139. Oscar-Berman M, Shagrin B, Evert DL, Epstein C. Impairments of Brain and Behavior. *Alcohol Health Res World*. 1997;21(1):65-75.

140. Mihic SJ, Ye Q, Wick MJ, et al. Sites of alcohol and volatile anaesthetic action on GABAA and glycine receptors. *Nature*. 1997;389(6649):385-389. doi:10.1038/38738

141. Boyle AE, Segal R, Smith BR, Amit Z. Bidirectional effects of GABAergic agonists and antagonists on maintenance of voluntary ethanol intake in rats. *Pharmacol Biochem Behav*. 1993;46(1):179-182. doi:10.1016/0091-3057(93)90338-T

142. Petry NM. Benzodiazepine-GABA modulation of concurrent ethanol and sucrose reinforcement in the rat. *Exp Clin Psychopharmacol*. 1997;5(3):183-194. doi:10.1037/1064-1297.5.3.183

143. Rassnick S, D'Amico E, Riley E, Koob GF. GABA antagonist and benzodiazepine partial inverse agonist reduce motivated responding for ethanol. *Alcohol Clin Exp Res*. 1993;17(1):124-130. doi:10.1111/j.1530-0277.1993.tb00736.x

144. Buck KJ, Finn DA. Genetic factors in addiction: QTL mapping and candidate gene studies implicate GABAergic genes in alcohol and barbiturate withdrawal in mice. *Addiction*. 2001;96(1):139-149. doi:10.1046/j.1360-0443.2001.96113910.x

145. Saba LM, Bennett B, Hoffman PL, et al. A Systems Genetic Analysis of Alcohol Drinking by Mice, Rats and Men: Influence of Brain GABAergic Transmission. *Neuropharmacology*. 2011;60(7-8):1269-1280. doi:10.1016/j.neuropharm.2010.12.019

146. Enoch MA, Zhou Z, Kimura M, Mash DC, Yuan Q, Goldman D. GABAergic Gene Expression in Postmortem Hippocampus from Alcoholics and Cocaine Addicts; Corresponding Findings in Alcohol-Naïve P and NP Rats. *PLoS ONE*. 2012;7(1):e29369. doi:10.1371/journal.pone.0029369

147. Bubier JA, Jay JJ, Baker CL, et al. Identification of a QTL in Mus musculus for Alcohol Preference, Withdrawal, and Ap3m2 Expression Using Integrative Functional Genomics and Precision Genetics. *Genetics*. 2014;197(4):1377-1393. doi:10.1534/genetics.114.166165

148. Langendorf CG, Tuck KL, Key TLG, et al. Structural characterization of the mechanism through which human glutamic acid decarboxylase auto-activates. *Biosci Rep*. 2013;33(1):e00013. doi:10.1042/BSR20120111

149. Soghomonian JJ, Martin DL. Two isoforms of glutamate decarboxylase: why? *Trends Pharmacol Sci*. 1998;19(12):500-505. doi:10.1016/S0165-6147(98)01270-X

150. Erlander MG, Tillakaratne NJK, Feldblum S, Patel N, Tobin AJ. Two genes encode distinct glutamate decarboxylases. *Neuron*. 1991;7(1):91-100. doi:10.1016/0896-6273(91)90077-D

151. Pinal CS, Tobin AJ. Uniqueness and redundancy in GABA production. *Perspect Dev Neurobiol*. 1998;5(2-3):109-118.

152. Gorini G, Roberts AJ, Mayfield RD. Neurobiological Signatures of Alcohol Dependence Revealed by Protein Profiling. *PLoS ONE*. 2013;8(12):e82656. doi:10.1371/journal.pone.0082656

153. Addolorato G, Ancona C, Capristo E, Gasbarrini G. Metadoxine in the Treatment of Acute and Chronic Alcoholism: A Review. *Int J Immunopathol Pharmacol*. 2003;16(3):207-214. doi:10.1177/039463200301600304

154. Montioli R, Borri Voltattorni C. Aromatic Amino Acid Decarboxylase Deficiency: The Added Value of Biochemistry. *Int J Mol Sci*. 2021;22(6):3146. doi:10.3390/ijms22063146

155. Söderpalm B, Ericson M. Neurocircuitry Involved in the Development of Alcohol Addiction: The Dopamine System and its Access Points. In: Sommer WH, Spanagel R, eds. *Behavioral Neurobiology of Alcohol Addiction*. Springer; 2013:127-161. doi:10.1007/978-3-642-28720-6_170

156. Wise RA, Jordan CJ. Dopamine, behavior, and addiction. *J Biomed Sci*. 2021;28(1):83. doi:10.1186/s12929-021-00779-7

157. Koob GF, Volkow ND. Neurocircuitry of Addiction. *Neuropsychopharmacology*. 2010;35(1):217-238. doi:10.1038/npp.2009.110

158. Wanat MJ, Willuhn I, Clark JJ, Phillips PEM. Phasic dopamine release in appetitive behaviors and drug abuse. *Curr Drug Abuse Rev*. 2009;2(2):195-213.

159. Flores-Hernandez J, Hernandez S, Snyder GL, et al. D1 Dopamine Receptor Activation Reduces GABAA Receptor Currents in Neostriatal Neurons Through a PKA/DARPP-32/PP1 Signaling Cascade. *J Neurophysiol*. 2000;83(5):2996-3004. doi:10.1152/jn.2000.83.5.2996

160. Guzmán JN, Hernández A, Galarraga E, et al. Dopaminergic Modulation of Axon Collaterals Interconnecting Spiny Neurons of the Rat Striatum. *J Neurosci*. 2003;23(26):8931-8940. doi:10.1523/JNEUROSCI.23-26-08931.2003

161. Laciak AR, Korasick DA, Wyatt JW, Gates KS, Tanner JJ. Structural and Biochemical Consequences of Pyridoxine-Dependent Epilepsy Mutations That Target the Aldehyde Binding Site of Aldehyde Dehydrogenase ALDH7A1. *FEBS J*. 2020;287(1):173-189. doi:10.1111/febs.14997

162. Edenberg HJ, McClintick JN. Alcohol dehydrogenases, aldehyde dehydrogenases and alcohol use disorders: a critical review. *Alcohol Clin Exp Res*. 2018;42(12):2281-2297. doi:10.1111/acer.13904

163. Jin S, Cinar R, Hu X, et al. Spinal astrocyte aldehyde dehydrogenase-2 mediates ethanol metabolism and analgesia in mice. *BJA Br J Anaesth*. 2021;127(2):296-309. doi:10.1016/j.bja.2021.02.035

164. Chvilicek MM, Titos I, Rothenfluh A. The Neurotransmitters Involved in Drosophila Alcohol-Induced Behaviors. *Front Behav Neurosci*. 2020;14. doi:10.3389/fnbeh.2020.607700

165. Moore MS, DeZazzo J, Luk AY, Tully T, Singh CM, Heberlein U. Ethanol Intoxication in *Drosophila*: Genetic and Pharmacological Evidence for Regulation by the cAMP Signaling Pathway. *Cell*. 1998;93(6):997-1007. doi:10.1016/S0092-8674(00)81205-2

166. Carnicella S, Amamoto R, Ron D. Excessive alcohol consumption is blocked by glial cell line–derived neurotrophic factor. *Alcohol Fayettev N*. 2009;43(1):35-43. doi:10.1016/j.alcohol.2008.12.001

167. Kaun KR, Sokolowski MB. cGMP-dependent protein kinase: linking foraging to energy homeostasis. *Genome*. 2009;52(1):1-7. doi:10.1139/G08-090

168. Schnaitmann C, Pagni M, Reiff DF. Color vision in insects: insights from Drosophila. *J Comp Physiol A*. 2020;206(2):183-198. doi:10.1007/s00359-019-01397-3

169. Little CM, Rizzato AR, Charbonneau L, Chapman T, Hillier NK. Color preference of the spotted wing Drosophila, Drosophila suzukii. *Sci Rep*. 2019;9:16051. doi:10.1038/s41598-019-52425-w

170. Lazopulo S, Lazopulo A, Baker JD, Syed S. Daytime colour preference in Drosophila depends on the circadian clock and TRP channels. *Nature*. 2019;574(7776):108-111. doi:10.1038/s41586-019-1571-y

171. Addicott MA, Marsh-Richard DM, Mathias CW, Dougherty DM. The Biphasic Effects of Alcohol: Comparisons of Subjective and Objective Measures of Stimulation, Sedation, and Physical Activity. *Alcohol Clin Exp Res*. 2007;31(11):1883-1890. doi:10.1111/j.1530-0277.2007.00518.x

172. Van Reen E, Rupp TL, Acebo C, Seifer R, Carskadon MA. Biphasic Effects of Alcohol as a Function of Circadian Phase. *Sleep*. 2013;36(1):137-145. doi:10.5665/sleep.2318

173. Cadieu N, Cadieu JC, El Ghadraoui L, Grimal A, Lambœuf Y. Conditioning to ethanol in the fruit fly—a study using an inhibitor of ADH. *J Insect Physiol*. 1999;45(6):579-586. doi:10.1016/S0022-1910(99)00041-4

174. Devineni AV, Heberlein U. Preferential Ethanol Consumption in Drosophila Models Features of Addiction. *Curr Biol CB*. 2009;19(24):2126-2132. doi:10.1016/j.cub.2009.10.070

175. Dudley R. Ethanol, Fruit Ripening, and the Historical Origins of Human Alcoholism in Primate Frugivory1. *Integr Comp Biol*. 2004;44(4):315-323. doi:10.1093/icb/44.4.315

176. Richmond RC, Gerking JL. Oviposition site preference in Drosophila. *Behav Genet*. 1979;9(3):233-241. doi:10.1007/BF01071304

177. Rodan AR, Rothenfluh A. The Genetics of Behavioral Alcohol Responses in Drosophila. *Int Rev Neurobiol*. 2010;91:25-51. doi:10.1016/S0074-7742(10)91002-7

178. Tan KR, Brown M, Labouèbe G, et al. Neural bases for addictive properties of benzodiazepines. *Nature*. 2010;463(7282):769-774. doi:10.1038/nature08758

179. O'Brien CP. Benzodiazepine Use, Abuse, and Dependence. *Prim Care Companion CNS Disord*. 2005;7(Suppl 1: Editor Choice):1829.

180. Garey RE. PCP (phencyclidine): an update. *J Psychedelic Drugs*. 1979;11(4):265-275. doi:10.1080/02791072.1979.10471408

181. Baldridge EB, Bessen HA. Phencyclidine. *Emerg Med Clin North Am*. 1990;8(3):541-550.

182. Liu Y, Lin D, Wu B, Zhou W. Ketamine abuse potential and use disorder. *Brain Res Bull*. 2016;126:68-73. doi:10.1016/j.brainresbull.2016.05.016

183. Lennox WG. Alcohol and Epilepsy. *Q J Stud Alcohol*. 1941;2(1):1-11. doi:10.15288/qjsa.1941.2.001

184. Koob GF. Drug Addiction: Hyperkatifeia/Negative Reinforcement as a Framework for Medications Development. *Pharmacol Rev*. 2021;73(1):163-201. doi:10.1124/pharmrev.120.000083

185. Symonds JD, Zuberi SM, Stewart K, et al. Incidence and phenotypes of childhood-onset genetic epilepsies: A prospective population-based national cohort. *Brain*. 2019;142(8):2303-2318. doi:10.1093/brain/awz195

186. Rubenstein JLR, Merzenich MM. Model of autism: increased ratio of excitation/inhibition in key neural systems. *Genes Brain Behav*. 2003;2(5):255-267.

187. Uhlhaas PJ, Singer W. Abnormal neural oscillations and synchrony in schizophrenia. *Nat Rev Neurosci*. 2010;11(2):100-113. doi:10.1038/nrn2774

188. Holmes GL. Cognitive impairment in Epilepsy: The Role of Network Abnormalities. *Epileptic Disord Int Epilepsy J Videotape*. 2015;17(2):101-116. doi:10.1684/epd.2015.0739

189. Novak A, Vizjak K, Rakusa M. Cognitive Impairment in People with Epilepsy. *J Clin Med*. 2022;11(1):267. doi:10.3390/jcm11010267

190. Fox J, Samudra N, Johnson M, Humayun MJ, Abou-Khalil BW. Temporal intermittent rhythmic theta activity (TIRTA): A marker of epileptogenicity? *eNeurologicalSci*. 2022;29:100433. doi:10.1016/j.ensci.2022.100433

191. Doose H, Baier WK. Theta rhythms in the EEG: A genetic trait in childhood epilepsy. *Brain Dev*. 1988;10(6):347-354. doi:10.1016/S0387-7604(88)80091-3

192. Marvin JS, Shimoda Y, Magloire V, et al. A genetically encoded fluorescent sensor for in vivo imaging of GABA. *Nat Methods*. 2019;16(8):763-770. doi:10.1038/s41592-019-0471-2

193. Asada H, Kawamura Y, Maruyama K, et al. Cleft palate and decreased brain γ-aminobutyric acid in mice lacking the 67-kDa isoform of glutamic acid decarboxylase. *Proc Natl Acad Sci*. 1997;94(12):6496-6499. doi:10.1073/pnas.94.12.6496

194. Asada H, Kawamura Y, Maruyama K, et al. Mice Lacking the 65 kDa Isoform of Glutamic Acid Decarboxylase (GAD65) Maintain Normal Levels of GAD67 and GABA in Their Brains but Are Susceptible to Seizures. *Biochem Biophys Res Commun*. 1996;229(3):891-895. doi:10.1006/bbrc.1996.1898

195. Kakizaki T, Ohshiro T, Itakura M, et al. Rats deficient in the GAD65 isoform exhibit epilepsy and premature lethality. *FASEB J*. 2021;35(2):e21224. doi:10.1096/fj.202001935R

196. Shimazaki K, Kobari T, Oguro K, et al. Hippocampal GAD67 Transduction Using rAAV8 Regulates Epileptogenesis in EL Mice. *Mol Ther - Methods Clin Dev*. 2019;13:180-186. doi:10.1016/j.omtm.2018.12.012

197. Neuray C, Maroofian R, Scala M, et al. Early-infantile onset epilepsy and developmental delay caused by bi-allelic GAD1 variants. *Brain*. 2020;143(8):2388-2397. doi:10.1093/brain/awaa178

198. Kuo PH, Kalsi G, Prescott CA, et al. Associations of glutamate decarboxylase genes with initial sensitivity and age-at-onset of alcohol dependence in the Irish Affected Sib Pair Study of Alcohol Dependence. *Drug Alcohol Depend*. 2009;101(1-2):80-87. doi:10.1016/j.drugalcdep.2008.11.009

199. Terranova C, Tucci M, Forza G, Barzon L, Palù G, Ferrara SD. Alcohol dependence and glutamate decarboxylase gene polymorphisms in an Italian male population. *Alcohol*. 2010;44(5):407-413. doi:10.1016/j.alcohol.2010.05.011

200. Loh EW, Lane HY, Chen CH, et al. Glutamate Decarboxylase Genes and Alcoholism in Han Taiwanese Men. *Alcohol Clin Exp Res*. 2006;30(11):1817-1823. doi:10.1111/j.1530-0277.2006.00218.x

201. Todorova MT, Mantis JG, Le M, Kim CY, Seyfried TN. Genetic and environmental interactions determine seizure susceptibility in epileptic EL mice. *Genes Brain Behav*. 2006;5(7):518-527. doi:10.1111/j.1601-183X.2006.00204.x

202. Steinlein OK. Idiopathic Epilepsies with a Monogenic Mode of Inheritance. *Epilepsia*. 1999;40(s3):9-11. doi:10.1111/j.1528-1157.1999.tb00892.x

203. Nicita F, De Liso P, Danti FR, et al. The genetics of monogenic idiopathic epilepsies and epileptic encephalopathies. *Seizure*. 2012;21(1):3-11. doi:10.1016/j.seizure.2011.08.007

204. Barr PB, Ksinan A, Su J, et al. Using polygenic scores for identifying individuals at increased risk of substance use disorders in clinical and population samples. *Transl Psychiatry*. 2020;10(1):1-9. doi:10.1038/s41398-020-00865-8

205. Kiiskinen T, Mars NJ, Palviainen T, et al. Genomic prediction of alcohol-related morbidity and mortality. *Transl Psychiatry*. 2020;10:23. doi:10.1038/s41398-019-0676-2